Nonquadratic design algorithms for input-saturated linear systems

Santiago Pantano-Calderón

RÉPUBLIQUE FRANÇAISE
Liberté Égalité Fraternité

Université de Toulouse

Doctorat de l'Université de Toulouse

préparé à l'INSA Toulouse

Algorithmes de conception non quadratiques pour les systèmes linéaires soumis à saturation d'entrée

Thèse présentée et soutenue, le 18 octobre 2024 par

Santiago PANTANO CALDERÓN

École doctorale
SYSTEMES

Spécialité
Automatique

Unité de recherche
LAAS - Laboratoire d'Analyse et d'Architecture des Systèmes

Thèse dirigée par
Sophie TARBOURIECH et Luca ZACCARIAN

Composition du jury
M. Jean-Marc BIANNIC, Président, ONERA
M. Mirko FIACCHINI, Rapporteur, CNRS Alpes
M. Matthew TURNER, Rapporteur, University of Southampton
M. Gianluca RIZZELLO, Examinateur, Universität des Saarlandes
Mme Sophie TARBOURIECH, Directrice de thèse, CNRS Occitanie Ouest
M. Luca ZACCARIAN, Co-directeur de thèse, CNRS Occitanie Ouest

RÉPUBLIQUE FRANÇAISE
Liberté
Égalité
Fraternité

Université de Toulouse

Titre : Algorithmes de conception non quadratiques pour les systèmes linéaires soumis à saturation d'entrée

Mots clés : Automatique, Systèmes saturés, LMI, Méthodes de Lyapunov, Stabilité

Résumé : Ce manuscrit propose de nouvelles conditions suffisantes pour la synthèse de contrôleurs dynamiques et stabilisateurs par retour de sortie incluant une boucle d'anti-windup statique pour les systèmes soumis à saturation d'entrée. Étant donné un contrôleur dynamique stabilisant la boucle fermée lorsque l'on néglige la saturation de l'entrée, la synthèse de la boucle d'anti-windup statique est également abordée. Basés sur des inégalités matricielles linéaires et bilinéaires (LMIs et BMIs, respectivement), ainsi que sur des transformations appropriées et des conditions de secteur, les résultats exposés exploitent les formes quadratiques indéfinies en signe impliquant l'état en boucle fermée et la zone morte de la commande d'entrée pour définir des fonctions de Lyapunov par morceaux. Les solutions proposées utilisent des degrés de liberté supplémentaires par rapport à l'approche classique de stabilisation quadratique pour construire des certificats de stabilité exponentielle globale ou régionale de l'origine du système en boucle fermée.

Les conditions LMI peuvent être utilisées comme contraintes de schémas d'optimisation convexes qui peuvent être facilement résolus à l'aide de solveurs et d'optimiseurs commerciaux. Pour les conditions formulées en termes de BMIs, des algorithmes itératifs basés sur une décomposition convexe-concave sont donnés pour obtenir des solutions. Pour exécuter ces algorithmes, il est nécessaire d'aussi des conditions initiales faisables que nous fournissons en exploitant la structure des BMIs. Avec une stabilité exponentielle globale ou régionale garantie, les solutions exposées dans ce manuscrit assurent également un taux de convergence exponentielle locale prescrit. De plus, lorsque seule la stabilité exponentielle régionale est atteignable, les conceptions régionales proposées permettent de déterminer des estimations du bassin d'attraction de l'origine pour le système en boucle fermée, avec un volume maximisé. Des applications numériques sont présentées dans ce manuscrit pour illustrer l'efficacitéet les désavantages de chacune des méthodes.

Title: Nonquadratic design algorithms for input-saturated linear systems

Key words: Automatic control, Saturated systems, LMI, Lyapunov methods, Stability

Abstract: This manuscript provides novel sufficient conditions for the synthesis of stabilizing dynamic output-feedback controllers with anti-windup compensation for linear systems subject to input saturation. Given a dynamic output-feedback controller, stabilizing the linear closed-loop, the design of a static anti-windup loop is also addressed. Based on Linear and Bilinear Matrix Inequalities (LMIs and BMIs, respectively), together with appropriate transformations and sector conditions, the results exposed exploit the sign-indefinite quadratic forms involving the closed-loop state and the deadzone of the control input to define piecewise smooth Lyapunov functions. The proposed solutions leverage additional degrees of freedom with respect to the classical quadratic stabilization approach to construct global or regional exponential stability certificates of the origin of the closed-loop system.

The obtained LMIs are used as constraints in convex optimization schemes and may be easily solved with commercial solvers and optimizers. For the conditions formulated in terms of BMIs, iterative algorithms based on a convex-concave decomposition are given to solve such bilinear conditions. To be executed, such algorithms require feasible initial conditions that we provide by exploiting the structure of the BMIs. With guaranteed global or regional exponential stability, the solutions exposed in this manuscript also ensure a prescribed local exponential convergence rate. Additionally, when only regional exponential stability is attainable, the proposed regional designs allow determining inner-approximations of the basin of attraction of the origin for the closed-loop system, with maximized volume. Numerical applications are presented in this manuscript to illustrate the effectiveness and drawbacks of each one of the proposed methods.

Para Nestor y Ruby

Para Tato y Lucila

Foreword

The results presented in this manuscript were obtained at the « Laboratoire d'analyse et architecture des systèmes du CNRS » (LAAS-CNRS), and more specifically, at the « Méthodes et Algorithmes en Commande » (MAC) team. I express thanks to Dr. Lucie Badouin, for letting me join the MAC team during the realization of my doctoral studies. Also, I express thanks to the « École Doctorale Systèmes » (EDSYS) and the « Institut National des Sciences Appliquées de Toulouse » (INSA Tououse), for giving me the financial support required to carry out this thesis.

I would like to express deep gratitude to Dr. Sophie Tarbouriech and Dr. Luca Zaccarian, researchers at LAAS-CNRS, for supporting me in all the imaginable ways from the beginning and until the finishing of this work. Without their support, this research would not have even been thought up. I am and will always be honored for being able to complete this thesis under their supervision.

I express thanks to Dr. Mirko Fiacchini, researcher at GIPSA-Lab, and Dr. Matthew Turner, Professor at the University of Southampton, for accepting to be examiners of my doctoral thesis. Also, I express thanks to Dr. Jean Marc Biannic, researcher at ONERA and Dr. Gianluca Rizzello, professor at the Saarland University, for accepting to be part of my dissertation jury.

Finally, I express special gratitude the most important people in my life: Ruby, Nestor, Lucila, Reynaldo, Sandra, Alex, María, Paula, Juan Camilo, Sofía, Matías and all the members of my family. After all these years of studies, that one thing that I can claim with all guarantees is that, without you, I would not have been able to get here. From the depths of my soul, thank you!

Contents

List of Figures

Notation

a	generic scalar
$\mathbf{a}$	Optimization decision scalar variable
$\mathrm{Re}(a)$	Real part of the complex number a
A	Generic matrix
$\mathbf{A}$	Optimization decision matrix variable
A^T	Transpose of the matrix A
A^{-1}	Inverse of the invertible matrix A
$A^{-\mathsf{T}}$	Transpose of the invertible matrix A^{-1}
$\lambda(A)$	Set of eigenvalues of the square matrix A
$\lambda_{\max}(A)$	Maximum eigenvalue of the square matrix A
$\lambda_{\min}(A)$	Minimum eigenvalue of the square matrix A
$\lambda_i(A)$	i^{th} eigenvalue of the square matrix A
$\mathrm{He}(A)$	Matrix resulting from the sum $A + A^\mathsf{T}$
$\mathbb{R}^m$	Euclidean space of dimensions m
$\mathbb{D}^m$	Set of diagonal matrices of dimensions $m \times m$
$\mathbb{D}^m_{>0}$ $\left(\mathbb{D}^m_{\geq 0}\right)$	Set of diagonal positive (semi-)definite matrices of dimensions $m \times m$
$\mathbb{S}^m$	Set of symmetric matrices of dimensions $m \times m$
$\mathbb{S}^m_{>0}$ $\left(\mathbb{D}^m_{\geq 0}\right)$	Set of symmetric positive (semi-)definite matrices of dimensions $m \times m$
I_m	Identity matrix of dimensions $m \times m$
0	Null matrix of appropriate dimensions

General introduction

Introductory discussion

Physical and technological limitations of sensors and actuators are intrinsic to real-life control systems: Motors can not give unlimited torque, flaps may not turn indefinitely, ovens have a maximum operating temperature and amplifiers are incapable of producing infinite gains. When a controller demands a signal that is not attainable by the actuator, we say that an actuator saturation occurred. Indeed, actuator saturation may occur not only in magnitude terms, but also in rate terms, i.e. they are not able to respond limitlessly fast. Such actuator limits have been considered to extensively study the behavior of systems subject to input saturation in the last decades, since neglecting the existence of these limitations may produce poor performance or undesirable behaviors of dynamic controlled closed-loop systems, including overshoot, slow convergence or even, in some cases, divergent responses [2], [62]. In general, any real technological application can benefit from accounting the saturation effect, since oversizing actuators may lead to increased construction or operating costs [30].

Historical overview

Throughout the last century, it has been discovered that considering the effects of actuator saturation is especially critical in high-gain systems, such as aircrafts, rockets and power electronic applications. As an example, magnitude and rate actuator limitations where the cause of the Chernobyl nuclear power plant accident [62] and both JAS 39 Gripen crashes in 1989 and 1994 [46]. However, beyond the fast-dynamics systems, the need to mitigate the effects of actuator saturation is already evidenced in works published in the 1950s, years when control systems were implemented by analog controllers [45]. More specifically, it was proposed that a control system should be able to resolve the large signal issues stemming from the saturation, instead of restricting the system dynamics to a small signal dynamics behavior to avoid saturation [45]. Then, it can be concluded that [45] is an early

observation of the nonlinear nature of the saturation phenomenon [18].

These real-life issues motivated the study on the so-called *windup* phenomenon [28], which denotes the performance or stability loss of the control system when saturation events occur, and pushed forward the works on systematic solutions to the windup problem that, naturally, were baptized as *anti-windup* compensations. This research interest continued being extended until the arise of digital control, where some early results were published on anti-windup solutions (see, for example, [16], [1]), evolving into relatively simple conditioning techniques for input-saturated systems [57]. This early core of literature, well summarized in [38], was focused on proposing ad-hoc strategies, thus in those years, there were no rigorous guarantees on stability or performance. It was not until the 1990s that researchers started addressing the anti-windup problem from a nonlinear control systems stability scope and, since then, an extensive literature rigorously analyzing control systems subject to input saturation and addressing synthesis of constrained stabilizing controllers is available.

Today, not only articles, but even books, such as [69], [41] and [65], may be found in the literature addressing these problems and providing *modern* approaches to mitigate the windup phenomenon. Certainly, modern in the sense that they were proposed after the year 2000. Moreover, there are some tutorial papers compiling the modern formal theoretical stability analysis and stabilization, such as [18] and [54]. Indeed, some of the recent works present results based in convex optimization strategies, exploiting Lyapunov methods and linear matrix inequality (LMI) [4] tools that can be easily implemented in algebraic solvers and optimizer software. These anti-windup designs can be roughly classified in tree different strands: The stability analysis, the direct controller synthesis and the anti-windup design.

It has been extensively shown that the presence of saturation in a closed-loop control system can lead to the emergence of parasitic equilibrium points and divergent trajectories (see, e.g., [2], [28] and [65, Example 1.1]). Moreover, it was found in the early 1980s that global asymptotic stability of the closed-loop system requires the uncontrolled input-saturated linear plant not to be exponentially unstable [61] (see also [59] and [63]), a class of systems denoted asymptotically null controllable with bounded controls (ANCBC) [68]. Hence, whenever these requirements are not fulfilled, i.e. when a linear plant is not ANCBC, only regional exponential stability is attainable, and therefore, it is imperative to analyze the closed-loop system in such a way that certain local conditions are satisfied, so that not only regional exponential stability is guaranteed, but also an approximation of the basin of attraction is computed, and possibly maximized. Consequently, stability analysis of saturating controller-plant feedback emerges as a fundamental problem and, in this direction, several works following an LMI approach have proposed certificates of global or regional exponential stability using quadratic Lyapunov functions [6], [30],

[65], nonquadratic Lyapunov functions [37], [43], [39], piecewise quadratic Lyapunov functions [13], [12] and sign-indefinite piecewise quadratic Lyapunov functions [56].

The second strand, the direct controller synthesis problem, addresses the problem of designing a stabilizing controller while simultaneously considering the actuator saturation limits in such a way that global or regional exponential stability of the saturated closed-loop system is guaranteed, depending on whether the plant is AN-CBC or not. Based on Lyapunov functions and LMI methods, this approach has been used to conceive full state-feedback laws with anti-windup compensation, as, for example, in [5], [20], [36] and [68]. Moreover, [11], [19], [22], [48], [49] and [58] have also proposed rigorous methods for the synthesis of dynamic output-feedback controllers with anti-windup compensation term. A common feature of these works is the use of classical quadratic Lyapunov functions or nonquadatic Popov-like Lyapunov functions to certify the closed-loop stability, combined with adequate ways to embed the saturation nonlinearity in a sector description. These specific Lyapunov function structures may lead to numerical conservative results (see, for example, the discussion in [69, Section 4.4.1.1], [12] or [65, Example 3.3]). For this reason, recent efforts have been made to exploit sign-indefinite quadratic forms involving a deadzone nonlinearity, thereby providing piecewise quadratic and piecewise smooth Lyapunov functions [56]. This functions provide sufficient and less conservative LMI conditions, allowing for the synthesis of global and regional stabilizing state-feedbacks [56] and dynamic output-feedback controllers [51], [52].

The last strand, the anti-windup design approach, requires a given pre-computed controller locally stabilizing the saturating closed-loop system and specifying a prescribed (or required) local closed-loop behavior when the saturation is inactive. Thereafter, an anti-windup compensator is synthesized to mitigate the performance, robustness or stability degradation when saturation occurs. Some results based on LMIs and quadratic Lyapunov functions following this approach are presented in [10] and [17] using model recovery anti-windup (MRAW) techniques, and in [7], [9], [21], [24], [23], [26], [27] and [60] exploiting direct linear anti-windup (DLAW) augmentations. Once again, to mitigate the conservativeness arising from the use of quadratic Lyapunov functions, [47] developed design methods for DLAW compensators using piecewise quadratic Lyapunov functions and, more recently, [55] and [50] proposed positivity-relaxed approaches using the sign-indefinite quadratic forms of [56] to compute the gains of a linear static anti-windup scheme while certifying, respectively, global and regional exponential stability.

Manuscript overview

As compared to traditional quadratic and piecewise quadratic Popov-like approaches, the sign-indefinite quadratic forms presented in [56] may produce less

conservative results due to:

1. the use of the information on the gradient of the nonlinearity [12], [44], and
2. the relaxed positivity conditions for the ensuing piecewise smooth Lyapunov functions stemming from the use of appropriate sector properties of the nonlinearity [56].

Therefore, this manuscript exploits the versatility of the piecewise smooth nonquadratic Lyapunov functions constructed with the sign-indefinite quadratic forms of [56] to develop regional and global stability certificates. We provide novel conditions with reduced conservativeness in the form of LMIs, for the design of dynamic output-feedback controllers [51], [52] for an input-saturated plant, and in the form of bilinear matrix inequalities (BMIs), for the synthesis of a static linear anti-windup compensators [50], [55] implementing a prescribed linear controller that locally stabilizes the linear closed-loop system. While LMIs can be directly implemented in numerical solvers, in this manuscript we propose an iterative algorithm based on a convex-concave decomposition inspired by [15] to solve each one of the problems encompassing BMI conditions.

This manuscript is organized as follows. First, some fundamental concepts around stability are recalled in Chapter 1, such as the definitions of Lyapunov stability of linear and nonlinear systems and the domain of attraction. Afterwards, Chapter 2 defines the open-loop and closed-loop systems subject to actuator saturation with the help of state-space representations. Moreover, here we present some elements intimately linked to systems subject to input saturation, such as the regions of linearity and saturation, the consequences of bounded controllability, the windup phenomenon and the algebraic loops that may be induced when the control loop is closed. All the previous definitions are introduced to delve, in Chapter 3, into the motivations of this thesis and the problems addressed in this manuscript. Chapter 3 continues by presenting the sign-indefinite quadratic forms of [56] used to obtain the results of this work.

The novel results found during this research work are presented subsequently. Indeed, Chapter 4 establishes novel sufficient LMI conditions for the synthesis of dynamic output-feedback controllers for input-saturated plants, presented in [51] and [52]. More specifically, [51], compiled in Section 4.3.2, addresses the case of exponentially stable plants constructing output-feedback design procedures that use piecewise quadratic Lyapunov functions derived from the sign-indefinite quadratic forms of [56] to certify global exponential stability of the saturated closed loop. Using again the sign-indefinite quadratic forms of [56], Section 4.3.1, which analyzes [52] in detail, exploits a piecewise smooth Lyapunov function to construct regional stabilizing dynamic output-feedback controllers while maximizing estimates of the domain of attraction.

On the other hand, Chapter 5 proposes four novel algorithms allowing to compute the gains of static linear anti-windup schemes while ensuring global or regional exponential stability and a minimum convergence rate through sufficient BMI conditions stemming from sign-indefinite piecewise quadratic and sign-indefinite piecewise smooth Lyapunov functions based on the sign-indefinite quadratic forms of [56]. Such certificates and algorithms have been published in [50] and [55]. For the regional results, the algorithms presented in Section 5.3.1 also use the procedures exposed in [50] which allow maximizing the piecewise quadratic estimate of the basin of attraction for the saturated controller-plant feedback. Finally, general conclusions of the work results are given, together with different interesting perspectives and challenges for future work.

Chapter 1

Preliminary concepts

1.1 Introduction

Stability is arguably one of the fundamental concepts that need to be embraced to study control systems and their properties. This chapter focuses on recalling the stability in the sense of Lyapunov, and more specifically, the principles of the second method of Lyapunov. Afterwards, based on these concepts, the definitions of the basin of attraction and the region of stability are given. At the end of this chapter, we present the application of these concepts to linear control systems.

The elements defined along this chapter are rather fundamental, and, therefore, they can be found in classical linear and nonlinear control theory bibliography, as, for example, in the books of Khalil [37] and Goodwin [25]. Nevertheless, they are summarized here since they are necessary to understand the methods used to obtain the results presented in the following chapters, in terms of stability analysis or controller design for linear systems subject to input saturation.

1.2 Stability in the sense of Lyapunov

In general terms, the Lyapunov stability consist in showing that all the trajectories starting near an equilibrium point stay nearby. In such a case, we say that the equilibrium point is stable, and otherwise, that it is unstable. The notions of equilibrium point and trajectory are introduced later in this section, since, before delving into these definitions, it is necessary to contemplate some preceding elements. First, introduce the concept of Lipschitz continuity.

Definition 1.1: Given an open set $\mathcal{D} \in \mathbb{R}^n$, a function $V : \mathcal{D} \mapsto \mathbb{R}$ is Lipschitz continuous in $\mathcal{D}$ if, for each $x \in \mathcal{D}$, there exist positive scalars k and ε such that,

for each $y \in \mathbb{R}^n$,

$$|y - x| \leq \varepsilon \Rightarrow |V(y) - V(x)| < k|y - x|. \tag{1-1}$$

Consider the autonomous system

$$\dot{x} = f(x), \tag{1-2}$$

where $f : \mathcal{D} \mapsto \mathbb{R}^n$ is a locally Lipschitz function from $\mathcal{D} \subseteq \mathbb{R}^n$ to $\mathbb{R}^n$. Define then an equilibrium point as follows.

Definition 1.2: The state $\bar{x}$ is an equilibrium point of (1-2) if $f(\bar{x}) = 0$.

Furthermore, the definitions and theorems presented in this chapter are stated considering the following assumption.

Assumption 1.1

System (1-2) has an equilibrium at the origin $x = 0$. In other words, $f(x)$ satisfies $f(0) = 0$.

As shown in [37, Section 4.1], Assumption 1.1 does not produce any loss of generality in the study of the stability of any equilibrium point of system (1-2). Denote with $\phi(t, x_0)$ the solution (or trajectory) of the system (1-2) corresponding to the initial state $x(0) = x_0$ as a function of time t. This solution is unique due to the Lipschitz property of f. Then, the stability of an equilibrium point is defined as follows.

Definition 1.3: The origin of the system (1-2) is

- Lyapunov stable, if for each $\varepsilon > 0$, there exist $\delta = \delta(\varepsilon) > 0$ such that
$$|x_0| < \delta \Rightarrow |\phi(t, x_0)| < \varepsilon$$
for all $t \geq 0$.
- Asymptotically stable, if it is stable and, moreover, δ can be selected in such a way that
$$|x_0| < \delta \Rightarrow \lim_{t \to \infty} |\phi(t, x_0)| = 0.$$
- Globally asymptotically stable, if $\lim_{t \to \infty} |\phi(t, x_0)| = 0$ holds for any $x_0 \in \mathbb{R}^n$.
- Unstable, if it is not Lyapunov stable.

Definition 1.3 implies that the origin of the dynamic system (1-2) is Lyapunov stable if the trajectory $\phi(t, x_0)$, with $|x_0| < \delta$, stays in the neighborhood

$$\mathcal{D}(\varepsilon) = \{x \in \mathbb{R}^n : |x| \leq \varepsilon\} \tag{1-3}$$

for all $t \geq 0$. If, additionally, the trajectory $\phi(t, x_0)$ tends to the origin as t tends to ∞, then the origin $x = 0$ is asymptotically stable. On the contrary, if for any $\varepsilon > 0$ there exists always a solution $\phi(t, x_0)$ that leaves $\mathcal{D}(\varepsilon)$ in (1-3), then the origin of the system (1-2) is unstable.

The stability certificates that will be presented in Chapters 4 and 5 ensure not only Lyapunov stability but *exponential stability*, which is a special case of asymptotic stability. Exponential stability is define as follows.

Definition 1.4: The origin of system (1-2) is exponentially stable if there exist positive scalars α, δ and k such that

$$|x_0| < \delta \Rightarrow |\phi(t, x_0)| < ke^{-\alpha t}|x_0|$$

for all $t \geq 0$.

Definitions 1.3 and 1.4 certainly require solutions $\phi(t, x_0)$ to be defined for all $t \geq 0$, which may not be true in some cases. This means that Definitions 1.3 and 1.4 usually can not be directly applied to analyze the stability of an equilibrium point. Fortunately, the *Lyapunov's second method*, proposed by Aleksandr Lyapunov in 1882, ensures the global existence of these solutions and, further, proposes a generalized way to analyze the stability of an equilibrium point.

1.2.1 Lyapunov's second method

Broadly speaking, Lyapunov's second method consists in showing that there exists a positive-definite function of the states of a dynamical system that decreases along this latter's trajectories, similar as, for example, the energy in mechanical or electrical systems, where the presence of non-conservative acting forces yields to energy dissipation in form of heat or noise. This means that, although the analytic identification of all the trajectories $\phi(t, x_0)$ remains an open problem, we may use Lyapunov's second method to analyze the stability of an equilibrium point without having any explicit determination of the trajectories at the neighborhood of the origin. The next theorem presents the sufficient conditions that ensure the stability of the origin of system (1-2) in a neighborhood $\mathcal{D}$ containing the state $x = 0$.

Theorem 1.1

[37, Theorem 4.1] *Regional stability.* Let the origin $x = 0$ be an equilibrium point of system (1-2), $\mathcal{D} \subset \mathbb{R}^n$ be an open set containing $x = 0$ and the function $V : \mathcal{D} \mapsto \mathbb{R}$ be a continuously differentiable function in $\mathcal{D}$. If

a) $V(0) = 0$, $V(x) > 0$ for all $x \in \mathcal{D} \setminus \{0\}$ and
b) $\dot{V}(x) \leq 0$ for all $x \in \mathcal{D}$,

then the origin of (1-2) is Lyapunov stable. Moreover, if

c) $\dot{V}(x) < 0$ for all $x \in \mathcal{D} \setminus \{0\}$,

then the origin of (1-2) is asymptotically stable from $\mathcal{D}$.

Definition 1.5: Any function V satisfying the conditions *b)* and *c)* in Theorem 1.1 is called a *Lyapunov function* for system (1-2).

The set $V(x) = c$, for some $c > 0$, is called a Lyapunov level set, and condition *c)* of Theorem 1.1 implies that, when a trajectory $\phi(t, x_0)$ crosses a Lyapunov level set $V(x) = c$, it does not leave the sublevel set $\Omega_c := \{x \in \mathbb{R}^n : V(x) \leq c\}$.

Of course, the local stability result proposed in Theorem 1.1 can be extended to determine global asymptotic stability conditions, which ensure that, for any initial state x_0 in the state-space $\mathbb{R}^n$, all the solutions $\phi(t, x_0)$ converge to the origin. Although intuitively considering that Theorem 1.1 ensures global asymptotic stability when $\mathcal{D} = \mathbb{R}^n$, this is not the case because radial unboundedness of V is also required for the global stability problem. With this in mind, the next theorem provides sufficient conditions for global asymptotic stability.

Theorem 1.2

[37, Theorem 4.2] *Global stability.* Let the origin $x = 0$ be an equilibrium point of the system (1-2) and function $V : \mathbb{R}^n \mapsto \mathbb{R}$ be a continuously differentiable function. If

a) $V(0) = 0$, $V(x) > 0$ for all $x \neq 0$,
b) $|x| \to \infty \Rightarrow V(x) \to \infty$ and
c) $\dot{V}(x) < 0$ for all $x \in \mathbb{R}^n \setminus \{0\}$,

then the origin of (1-2) is globally asymptotically stable.

It is important to remark that Theorems 1.1 and 1.2 provide *sufficient* conditions for regional and global asymptotic stability. This means that not finding a Lyapunov function leads to inconclusive results on stability, and, consequently, an autonomous system (1-2) may be regionally or globally asymptotically stable even though no Lyapunov function was found. Therefore, the main challenge stemming from applying these theorems relies on finding a function V that actually satisfies the conditions for global or regional stability. In the particular case of physical systems models, the energy function usually satisfies these conditions and may be often used as a Lyapunov function, but, for some abstract cases, the selection of function V may become a challenging task, and different selections of function V may lead to different stability analysis results.

The results presented in [14] turn out to be especially advantageous for the selection of a Lyapunov function, since they may be exploited to construct a broad class of Lyapunov functions. In fact, the continuous differentiability of V required in Theorems 1.1 and 1.2 can be relaxed into Lipschitz continuity. This result will be further made precise in Section 3.4.2 and, as an example, it allows to construct stability certificates based on piecewise smooth Lyapunov functions.

1.2.2 The basin of attraction

Even though determining if an equilibrium point is Lyapunov stable is useful, there is further information on stability that we might desire to extract. This is the case of the domain of attraction of the system (1-2), which allows us to determine the set of initial states generating solutions that converge to the origin. In fact, this is directly related to the definition of the *basin of attraction* of the origin.

Definition 1.6: Consider the autonomous system (1-2). The basin of attraction of the origin of (1-2) is the set of initial states $x_0 = x(0) \in \mathbb{R}^n$ such that the trajectories $\phi(t, x_0)$ converge to the origin. Rigorously speaking, the basin of attraction is defined as

$$\mathcal{R}_A := \{x_0 \in \mathbb{R}^n : t \to \infty \Rightarrow \phi(t, x_0) \to 0\}. \tag{1-4}$$

Based on Definition 1.6, it is immediate to note that if the autonomous system (1-2) is globally asymptotically stable, then $\mathcal{R}_A = \mathbb{R}^n$. However, when (1-2) is not globally asymptotically stable but regionally asymptotically stable, the analytical determination of $\mathcal{R}_A$ remains an open problem, generally difficult and, in some cases, impossible [65].

Figure 1.1 shows a phase plane with several trajectories and illustrates the non-trivial nature of the basin of attraction of the origin for a nonlinear system with three equilibrium points. For all $t \in [0, 50]$, notice that the trajectories $\phi\big(t, \left[8, -1\right]^\mathsf{T}\big)$ and $\phi\big(t, \left[4, 1\right]^\mathsf{T}\big)$ belong to the basin of attraction $\mathcal{R}_A$ of the origin of the system, while $\phi\big(t, \left[3, -2\right]^\mathsf{T}\big)$ belongs to the basin of attraction of the equilibrium point $\left[-2, 1\right]^\mathsf{T}$ and, as far as the simulation allows us to see, $\phi\big(t, \left[5, -3\right]^\mathsf{T}\big)$ and $\phi\big(t, \left[4, 4\right]^\mathsf{T}\big)$ diverge.

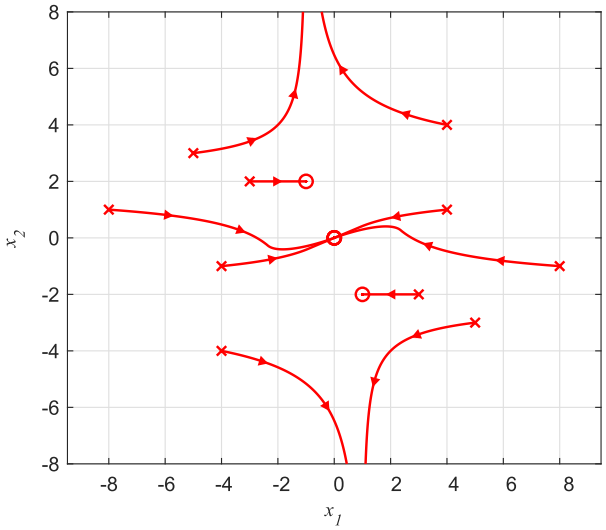

Figure 1.1: Presence of converging and diverging trajectories for a nonlinear system with multiple equilibrium points. Initial conditions ($\times$) and equilibrium points ($\circ$).

1.3 Linear systems stability

Linear systems are a particular class of dynamical systems, where the *principle of superposition* holds. This principle implies that any response obtained from the sum of k initial conditions is equal to the sum of the k responses obtained separately from the k initial conditions. Following the state-space modeling regular notation, consider the linear time-invariant system

$$\dot{x} = Ax, \tag{1-5}$$

where $x \in \mathbb{R}^n$. Assume that $\det(A) \neq 0$. Then, the unique equilibrium point of system (1-5) is the origin, since exactly and only $x = 0$ verifies

$$\dot{x} = A \cdot 0 = 0.$$

Recall that, for any initial state $x_0 = x(0) \in \mathbb{R}^n$, the solution of system (1-5) at a time t is

$$\phi(t, x_0) = e^{At} x_0 \tag{1-6}$$

Recall also from linear control theory (see, for example, [25]) that some properties of the solutions of the linear time-invariant system (1-5), including stability and time response, can be determined by observing the eigenvalues of matrix A. Regarding asymptotic stability, it is possible to state the following theorem.

Theorem 1.3

[37, Theorem 4.5] The equilibrium point $x = 0$ of the linear time-invariant system (1-5) is

- Globally asymptotically stable, if and only if $\mathrm{Re}(\lambda_{\max}(A)) < 0$.
- Unstable, if $\mathrm{Re}(\lambda_{\max}(A)) > 0$.

When all the eigenvalues of A satisfy $\mathrm{Re}(\lambda_i(A)) < 0$, we say that matrix A is Hurwitz. Then, exploiting Theorem 1.3, it is possible to state that the origin of (1-5) is globally exponentially stable if and only if A is Hurwitz. Moreover, since the solution (1-6) of the system (1-5) has an exponential form and is homogeneous, then the origin of (1-5) is also exponentially stable whenever it is locally asymptotically stable. Therefore, the stability of the linear system may be determined by observing the maximum eigenvalue of A, i.e. $\lambda_{\max}(A)$, which is usually known as the *dominant eigenvalue*.

Remark 1.1: The origin of linear system (1-5) may be Lyapunov stable if, for all $i = 1, \cdots, n$, $\mathrm{Re}(\lambda_i(A)) \leq 0$ and certain conditions on the algebraic multiplicity of the eigenvalues of A with real part equal to zero are satisfied. However, since global exponential stability is not obtainable when, for any $i = 1, \cdots, n$, $\mathrm{Re}(\lambda_i(A)) = 0$, this case is out of the scope of this work.

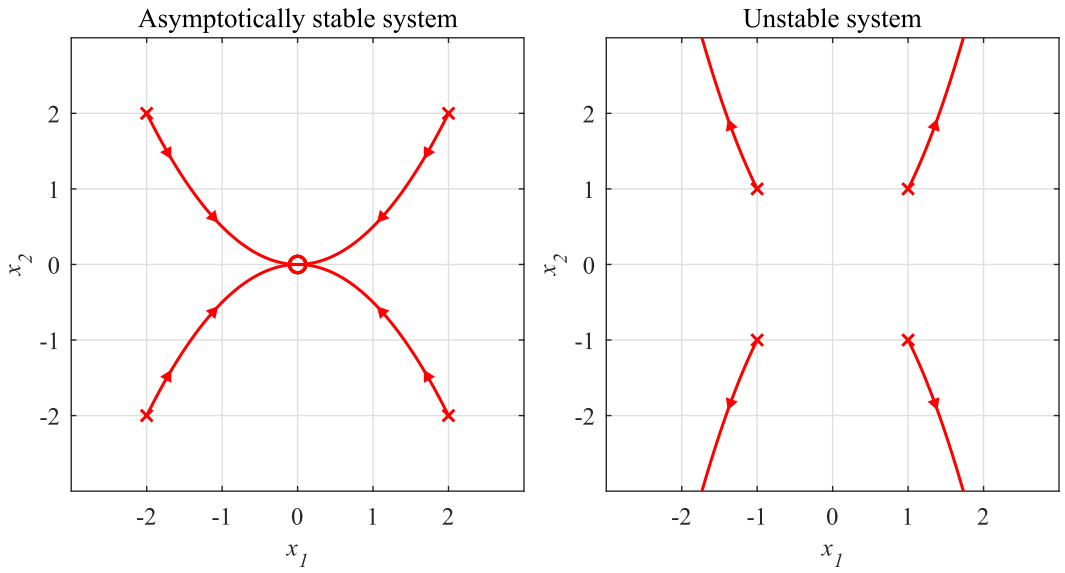

Figure 1.2: Examples of the trajectories of asymptotically stable and unstable linear systems.

Figure 1.2 illustrates the stability of linear systems. Following the definition of a linear system given in (1-5), it shows the trajectories $\phi(t, x_{0(i)})$, with $i = 1, \cdots, 4$, for:

- at the left, an asymptotically stable linear system, with a matrix A having eigenvalues $\lambda(A) = \{-1, -2\}$, from the initial states $x_{0(i)} = \begin{bmatrix} \pm 2 & \pm 2 \end{bmatrix}^\mathsf{T}$ and
- at the right, an unstable linear system, with a matrix A with eigenvalues $\lambda(A) = \{1, 2\}$, from the initial states $x_{0(i)} = \begin{bmatrix} \pm 1 & \pm 1 \end{bmatrix}^\mathsf{T}$.

The stability analysis based on eigenvalues may be also carried out with different strategies, such as Routh's Algorithm or Nyquist analysis. Nevertheless, these methods are not introduced in this manuscript since they are not used this thesis.

1.4 Summarizing comments

The definition of Lyapunov stability was introduced, together with the definition of exponential stability. Since the analytical determination of the trajectories of the system is rather hard, and sometimes impossible, we presented the second method of Lyapunov to study global or regional asymptotic stability of an equilibrium point. The concept of domain of attraction was also discussed. We introduced also some results for the stability analysis linear time-invariant systems, for which the Hurwitz property of the state matrix of the system is necessary to ensure global exponential stability. The definitions presented in this chapter are necessary to develop the constrictive methods for input-saturated linear systems in Chapters 4 and 5.

Chapter 2

Linear systems subject to actuator saturation

2.1 Introduction

Certainly, linear systems subject to input saturation can also be studied by using the state-space modeling, which, indeed, is one of the most common modeling approach in control engineering to develop analytical and constructive stability conditions. In this chapter, we introduce the concept of linear plant subject to input saturation in Section 2.2.1, and then, we present the controller forms used in this manuscript in Section 2.2.2. With these definitions, the controller-plant closed-loop system state-space model is given. Furthermore, in Section 2.2.1 we also depict the mathematical model of the saturation nonlinearity used in this research.

In Section 2.3, we focus the properties of the input-saturated systems. First, in Sections 2.3.1 and 2.3.2, we define some fundamental implications stemming from the saturation limits, such as the presence of bounded controllability and the appearance of regions of linearity and regions of saturation. Then, Section 2.3.3 discuss the issues on the stability and performance of the controller-plant saturated feedback, and proposes the implementation of a linear compensator to mitigate the appearing degradations. Except for the cases where it is explicitly specified, the concepts, definitions and results presented here can be found in [65], [69] and references therein.

2.2 Saturated systems control modeling

The linear systems subject to saturating inputs can be simultaneously described as linear and nonlinear systems. Regarding the open-loop system, it remains linear despite having a nonlinear input. However, it is shown later that, when the feedback

loop is closed, the closed-loop system follows a linear behavior in a certain region where the saturation is inactive, but the linearity property is lost when the loop feedback is closed and actuator saturation occurs.

2.2.1 The open-loop linear system

Suppose that the control signal u is subject to upper and lower magnitude constraints in the plant input, simulating a saturating actuator. Then, the linearity of the open-loop system can be straight evinced by considering the linear plant subject input saturation

$$\left| \begin{array}{ll} \dot{x}_{\mathrm{p}} & = A_{\mathrm{p}} x_{\mathrm{p}} + B_{\mathrm{p}} \mathrm{sat}\left(u\right) \\ y & = C_{\mathrm{p}} x_{\mathrm{p}} + D_{\mathrm{p}} \mathrm{sat}\left(u\right) \end{array} \right. , \tag{2-1}$$

where $x_{\mathrm{p}} \in \mathbb{R}^{n_{\mathrm{p}}}$ is the state vector of the plant, $y \in \mathbb{R}^{p}$ corresponds to the measured output and $u \mapsto \mathrm{sat}\left(u\right)$ denotes the decentralized asymmetric saturation function whose components are

$$\mathrm{sat}_{i}\left(u_{i}\right) := \max\left\{-\underline{u}_{i}, \min\left\{\overline{u}_{i}, u_{i}\right\}\right\}, \tag{2-2}$$

with lower saturation limits $\underline{u}_{i} > 0$ and upper saturation limits $\overline{u}_{i} > 0$ for all $i = 1, ..., m$; $\underline{u}_{i}$, $\overline{u}_{i}$ and u_{i} being the i^{th} entry of vectors $\underline{u}$, $\overline{u}$ and u, respectively. A depiction of the symmetric saturation function is shown in Figure 2.1, in which the upper limits and lower limits have the same absolute value, or $\underline{u} = \overline{u}$.

2.2.2 The controller-plant feedback

In order to improve the behavior or performance of the input-saturated plant, we may let a controller handle the input signals of the plant. It is important to remark that real-world actuators usually transduce the input magnitude into a different output physical quantity. For example, a DC motor transduces an electric field into mechanical movement, and a microphone converts air vibrations into electric signals. However, for simplicity, we consider that the actuator has no dynamics and that it is only represented by a saturation map. Therefore, the controller presented here takes the input signal, which turns out to be the output signal of the plant y, to compute the output signal u. Thereafter, this control signal u is injected into a saturation mapping to produce the signal $\mathrm{sat}\left(u\right)$.

Furthermore, introduce the deadzone function $\mathrm{dz}\left(u\right) := u - \mathrm{sat}\left(u\right)$. The figure 2.2 shows the symmetric deadzone function. Then, it is possible to set up two control strategies: a state-feedback controller and an output-feedback controller. Depending on the selected control law, stabilizability of plant (2-1) requires different necessary conditions, evoked below. Besides, for both control strategies, the closed-

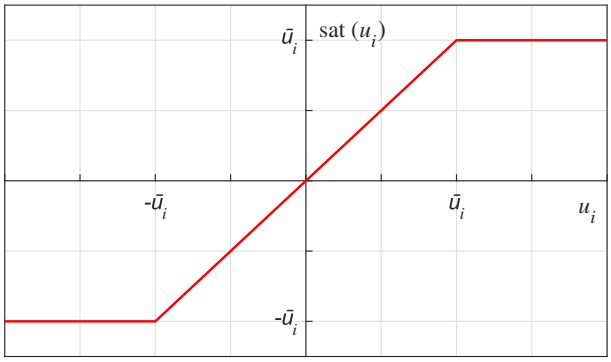

Figure 2.1: The symmetric saturation function.

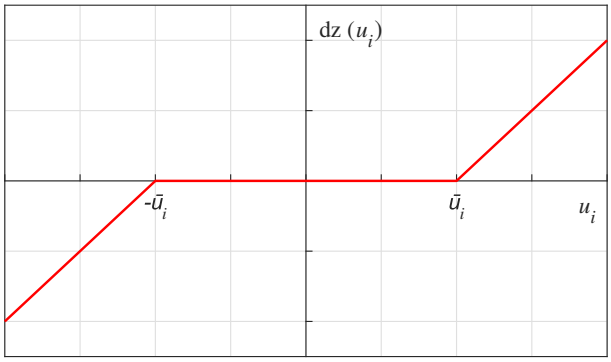

Figure 2.2: The symmetric deadzone function.

loop dynamics may be compactly written as

$$\left| \begin{array}{l} \dot{x} = Ax + B\mathrm{dz}\,(u) \\ u = Cx + D\mathrm{dz}\,(u) \end{array} \right. , \tag{2-3}$$

where the definition of the state vector x and the matrices A, B, C and D depends on the selected control law, as verified in the next two sections.

State-feedback control modeling

Assume that the plant (2-1) is observable and stabilizable. Then, considering the state-feedback control law

$$| \, u = K_1 x_\mathrm{p} + K_2 \mathrm{dz}\,(u)\,, \tag{2-4}$$

with output $u \in \mathbb{R}^m$, the closed-loop system stemming from the controller (2-6) and plant (2-1) is nonlinear due to the presence of the actuator saturation in the controller output. Moreover, for the purposes of this work, a control augmentation is implemented with the term $K_2\mathrm{dz}\,(u)$ in the state feedback controller (2-4). The advantages of applying this control augmentation, called anti-windup compensation, are explained in Section 2.3. Figure 2.3 presents the block diagram of the controller-plant feedback. Moreover, note that whenever $K_2 \neq 0$, the presence of the deadzone function in the state-feedback control law (2-4) induces an algebraic loop, whose well-posedness is required to be able to ensure the existence of a unique (piece-

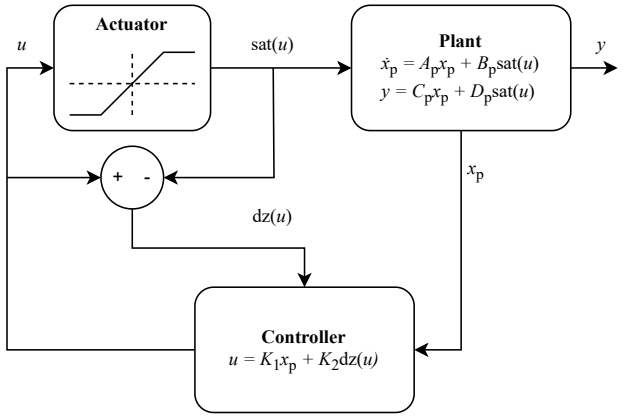

Figure 2.3: The state-feedback controller-plant closed-loop system.

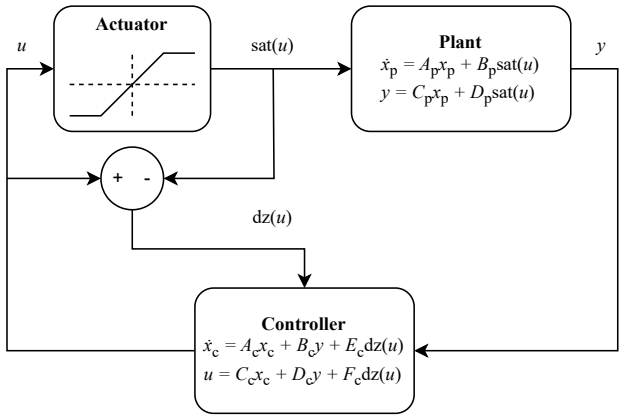

Figure 2.4: The output-feedback controller-plant closed-loop system.

wise affine) solution $x_p \mapsto v(x_p)$ to equation (2-4) [70]. The sufficient conditions guaranteeing well-posedness of this algebraic loop are addressed in Section 2.3 and can be originally found in [70] and [3, Proposition 1].

Hence, combining (2-4) and (2-1), the dynamics of the controller-plant closed-loop system are given by (2-3), with

$$x := x_\mathrm{p}, \quad A := A_\mathrm{p} + B_\mathrm{p} K_1, \quad B := B_\mathrm{p}(K_2 - I_m), \quad C := K_1, \quad D := K_2. \tag{2-5}$$

Ouptut-feedback control modeling

Assume that the plant (2-1) is detectable and stabilizable. Then, by setting up an unconstrained linear feedback control law

$$\left| \begin{array}{rl} \dot{x}_\mathrm{c} &= A_\mathrm{c} x_\mathrm{c} + B_\mathrm{c} y + \nu_x \\ u &= C_\mathrm{c} x_\mathrm{c} + D_\mathrm{c} y + \nu_u \end{array} \right. , \tag{2-6}$$

with state vector $x_\mathrm{c} \in \mathbb{R}^{n_\mathrm{c}}$ and output $u \in \mathbb{R}^m$, the resulting closed-loop system turns out to be certainly nonlinear and its dynamics are directly affected by the presence of the actuator saturation. Following [69, Section 4.2], the controller-plant feedback resulting from (2-1) and (2-6) is well-posed if and only if there exist the

matrix inverses

$$\begin{aligned} \Delta_u &= (I_m - D_\mathrm{c} D_\mathrm{p})^{-1} \ , \\ \Delta_y &= (I_q - D_\mathrm{p} D_\mathrm{c})^{-1} \ , \end{aligned} \tag{2-7}$$

where Δ_u exists if and only if Δ_y exists.

As in the state-feedback control law (2-4), an anti-windup augmentation may be implemented with the terms ν_x and ν_u, which are selected as

$$\begin{aligned} \nu_x &:= E_\mathrm{c} \mathrm{dz}\,(u) \ , \\ \nu_u &:= F_\mathrm{c} \mathrm{dz}\,(u) \ . \end{aligned} \tag{2-8}$$

As in the state-feedback control case, an algebraic loop is also induced when F_c is not null for the output-feedback control strategy, and well-posedness is a necessary condition for the existence of a unique solution $x \mapsto v(x)$ to the output equation in (2-6) [70]. Figure 2.4 presents the block diagram of the controller-plant feedback. The nonlinear dynamics of the closed-loop system derived from (2-1), (2-6) and (2-8) are given by the compact system (2-3), with the extended state vector $x := \begin{bmatrix} x_\mathrm{p}^\mathsf{T} & x_\mathrm{c}^\mathsf{T} \end{bmatrix}^\mathsf{T} \in \mathbb{R}^n$, $n = n_\mathrm{p} + n_\mathrm{c}$ and

$$\left[\begin{array}{c|c} A & B \\ \hline C & D \end{array}\right] := \left[\begin{array}{cc|c} A_\mathrm{p} + B_\mathrm{p}\Delta_u D_\mathrm{c} C_\mathrm{p} & B_\mathrm{p}\Delta_u C_\mathrm{c} & -B_\mathrm{p}\Delta_u + B_\mathrm{p}\Delta_u F_\mathrm{c} \\ B_\mathrm{c}\Delta_y C_\mathrm{p} & A_\mathrm{c} + B_\mathrm{c}\Delta_y D_\mathrm{p} C_\mathrm{c} & E_\mathrm{c} + B_\mathrm{c}\Delta_y D_\mathrm{p}\,(F_\mathrm{c} - I_m) \\ \hline \Delta_u D_\mathrm{c} C_\mathrm{p} & \Delta_u C_\mathrm{c} & I_m + \Delta_u\,(F_\mathrm{c} - I_m) \end{array}\right] . \tag{2-9}$$

2.3 Properties of saturated systems

2.3.1 Bounded controllability and stabilization

The concepts and definitions compiled in this section may be found in [61], [40] and [65]. Introduce the linear plant

$$\left|\begin{aligned} \dot{x}_\mathrm{p} &= A_\mathrm{p} x_\mathrm{p} + B_\mathrm{p} v \\ y &= C_\mathrm{p} x_\mathrm{p} + D_\mathrm{p} v \end{aligned}\right. , \tag{2-10}$$

with state $x_\mathrm{p} \in \mathbb{R}^{n_p}$, input $v \in \mathbb{R}^m$ and output $y \in \mathbb{R}^p$. Then, considering (2-10), the following assumptions are made.

Assumption 2.1

The pairs $(A_\mathrm{p}, B_\mathrm{p})$, $(C_\mathrm{p}, A_\mathrm{p})$ of the plant (2-10) are stabilizable and detectable, respectively.

Assumption 2.2

The input v is restricted to the compact set

$$\mathcal{U}(I_m) := \{v \in \mathbb{R}^m : -\underline{u} \leq v \leq \overline{u}\}, \tag{2-11}$$

where $-\underline{u} \leq v \leq \overline{u}$ is a component-wise inequality and $\underline{u} \in \mathbb{R}^m$, $\overline{u} \in \mathbb{R}^m$ have positive components.

Once the control signal is restricted to $\mathcal{U}(I_m)$, the characterization of the trajectories that converges to the origin despite using bounded control signals becomes a major issue, leading to the concept of *null-controllable region* [61].

Definition 2.1: Considering the plant (2-10), a state x_0 is a null-controllable state of the plant (2-10) if there exist a finite time t_{ss} and an admissible control signal $v(t) \in \mathcal{U}(I_m)$, $\forall t \in [0, t_{ss}]$ such that, for an initial state $x_p(0) = x_0$,

$$\lim_{t \to t_{ss}} \phi(t, x_0) = 0. \tag{2-12}$$

Definition 2.2: The null-controllable region of plant (2-10) is defined as the set of null-controllable states of the same plant.

Moreover, we say that:

Definition 2.3: The linear plant (2-10) is null-controllable if the region of null-controllability is equal to $\mathbb{R}^n$ [40].

Note that plant (2-10) with input v restricted to the compact set $\mathcal{U}(I_m)$ is equivalent to plant (2-1) due to the definition of the saturation mapping in (2-2). It may be proven that, due to Definition 2.3, global exponential stability of the closed-loop system (2-3) is obtainable if and only if the state matrix A_p of the input-saturated plant (2-1) is Hurwitz, while local exponential stability holds whenever A_p is not Hurwitz but A in (2-3) is Hurwitz.

2.3.2 Regions of linearity and saturation

Consider the controller-plant saturated feedback (2-3) and the definition of the saturation function in (2-2). For the states close to the origin, the control signal is not saturated, thus

$$\mathrm{dz}\,(u) = 0$$

and the dynamics of the state of the closed-loop system are given by

$$\left| \begin{array}{l} \dot{x} = Ax \\ u = Cx \end{array} \right. . \tag{2-13}$$

Therefore, we can define the region of linearity as follows.

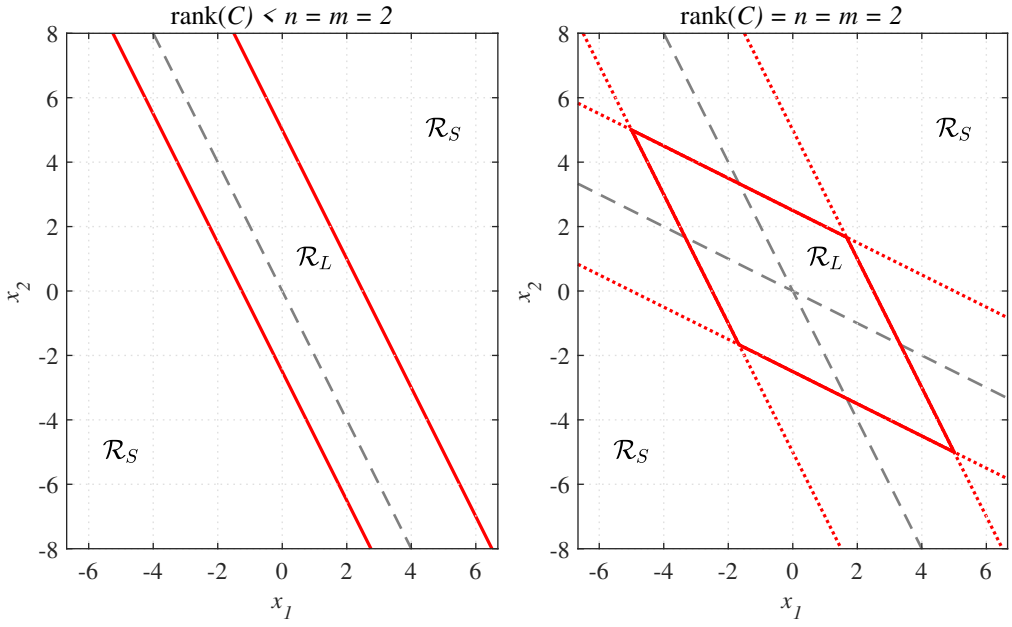

Figure 2.5: The asymmetric unbounded (in the left) and symmetric bounded (in the right) regions of linearity $\mathcal{R}_L$ and saturation $\mathcal{R}_S$ with matrix $D = 0$.

Definition 2.4: The region of linearity $\mathcal{R}_L$ of the closed-loop system (2-3) is defined as the set of states $x \in \mathbb{R}^n$ such that $\text{sat}\,(u) = u$.

The region of linearity can be also defined as the intersection of the half-spaces

$$\mathcal{R}_i^{\max} = \{x \in \mathbb{R}^n : u_i \leq \overline{u}_i\},$$
$$\mathcal{R}_i^{\min} = \{x \in \mathbb{R}^n : u_i \geq \underline{u}_i\},$$

with $i = 1, \cdots, m$, which is equivalent to

$$\mathcal{R}_L = \mathcal{R}_i^{\max} \cap \mathcal{R}_i^{\min}. \tag{2-14}$$

With this definition, it is possible to observe that the region $\mathcal{R}_L$

- is symmetric if $\underline{u} = \overline{u}$, and asymmetric otherwise.
- is bounded if $\text{rank}(C) = n$ and unbounded if $\text{rank}(C) < n$, where the matrix C is the output matrix of the closed-loop system (2-3).

Furthermore, the region of saturation $\mathcal{R}_S$ can be straight defined as

$$\mathcal{R}_S := \mathbb{R}^n \setminus \mathcal{R}_L, \tag{2-15}$$

since the region of linearity encompasses all the states x in which the saturation is inactive. Figure 2.5 illustrates the linearity and saturation regions, together with the two properties described above.

Since the closed-loop system dynamics in the region of linearity are linear, it is possible to adapt the next theorem, presented and proven in [65, Theorem 1.1], which

proposes some guarantees about the trajectories of the controller-plant feedback (2-3) from a initial state contained in any subset of the region of linearity.

Theorem 2.1

[65, Theorem 1.1] If the matrix A of system (2-3) is Hurwitz, then there always exists a set $\mathcal{S}_L$ for which the following properties hold:

1. $\mathcal{S}_L \subseteq \mathcal{R}_L$,
2. $\forall x_0 \in \mathcal{S}_L$, $\phi(t, x_0)$ is a trajectory of the linear system (2-13) and
3. $\forall x_0 \in \mathcal{S}_L$, the trajectory $\phi(t, x_0)$ asymptotically converges to the origin.

Furthermore, any positive invariant set contained in the region of linearity can be considered as a region $\mathcal{S}_L$.

2.3.3 The windup phenomenon

Physical control systems are usually limited by the actuator capabilities. Consequently, most control systems may suffer a degradation in performance, robustness or stability when actuator saturation occurs in the plant input. This well-known phenomenon is called "windup" [28], [29]. One of the most known windup events in the control domain is the integral windup, in which the saturation nonlinearity produces excessively large error values in the integrator component of PID controllers, thus slowing down and overshooting the output response of the feedback control loop system [1].

Perhaps one of the simplest solutions to eliminate the windup effects is to invest in less-restrictive actuators, so that saturation occurs less frequently or never occurs. However, the windup phenomenon can also be mitigated by implementing a controller design augmentation, namely an anti-windup compensation, a filter that is typically activated when the actuator is saturated and relieves the saturation effects. In controllers (2-4), the anti-windup component is represented by the nonlinear term $K_2\mathrm{dz}\,(u)$ while, in controller (2-6), it is represented by the terms $\nu_x = E_\mathrm{c}\mathrm{dz}\,(u)$ and $\nu_u = F_\mathrm{c}\mathrm{dz}\,(u)$, as selected in (2-8). Among other results, this thesis provides different guidelines, strategies and algorithms to synthesize the static gains E_c and F_c (see Chapter 3 for the description of the design problems and Chapters 4 and 5 for the results). The following examples depict the effectiveness of the static linear anti-windup scheme in mitigating the windup effects.

Example 2.1: Academic example. Consider the following saturated system with $\bar{u} = 0.5$, state-space model plant matrices

$$A_\mathrm{p} = \begin{bmatrix} -1 & 0 \\ 0 & 0.1 \end{bmatrix}, \qquad B_\mathrm{p} = \begin{bmatrix} 1 \\ 1 \end{bmatrix}, \qquad C_\mathrm{p} = \begin{bmatrix} 1 & 1 \end{bmatrix}, \qquad D_\mathrm{p} = 0 \tag{2-16}$$

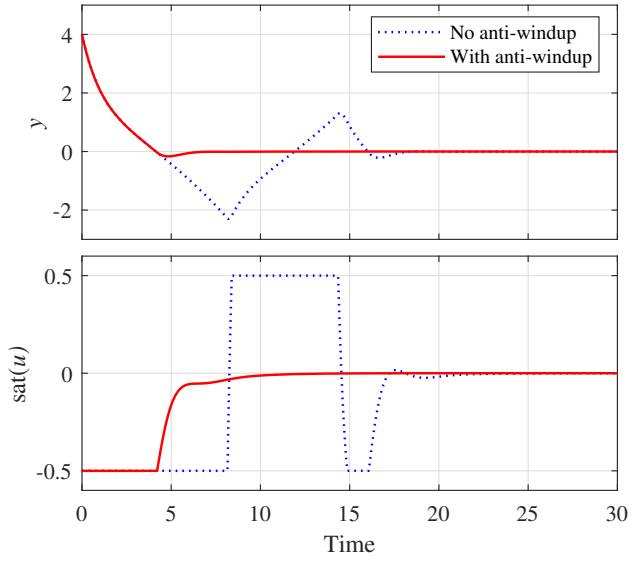

Figure 2.6: Response of the controller-plant closed-loop system (2-3) with plant (2-16) and controller (2-17) from the initial state $x(0) = \begin{bmatrix} 2 & 2 & 0 \end{bmatrix}^{\mathsf{T}}$. In dotted blue, with $E_{\mathrm{c}} = F_{\mathrm{c}} = 0$ and, in red, with $E_{\mathrm{c}} = 20$ and $F_{\mathrm{c}} = -10$.

and output-feedback controller matrices

$$A_{\mathrm{c}} = 0, \qquad B_{\mathrm{c}} = 2, \qquad C_{\mathrm{c}} = -1, \qquad D_{\mathrm{c}} = -1. \tag{2-17}$$

With (2-16), (2-17) and no anti-windup compensation, i.e. $E_{\mathrm{c}} = F_{\mathrm{c}} = 0$, Figure 2.6 shows the response of the plant-controller feedback to the initial state $x(0) = \begin{bmatrix} 2 & 2 & 0 \end{bmatrix}^{\mathsf{T}}$ in blue. Observe that the controller saturates three times over the first 17 time units of simulation, causing an erratic output response of the closed-loop system. However, if the static linear anti-windup compensation strategy is implemented by fixing $E_{\mathrm{c}} = 20$ and $F_{\mathrm{c}} = -10$ (computed with the procedure presented Chapter 5), the overshoot is mitigated and the settling time is reduced in the output response depicted in red, thus showing the importance and effectiveness of the anti-windup loop in saturated systems.

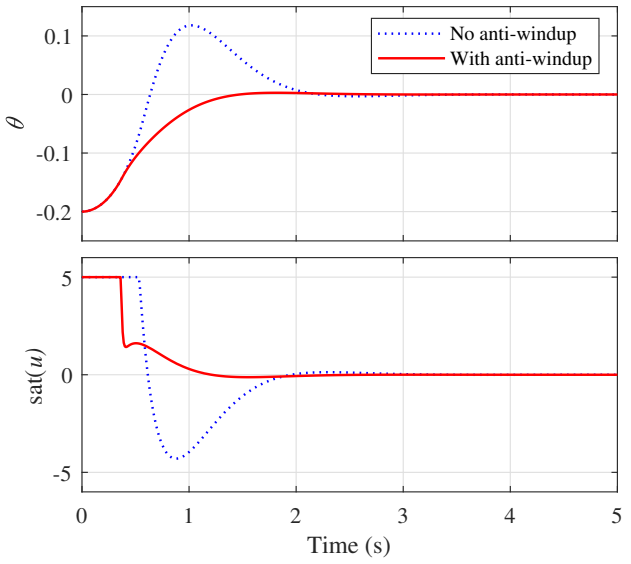

Figure 2.7: Response of the controller-plant closed-loop system (2-3) with plant (2-19) and controller (2-20) from the initial state $x(0) = \begin{bmatrix} -0.2 & 0 & 0 & 0 \end{bmatrix}^{\mathsf{T}}$. In dotted blue, with $E_{\mathrm{c}} = F_{\mathrm{c}} = 0$ and, in red, with $E_{\mathrm{c}} = \begin{bmatrix} 0.003 & -0.06 \end{bmatrix}^{\mathsf{T}}$ and $F_{\mathrm{c}} = 0$.

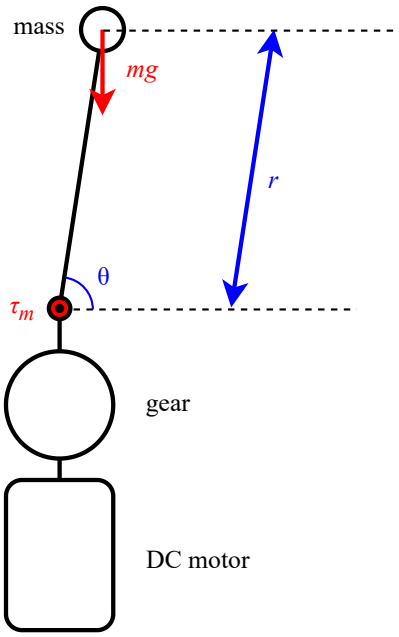

Figure 2.8: Inverted pendulum system controlled with a DC motor connected to a gear coupling.

Example 2.2: Linearized pendulum. Consider the inverted pendulum shown in Figure 2.8, where the angle θ is controlled throughout a torque τ_m produced by a DC motor connected to a n:1 ratio gear. Motor internal inductance is negligible. Selecting $x_1 = \theta$ and $x_2 = \dot{\theta}$, the state-space nonlinear model describing the dynamics of this plant is

$$\left|\begin{array}{rcl} \dot{x}_1 &=& x_2 \\ \dot{x}_2 &=& -\frac{mgr}{J}\cos(x_1) - \frac{nK_\mathrm{b}K_\mathrm{t}+bR}{JR}x_2 + \frac{nK_\mathrm{t}}{JR}u \\ y &=& x_1 \end{array}\right. , \tag{2-18}$$

where u is the voltage sent to the DC motor in volts. The pendulum parameters are:

- load mass $m = 1\,kg$,
- arm length $r = 0.2\,m$ and
- inertia $J_l = m \cdot r^2 = 0.04\,kg \cdot m^2$,

Additionally, the motor parameters are:

- shaft inertia $J_m = 0.1\,kg \cdot m^2$,
- internal friction coefficient $b = 0.001\,\frac{N}{m \cdot s^{-1}}$,
- electromechanical constants $K_\mathrm{t} = 1\frac{n \cdot m}{A}$ and $K_\mathrm{b} = 1\frac{V}{rad \cdot s}$ and
- internal electrical resistance $R = 100\,\Omega$,

and the gear parameters are:

- inertia $J_g = 0.04\,kg \cdot m^2$ and
- gear ratio $n = 10$.

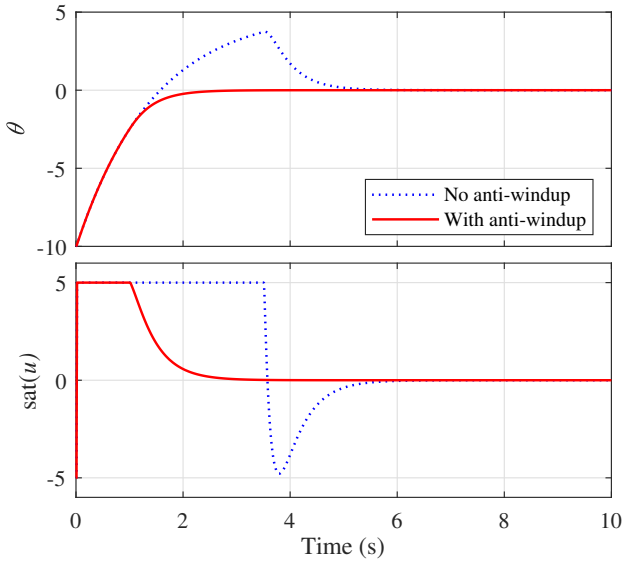

Figure 2.9: Response of the controller-plant closed-loop system (2-3) with plant (2-21) and controller (2-22) from the initial state $x(0) = \begin{bmatrix}-10 & 0 & 0\end{bmatrix}^\mathsf{T}$. In dotted blue, with $E_\mathrm{c} = F_\mathrm{c} = 0$ and, in red, with $E_\mathrm{c} = \begin{bmatrix}0.5 & 1\end{bmatrix}^\mathsf{T}$ and $F_\mathrm{c} = 0$.

With these values, the total inertia on the motor rotor is $J = J_m + J_g + J_l/n^2 = 0.1404$ and, therefore, the linearized model of plant (2-18) around $\theta = 0, \dot{\theta} = \frac{\pi}{2}$ has state-space matrices

$$\left[\begin{array}{c|c} A_\mathrm{p} & B_\mathrm{p} \\ \hline C_\mathrm{p} & D_\mathrm{p} \end{array}\right] = \left[\begin{array}{cc|c} 0 & 1 & 0 \\ \frac{mgr}{J} & \frac{-nK_\mathrm{b}K_\mathrm{t}+bR}{JR} & \frac{nK_t}{JR} \\ \hline 1 & 0 & 0 \end{array}\right] = \left[\begin{array}{cc|c} 0 & 1 & 0 \\ 13.9744 & -0.7051 & 0.7123 \\ \hline 1 & 0 & 0 \end{array}\right]. \tag{2-19}$$

Consider also the output-feedback controller matrices

$$A_\mathrm{c} = \begin{bmatrix}0 & 0 \\ 0 & -100\end{bmatrix}, \quad B_\mathrm{c} = \begin{bmatrix}1 \\ -100\end{bmatrix}, \quad C_\mathrm{c} = \begin{bmatrix}-100 & -1500\end{bmatrix}, \quad D_\mathrm{c} = -1580. \tag{2-20}$$

The output and control responses from the initial state $x(0) = \begin{bmatrix}-0.2 & 0 & 0 & 0\end{bmatrix}^\mathsf{T}$ of the output feedback closed-loop system composed by (2-19) and (2-20), with and without anti-windup compensation, are presented in Figure 2.7. In this example, it is possible to observe that the implementation of the static linear anti-windup strategy, with $E_\mathrm{c} = \begin{bmatrix}0.003 & -0.06\end{bmatrix}^\mathsf{T}$ and $F_\mathrm{c} = 0$, is able to completely eliminate the overshoot and also reduces the settling time of the controller-plant closed-loop system.

Example 2.3: Potter's wheel. Consider a Potter's wheel for which the angular speed is driven by the same DC motor and gear as in the Example 2.2. This time, nonetheless, the charge is a disc of radius $r = 0.15m$ and mass $m = 10kg$. The state-space matrices describing the dynamics of this system are then

$$A_\mathrm{p} = \frac{bR - nK_\mathrm{b}K_\mathrm{t}}{JR} = -0.6960, \qquad B_\mathrm{p} = \frac{nK_t}{JR} = 0.7030, \qquad C_\mathrm{p} = 1, \qquad D_\mathrm{p} = 0, \tag{2-21}$$

with $J = J_m + J_g + J_l/n^2$, and the output-feedback controller, regulating the disc

angular speed, is defined by

$$A_{\mathrm{c}} = \begin{bmatrix} 0 & 0 \\ 0 & -100 \end{bmatrix}, \qquad B_{\mathrm{c}} = \begin{bmatrix} 1 \\ -100 \end{bmatrix}, \qquad C_{\mathrm{c}} = \begin{bmatrix} -20 & -30 \end{bmatrix}, \qquad D_{\mathrm{c}} = 20. \quad (2\text{-}22)$$

For this example, Figure 2.9 shows the output and control dynamics of the closed-loop system (2-3) stemming from both plant (2-21) and controller (2-22) when released from the initial state $x(0) = \begin{bmatrix} -10 & 0 & 0 \end{bmatrix}^{\mathsf{T}}$. For this system, where the plant is globally exponentially stable, it is possible to observe that selecting $E_{\mathrm{c}} = \begin{bmatrix} 0.5 & 1 \end{bmatrix}^{\mathsf{T}}$, $F_{\mathrm{c}} = 0$ produces a faster response as compared with the system without anti-windup compensation. Moreover, this latter is also able to completely eliminate the overshoot produced by the saturation nonlinearity.

2.3.4 The induced algebraic loop

As stated in Section 2.2, the algebraic loop induced by the static linear anti-windup component in controller (2-6) is said to be well-posed if its implicit equation resulting from

$$u = Cx + D\mathrm{dz}\left(u\right) \quad (2\text{-}23)$$

has an unique solution $x \mapsto v(x)$. Based on this definition, the results in [70] provide and prove the following sufficient condition guaranteeing well-posedness of the nonlinear algebraic loop in (2-3) [64].

Lemma 2.1

The nonlinear algebraic loop $u = Cx + D\mathrm{dz}\left(u\right)$ is well-posed if there exists a matrix $L \in \mathbb{D}^{m}_{>0}$ satisfying

$$DL + LD^{\mathsf{T}} - 2L < 0. \quad (2\text{-}24)$$

Under well-posedness, a second challenge shows up when solving the nonlinear algebraic loop in (2-3). Indeed, Lemma 2.1 does not give any procedure to solve the implicit equation to find the explicit value of v. However, according to [69, Section 2.3.7], there exist four main approaches to determine the explicit controller output:

1. Simulation software, which generally use solvers based on a Newton method.
2. Hand-crafted solver, which usually relies on an iterative algorithm to find an approximation of the explicit solution.
3. Lookup table, when the number of input variables is sufficiently small.
4. Dynamic extension methods, as for example, the solution presented in [3].

In this work, opting to use the simulation software approach whenever $D \neq 0$ in (2-3) and an algebraic loop is induced, we make use of MATLAB Simulink [33] to determine the value of v.

2.4 Sector models of the deadzone

Recall the definition of the saturation function in (2-2) and consider the following identity.

$$u = \text{sat}\,(u) + \text{dz}\,(u)\,. \tag{2-25}$$

Note that, if $u = Cx + D\text{dz}\,(u)$ is a stabilizing control law, then the matrix A in (2-3) is Hurwitz (i.e. the closed-loop system (2-3) is asymptotically stable). Furthermore, both the saturation and the deadzone functions are decentralized memoryless nonlinearities [53], which means that the closed-loop system (2-3) may be studied as a Lur'e problem [37], and that the deadzone satisfies the following sector conditions (see discussion in [65, Section 1.7.2]). First, the following well-known fact, initially found in [23], can be stated.

Fact 2.1

Global sector condition: For any $T_1 \in \mathbb{D}^m_{>0}$ and all $u \in \mathbb{R}^m$, it holds that

$$\text{dz}\,(u)^\mathsf{T} T_1(u - \text{dz}\,(u)) \geq 0. \tag{2-26}$$

It is important to remark that the global sector condition in Fact 2.1 is applicable for any nonlinearity that is descentralized and vector-valued. Hence, some conservatism may arise when this sector condition is used to certify stability, since it implicitly ensures stability for a larger class of systems [65]. To mitigate this source of conservativeness, introduce the function $x \mapsto h(x)$, the matrix $\overline{U} := \text{diag}(\overline{u})$ and the set

$$\mathcal{S}_h := \{x \in \mathbb{R}^n : |h(x)|_\infty \leq 1\}. \tag{2-27}$$

Then, the following sector condition, proposed and proven in [66] (see also [11], [56]) specifically applies for a symmetric deadzone and produces less conservative conditions as compared to the global sector condition [65, Section 1.7.2.2].

Fact 2.2

Local sector condition: For any $T_2 \in \mathbb{D}^m_{>0}$, it holds that for all $x \in \mathcal{S}_h$ and any $u \in \mathbb{R}^m$,

$$\text{dz}\,(u)^\mathsf{T} T_2(u - \text{dz}\,(u) - \overline{U}h(x)) \geq 0. \tag{2-28}$$

Additionally, denote with $x \mapsto v(x)$ the explicit solution of the algebraic loop in (2-23). Exploiting the properties of the directional derivatives $x \mapsto \dot{v}(x)$ and $x \mapsto \dot{\text{dz}}\,(v(x))$ along the solutions of (2-3), we may complete this background by introducing the next inequalities proposed in [12, Fact 4] (see also [56, Fact 5]).

Fact 2.3

Derivative of the deadzone: For any $T_3 \in \mathbb{D}^m$, any $T_4 \in \mathbb{D}^m$ and for almost all $x \in \mathbb{R}^n$,

$$\mathrm{dz}\left(v(x)\right)^{\mathsf{T}} T_3(\dot{v}(x) - \dot{\mathrm{dz}}\left(v(x)\right)) \equiv 0, \tag{2-29}$$

$$\dot{\mathrm{dz}}\left(v(x)\right)^{\mathsf{T}} T_4(\dot{v}(x) - \dot{\mathrm{dz}}\left(v(x)\right)) \equiv 0, \tag{2-30}$$

where $v(x)$ denotes the explicit solution of the nonlinear algebraic loop $u - D\mathrm{dz}\left(u\right) = Cx$ in (2-23) and $\dot{\mathrm{dz}}\left(v(x)\right)$ denotes the time-derivative of $x \mapsto \mathrm{dz}\left(v(x)\right)$, which is well defined for almost all values of $x \in \mathbb{R}^n$.

2.5 Conclusion

In this chapter, we proposed the state-space modeling of the plant subject to actuator saturation and the state-space modeling of the controller-plant feedback, in which two control laws are considered: The full state-feedback controller and the dynamic output-feedback controller. In the general case, the plant (2-1) is assumed to be observable and stabilizable to be suitable for the controller implementation since observability is a necessary condition for the state-feedback implementation, but this assumption can be relaxed when implementing the output-feedback control law (2-6), which only requires detectability and stabilizability of the plant. Moreover, when the feedback regulation law is applied, the closed-loop dynamics become nonlinear due to the saturating control signal.

On the other hand, we presented the main concepts and properties of the input-saturated control systems, whose behavior and stability are directly affected by the presence of bounded control signals. In fact, the bounded controllability may yield the appearance of the windup phenomenon. These stability and performance degradations can be mitigated by implementing an anti-windup compensator, but this strategy might induce algebraic loops that must be considered in the study of the closed-loop system. Finally, different useful sector conditions that the deadzone satisfies were also discussed.

Chapter 3

Problems considered and methods

3.1 Introduction

In this chapter, we consider the plant subject to input saturation as defined in Chapter 2 and we recall it here to ease the reading, with

$$\left|\begin{array}{l}\dot{x}_{\mathrm{p}} = A_{\mathrm{p}}x_{\mathrm{p}} + B_{\mathrm{p}}\mathrm{sat}\left(u\right)\\ y \;\; = C_{\mathrm{p}}x_{\mathrm{p}} + D_{\mathrm{p}}\mathrm{sat}\left(u\right)\end{array}\right. . \tag{3-1}$$

Similarly, we consider the dynamic output-feedback controller

$$\left|\begin{array}{l}\dot{x}_{\mathrm{c}} = A_{\mathrm{c}}x_{\mathrm{c}} + B_{\mathrm{c}}y + E_{\mathrm{c}}\mathrm{dz}\left(u\right)\\ u \;\; = C_{\mathrm{c}}x_{\mathrm{c}} + D_{\mathrm{c}}y + F_{\mathrm{c}}\mathrm{dz}\left(u\right)\end{array}\right. , \tag{3-2}$$

and the generic controller-plant saturated feedback

$$\left|\begin{array}{l}\dot{x} = Ax + B\mathrm{dz}\left(u\right)\\ u = Cx + D\mathrm{dz}\left(u\right)\end{array}\right. . \tag{3-3}$$

As a first step, we expose the motivations of this work. Then, the Section 3.2.2 presents the problems we are concerned throughout the manuscript, which are solved using the tools presented in Section 3.4, namely sign-indefinite quadratic Lyapunov functions constructed with the help of the sign-indefinite quadratic forms of [56]. The solutions of these problems are presented in Chapters 4 and 5. However, before that, a brief literature review describing the origins of the mentionned Lyapunov function is summarized in Sections 3.3 and 3.4.1.

As discussed in Section 2.3.1, it is possible to ensure global exponential stability of the origin of (3-3) only if certain conditions on the open-loop system (3-1) are satisfied. This implies that guaranteeing the global or regional stability of the closed-loop system (3-3) is a major interest of this work, but, whenever global exponential stability is not obtainable, it is also important to determine regions in the state space in which the exponential stability is ensured. Since the analytic determination of the region of exponential stability is a very challenging issue [65], Section 3.4 also

presents additional definitions that must be considered to obtain an estimate of the basin of attraction of the origin of (3-3).

3.2 Problem statement and motivations

3.2.1 Motivation

From the scope of the Lyapunov methods, the use of positive-definite quadratic forms of the state x is the common basis in most of the existing solutions to analyze and stabilize saturated systems in the literature (see, for example, [19], [11], [23]), revealing some conservative results emerging from the fact that the saturation limits are not considered during the choice of a Lyapunov function candidate, as discussed, for example, in [65, Example 3.4] and [69, Section 4.4.1.1]. In consequence, in the recent years, some rigorous theoretical stability analysis producing different constructive methods for static anti-windup gains, state feedback controller and dynamic output feedback controller synthesis have well overcome this conservatism by following the Popov criterion [37] to incorporate some saturation nonlinearity information to the Lyapunov function, thus relaxing the positivity conditions of the Lyapunov candidate function while ameliorating multiple performance indicators (see, for example, [50], [51], [52], [55], [56] and [67]).

3.2.2 Problems contemplated

Roughly speaking, we make use of sign-indefinite piecewise quadratic Lyapunov functions stemming from the sign-indefinite quadratic form presented in [56] in this work with the aim to address the main problems of this work: Anti-windup synthesis and dynamic output-feedback stabilization. Moreover, it is worth to remark that this thesis focuses on internal stability, in which the closed-loop system (3-3) is assumed to be free of exogenous signals and perturbations.

With respect to the dynamic output-feedback control design, we assume that the plant (3-1) is detectable and stabilizable and that its feedthough matrix D_{p} in (3-2) is null. Then, whenever the closed-loop system (3-3) is exponentially unstable, a main issue is the determination of the regions of initial states that converge to the origin when a saturating output-feedback control law is designed. Therefore, the regional stabilization problem may be formulated as follows.

Problem 3.1: *Regional output-feedback synthesis.* Given an input-saturated unstable plant (3-1) with feedthrough matrix $D_{\mathrm{p}} = 0$, compute the matrices A_{c}, B_{c}, C_{c}, D_{c} and E_{c} for the output-feedback control law (3-2) ensuring regional exponen-

tial stability and provide an estimate of the basin of the attraction of the origin for the closed-loop system (3-3) with maximized volume.

In the particular case where the input-saturated plant is null controllable with bounded controls, i.e. the matrix A_p in (3-1) is Hurwitz, the following problem concerns the global asymptotic stabilization.

Problem 3.2: *Global output-feedback synthesis.* Given an input-saturated stable plant (3-1) with feedthrough matrix $D_\mathrm{p} = 0$ and a prescribed minimum convergence rate α, compute the matrices A_c, B_c, C_c, D_c and E_c for the output-feedback control law (3-2) ensuring global exponential stability of the origin for the closed-loop system (3-3) with a spectral abscissa of the matrix A smaller than $-\alpha$.

On the other hand, regarding the static linear anti-windup synthesis for a pre-computed controller ensuring local exponential stability in the region of linearity $\mathcal{R}_L$, the following regional and global stabilization problems are formulated.

Problem 3.3: *Regional anti-windup synthesis.* Given an input-saturated unstable plant and a control law such that the matrix A of the closed-loop system (3-3) is Hurwitz, design the anti-windup gains E_c and F_c ensuring regional exponential stability and provide an estimate of the basin of the attraction of the origin for the closed-loop system (3-3) with maximized volume.

Problem 3.4: *Global anti-windup synthesis.* Given an input-saturated stable plant and a control law such that the matrix A of the closed-loop system (3-3) is Hurwitz, design the anti-windup gains E_c and F_c ensuring global exponential stability of the origin for the closed-loop system (3-3) with minimized spectral abscissa of the state matrix A.

3.3 The quadratic Lyapunov function

Before introducing the piece-wise sign-indefinite quadratic Lyapunov function uses in this work to address the problems previously formulated, we propose to recall some ingredients using the classical quadratic Lyapunov function. Except for the statements in which the source is explicitly cited, the results presented in this section can be found in an extensive Lyapunov control methods bibliography, including [37], [25], [65] and [69].

The quadratic Lyapunov function is a common Lyapunov functions used to study the stability following the second principle of Lyapunov, presented in the Section 1.2.1. It is defined as

$$V_\mathrm{Q}(x) := x^\mathsf{T} P x, \tag{3-4}$$

where $P \in \mathbb{S}^n_{>0}$ and x is the vector state of the closed-loop system (3-3). Consider the system (2-3) with A Hurwitz and denote with $x \mapsto v(x)$ the explicit solution of

the nonlinear algebraic loop defined by the second equation in (3-3). Then, defining the extended state vector

$$\eta = \begin{bmatrix} x^{\mathsf{T}} & \mathrm{dz}\left(v(x)\right)^{\mathsf{T}} \end{bmatrix}^{\mathsf{T}}, \tag{3-5}$$

it is possible to obtain

$$\begin{aligned} \dot{V}_{\mathrm{Q}}(x) &= \dot{x}^{\mathsf{T}} P x + x^{\mathsf{T}} P \dot{x} \\ &= \eta^{\mathsf{T}} \begin{bmatrix} A^{\mathsf{T}}P + PA & PB \\ B^{\mathsf{T}}P & 0 \end{bmatrix} \eta. \end{aligned} \tag{3-6}$$

Observe that due to the presence of a zero on the diagonal of the matrix in (3-6), it is not feasible to check the condition $\dot{V}_{\mathrm{Q}} < 0$ for all $x \in \mathbb{R}^n$ to ensure the asymptotic stability of the system (2-3). This clearly means that it is necessary to use information of the deadzone $\mathrm{dz}\left(u\right)$. Therefore, exploiting the Fact 2.1 allows to relieve this issue, given that

$$\dot{V}_{\mathrm{Q}}(x) < \dot{V}_{\mathrm{Q}}(x) + 2\mathrm{dz}\left(v(x)\right) T(v(x) - \mathrm{dz}\left(v(x)\right)) \tag{3-7}$$

$$= \eta^{\mathsf{T}} \begin{bmatrix} A^{\mathsf{T}}P + PA & PB + C^{\mathsf{T}}T \\ B^{\mathsf{T}}P + TC & -2T \end{bmatrix} \eta \tag{3-8}$$

To ensure that $\dot{V}_{\mathrm{Q}}(x) < 0$, or more specifically, to ensure that the matrix in (3-8) is negative-definite, the following theorem, which is an adaptation of the results presented in [34] and [35], provides sufficient conditions for asymptotic stability using the second method of Lyapunov.

Theorem 3.1

Consider the quadratic Lyapunov function candidate (3-4). Given any matrix $Q \in \mathbb{S}^n_{>0}$, the equilibrium point $x = 0$ of the closed-loop system (3-3) is asymptotically stable if there exists the matrices $P \in \mathbb{S}^n_{>0}$ and $T \in \mathbb{D}^m_{>0}$ satisfying the Lyapunov equation

$$A^{\mathsf{T}}P + PA + \tfrac{1}{2}(PB + C^{\mathsf{T}}T)T^{-1}(B^{\mathsf{T}}P + TC) = -Q. \tag{3-9}$$

Proof: Due to the definition of the matrix Q, it may be ensured that

$$A^{\mathsf{T}}P + PA + \tfrac{1}{2}(PB + C^{\mathsf{T}}T)T^{-1}(B^{\mathsf{T}}P + TC) < 0, \tag{3-10}$$

which turns out to be an suitable inequality for the use of the Schur complement. Therefore, leveraging the invertibility of T, inequality (3-10) yields the LMI

$$\begin{bmatrix} A^{\mathsf{T}}P + PA & PB + C^{\mathsf{T}}T \\ B^{\mathsf{T}}P + TC & -2T \end{bmatrix} < 0, \tag{3-11}$$

ensuring $\dot{V}_{\mathrm{Q}}(x) < \dot{V}_{\mathrm{Q}}(x) + 2\mathrm{dz}\left(v(x)\right) T(v(x) - \mathrm{dz}\left(v(x)\right)) < 0$ and, consequently, proving the asymptotic stability of the origin of the system (3-3). □

Although Theorem 3.1 does not provide any information about the basin of attraction of the origin of the system (3-3), it identifies the cases in which a quadratic Lyapunov function for (3-3) exists and presents some fundamental conditions the for

stability analysis of the closed-loop system with control saturation. The estimation of the region of stability using the quadratic Lyapunov function (3-4) is out of the scope of this manuscript, but it may be found in [32], exploiting the Fact 2.2 (local sector condition), instead of the Fact 2.1.

Nevertheless, it is worth to remark that the main problem of using the quadratic Lyapunov function (3-4) to study the stability of input-saturated systems rely on its intrinsic conservativeness. First, the classical quadratic approaches often require the feedthrough matrix D in (3-3) to be null, since it is not considered in the Lyapunov equation (3-9). Additionally, the function V_{Q} does not consider the evolution of the nonlinearities present in the input-saturated systems, but only the behavior of the states x. This conservativeness is the reason why some results came out towards the construction and application of less conservative Lyapunov functions leading to linear or bilinear matrix inequality stability conditions, as, for example, [24], [31] and [47]. Actually, the next section introduces the sign-indefinite quadratic form used in [56] to construct piecewise smooth and piecewise quadratic Lyapunov functions mitigating the classical quadratic approach conservativeness.

3.4 The sign-indefinite quadratic form

3.4.1 Origins from the quadratic Lyapunov function

The origins of the sign-indefinite quadratic form constructed in [56] are founded in the Popov-like Lyapunov functions introduced in [39, Section 2.5], in which, applying the Popov criterion [37] to capture certain Popov-like terms, it is shown that the Lure-Postnikov type Lyapunov function

$$V_{\mathrm{L}}(x) = x^{\mathsf{T}} Q x + 2 \sum_{i=1}^{m} \int_0^{\omega_i} \mathrm{dz}_i(\sigma) \Lambda_{ii} \mathrm{d}\sigma \tag{3-12}$$

proposed in [35], where $Q \in \mathbb{S}^n_{>0}$, $\Lambda \in \mathbb{D}^m_{>0}$ and $\omega = K_1 x$ is the state-feedback control law, is able to provide sufficient conditions for global and regional asymptotic stability. Recalling the definition of η in (3-5), generalizing the control output ω in (3-12) so that $\omega = u = Cx + D\mathrm{dz}\,(u)$ and exploiting the identity

$$2 \int_0^{u_i} \mathrm{dz}_i(\sigma) \mathrm{d}\sigma = \mathrm{dz}_i^2(u), \tag{3-13}$$

the Lyapunov function (3-12) can be simply rewritten as

$$V_{\mathrm{L}}(x) = x^{\mathsf{T}} Q x + \mathrm{dz}\,(v(x))^{\mathsf{T}} \Lambda \mathrm{dz}\,(v(x)) = \eta^{\mathsf{T}} \begin{bmatrix} Q & 0 \\ 0 & \Lambda \end{bmatrix} \eta,$$

where $\Lambda = \mathrm{diag}(\Lambda_{11}, \cdots, \Lambda_{mm})$. Nevertheless, it is important to remark that the positive-definiteness of Λ is still required in the procedures using the Lyapunov function V_{L}, such as [13] and [42]. As a second example, another Popov-like Lyapunov

function used in the literature to study the input-saturated control systems is

$$V_{\mathrm{K}} = x^{\mathsf{T}} Q x + 2 \sum_{i=1}^{m} \int_0^{u_i} \mathrm{sat}_i(\sigma) \Lambda_{ii} \mathrm{d}\sigma, \tag{3-14}$$

which was initially proposed in [37, Example 2.4] and where u_i is the i state-feedback controller output, for $i = 1, \cdots, m$. Unlike V_{L}, the function V_{K} can be represented by a sign-indefinite matrix P. This can be shown by rewrtting (3-14) as follows.

$$\begin{aligned} V_{\mathrm{K}} &= x^{\mathsf{T}} Q x + 2 \sum_{i=1}^{m} \int_0^{u_i} (\sigma - \mathrm{dz}_i(\sigma)) \Lambda_{ii} \mathrm{d}\sigma, \\ &= x^{\mathsf{T}} Q x + \sum_{i=1}^{m} (u_i^2 - \mathrm{dz}_i^2(u)) \Lambda_{ii} \\ &= \eta^{\mathsf{T}} \left(\begin{bmatrix} Q & 0 \\ 0 & -\Lambda \end{bmatrix} + \begin{bmatrix} K_1^{\mathsf{T}} \\ K_2^{\mathsf{T}} \end{bmatrix}^{\mathsf{T}} \Lambda \begin{bmatrix} K_1 & K_2 \end{bmatrix} \right) \eta = \eta^{\mathsf{T}} P \eta. \end{aligned} \tag{3-15}$$

Notice that, in the previous expression, the matrix P is sign-indefinite since its $(2,2)$ entry, namely $K_2^{\mathsf{T}} \Lambda K_2 - \Lambda$ may be nonpositive (for example, when $K_2 = 0$). However, (3-14) is still positive definite under mild conditions on the matrix Q, as it was proven in [56, Proposition 1].

3.4.2 Proposed structure

Inspired in the Lyapunov function V_{L} defined in (3-12), [12] proposes the piecewise quadratic Lyapunov function

$$V_{\mathrm{D}}(x) := \eta^{\mathsf{T}} P \eta = \eta^{\mathsf{T}} \begin{bmatrix} P_{11} & P_{12} \\ P_{12}^{\mathsf{T}} & P_{22} \end{bmatrix} \eta, \tag{3-16}$$

with $P \in \mathbb{S}_{>0}^{m+n}$. In fact, $V_{\mathrm{D}}(x)$ turns out to be a generalization of V_{L}, in the sense that V_{L} is a special case of V_{D} when P is a diagonal block matrix with diagonal P_{22}, or, in other words, when $P_{22} \in \mathbb{D}_{>0}^{m}$ and the cross terms $x^{\mathsf{T}} P_{12} \mathrm{dz}\,(u) = 0$ and $\mathrm{dz}\,(u)^{\mathsf{T}} P_{12}^{\mathsf{T}} x = 0$. It was also proven in [12] that $V_{\mathrm{D}}(x)$ in (3-16) is suitable for guaranteeing the global or regional exponential stability of the origin of (3-3). Further, unlike the quadratic function V_{Q} in (3-4), the Lyapunov function $V_{\mathrm{D}}(x)$ directly considers the feedthrough matrix D in (3-3).

Despite the less-conservative results presented in [12], the function V_{D} still requires the positive-definiteness of P, in contrast to the function V_{K} defined in (3-14). However, recent works have overcome this source of conservativeness by exploiting the sign indefinite quadratic form constructed in [56] to propose the sign-indefinite piecewise quadratic Lyapunov function

$$V(x) := \eta^{\mathsf{T}} P \eta = \eta^{\mathsf{T}} \begin{bmatrix} P_{11} & P_{12} \\ P_{12}^{\mathsf{T}} & P_{22} \end{bmatrix} \eta, \tag{3-17}$$

in which $P_{11} > 0$ so that V is locally positive definite, while admitting a sign-

indefinite matrix P_{22}. This property is illustrated in the Figure (3.1) for a example of V. Note that, even if the sign-indefinite quadratic form presented in [56] is quadratic, (3-17) is actually nonquadratic in x due to the piecewise affine dependence on x of the vector η.

Furthermore, unlike V_{L} and V_{K}, V is not differentiable in all $x \in \mathbb{R}^n$. This is because the deadzone mapping $x \mapsto \mathrm{dz}\,(v(x))$, stemming from the definition of the saturation function in (2-2) and the algebraic loop in the bottom equation of (3-3) with explicit solution $x \mapsto v(x)$, is not differentiable everywhere. Fortunately, making use of the results presented in [14, Proposition 1] and taking advantage of the fact that V is Lipschitz continuous, the time-derivative of V, here denoted by $\dot{V}$, is well defined for almost all $x \in \mathbb{R}^n$. Therefore, the following Lemma can be stated to ensure the negative-definiteness of $\dot{V}$ in the set $\mathcal{S}_h$ defined in (2-27) along the trajectories of system (3-3).

Lemma 3.1

[14, Proposition 1] Given a piecewise quadratic Lyapunov candidate function V as defined in (3-17) that is locally Lipschitz continuous in $\mathcal{S}_h$, if there exists a scalar $\beta_3 > 0$ such that

$$\dot{V}(x) = \left\langle \nabla V(x), \dot{x} \right\rangle \leq -\beta_3 |x|^2 \qquad \text{for almost all } x \in \mathcal{S}_h,$$

with $\dot{x} = Ax + B\mathrm{dz}\,(u)$, then, it holds that

$$\langle \delta_v, \dot{x} \rangle \leq -\beta_3 |x|^2, \qquad \forall x \in \mathcal{S}_h, \forall \delta_v \in \partial V(x), \tag{3-18}$$

where $\partial V(x)$ denotes the Clarke generalized gradient of V at x.

With Lemma 3.1, the areas where V is not differentiable may be ignored when analyzing the global or regional exponential stability of the origin of (3-3) in $\mathcal{S}_h$, or

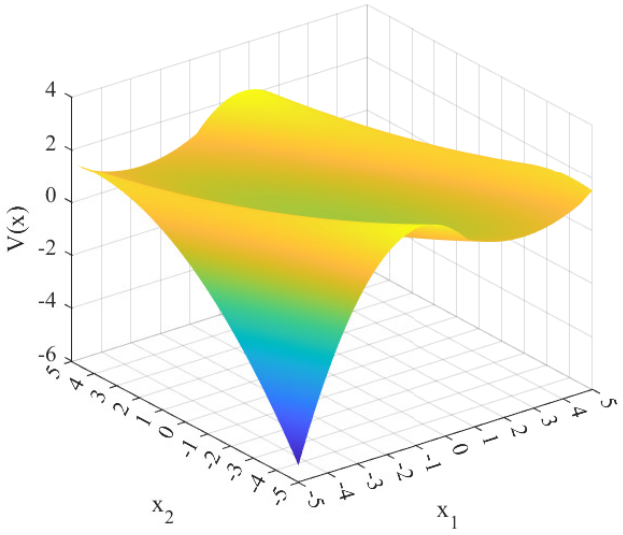

Figure 3.1: Example of the function V in the state space. Notice that V is locally positive definite.

when synthesizing a stabilizing controller the saturated closed-loop system. Additionally, it is worth to remark that the global problems listed in Section 3.2.2 are addressed in Chapters 4 and 5 by using the Lyapunov function V in (3-17) to certify global stability with the help of the second method of Lyapunov (see Chapter 1). In the regional case, we introduce, in Section 3.4.3, other preliminary considerations that must be contemplated before developing the stability certificates presented in Chapters 4 and 5.

3.4.3 Considerations for the regional results

In the general case, the determination of the region of attraction of saturated systems remains an open problem. However, one of the main problems addressed in recent works (see, for example, [11], [23], [19] and [56]) consists in providing an estimate $\mathcal{S}(W)$ of the basin of attraction of the origin of the closed-loop system (3-3), corresponding to

$$\mathcal{S}(W) := \{x \in \mathbb{R}^n : W(x) < 1\} \subset \mathcal{R}_A, \tag{3-19}$$

where W is a Lyapunov function defined in such a way that

$$\mathcal{S}(W) \subset \mathcal{S}_h, \tag{3-20}$$

with the set $\mathcal{S}_h$ as defined in (2-27).

As discussed in Section 2.3.1, whenever the plant subject to input saturation (3-1) has exponentially unstable poles, only regional exponential stability is obtainable due to the presence of the saturation limits and the resulting limitations of bounded stabilization [61]. Therefore, following a similar procedure to [56], characterizing estimates of the basin of attraction of the origin for (3-3) through $\mathcal{S}(W)$ in (3-19) requires selecting the function $x \mapsto h(x)$ in (2-27) and (2-28) as

$$h(x) = H_1 x + H_2 \mathrm{dz}\left(v(x)\right), \tag{3-21}$$

where $H_1 \in \mathbb{R}^{m\times n}$, $H_2 \in \mathbb{R}^{m\times m}$ are both arbitrary design parameters and $x \mapsto v(x)$ is the explicit solution of the bottom equation in (3-3). With the sign-indefinite quadratic form (3-17), the definition of h in (3-21) and the subset $\mathcal{S}_h$ in (2-27), impose the condition

$$V(x) \geq |h(x)|_\infty^2 \tag{3-22}$$

for all $x \in \mathcal{S}_h$ so that the Lyapunov function candidate

$$W(x) := \begin{cases} V(x) & \text{if } x \in \mathcal{S}_h \\ 1 & \text{otherwise} \end{cases} \tag{3-23}$$

is locally continuous and Lipschitz in $\mathcal{S}_h$ and the inclusion in Equation (3-20) holds. Now, thanks to the definition of $\mathcal{S}(W)$ in (3-19), it holds under (3-22) that

$$\mathcal{S}(W) = \mathcal{S}(V) \cap \mathcal{S}_h. \tag{3-24}$$

This property turns out to be useful for the construction of the regional stability

certificates for the four problems listed in the previous section, which are addressed in the next chapters.

Remark 3.1: Whether $H_1 = 0$ and $H_2 = 0$, then the set $\mathcal{S}_h = \mathbb{R}^n$ and, therefore, the Lyapunov function candidate W coincides with the sign-indefinite quadratic form V in (3-17) for all $x \in \mathbb{R}^n$.

3.5 Closing statements

In this chapter we stated the motivations of this work and listed the problems addressed in this manuscript, which concern different analysis and synthesis procedures for both regional and global exponential stability of the saturated controller-plant feedback. Moreover, the synthesis problems are related to the design of the state-feedback controller, the output-feedback controller and anti-windup compensator for the input-saturated plant. Then, we also introduced the sign-indefinite quadratic form, originally presented in [56], to reveal the sign-indefinite piecewise quadratic Lyapunov functions used in this manuscript to address the problems formulated in the Section 3.2.2.

Chapter 4

Output-feedback controller design

4.1 Introduction

This chapter addresses the synthesis of dynamic output-feedback controllers for input-saturated plants, which correspond to Problems 3.1 and 3.2 enunciated in Section 3.2.2. As a first step, based on the state-space model representation of the saturated closed-loop system and the second principle of Lyapunov, applied with sign-indefinite nonquadratic Lyapunov functions constructed with the sign-indefinite quadratic forms proposed in [56] and overviewed in Section 3.4, Section 4.2 introduces some preliminary concepts used along this chapter. Additionally, Section 4.3 compiles the global and regional results presented in [51] and [52] ensuring regional and global exponential stability, respectively.

Furthermore, the sufficient conditions formulated in this chapter are given in form of Linear matrix inequalities (LMIs) and, for the regional stability and stabilization problems, useful means are also given to determine and maximize estimates of the basin of the attraction of the origin of the saturated controller-plant feedback. Additionally, secondary sufficient LMI conditions are presented to guarantee a prescribed minimum convergence rate, which holds locally in the region of linearity.

4.2 Preliminaries

First, let $n = n_p$ to simplify notation. This chapter focuses on the stabilization of the linear plant subject to input saturation

$$\left| \begin{array}{rcl} \dot{x}_p & = & A_{\mathrm{p}} x_p + B_{\mathrm{p}} \mathrm{sat}\,(u) \\ y & = & C_{\mathrm{p}} x_p \end{array} \right. , \tag{4-1}$$

where $x_p \in \mathbb{R}^n$ denotes the state and $y \in \mathbb{R}^m$ the output of the plant, respectively, and $u \mapsto \mathrm{sat}\,(u)$ denotes the decentralized asymmetric saturation function, with

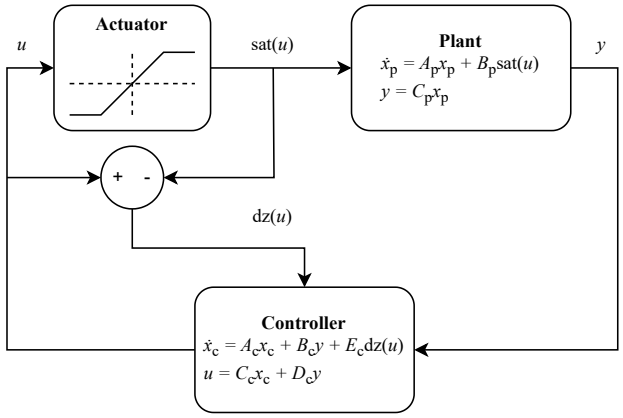

Figure 4.1: The output-feedback controller-plant closed-loop system

components

$$\text{sat}_i(u_i) := \max\{-\underline{u}_i, \min\{\overline{u}_i, u_i\}\} \tag{4-2}$$

for all $i = 1, \cdots, m$, where $\underline{u}_i > 0$ and $\overline{u}_i > 0$ are the saturation lower and upper limits on the input u_i, with u_i, $\underline{u}_i$ and $\overline{u}_i$ being the ith entry of the vectors u, $\underline{u}$ and $\overline{u}$, respectively. Defining now the deadzone function as

$$\text{dz}\,(u) := u - \text{sat}\,(u)\,, \tag{4-3}$$

and assuming that (4-1) is stabilizable and detectable, which is a necessary condition for output feedback stabilizability, the aim of this chapter is to design a dynamic output feedback controller with anti-windup compensation with the form

$$\left|\begin{array}{ll} \dot{x}_\text{c} &= A_\text{c} x_\text{c} + B_\text{c} y + \nu_x \\ u &= C_\text{c} x_\text{c} + D_\text{c} y \end{array}\right. , \tag{4-4}$$

which has the same order as the plant, i.e. with state $x_c \in \mathbb{R}^n$ and output $u \in \mathbb{R}^m$, and where the term ν_x plays the role of the anti-windup compensation. With (4-3), select

$$\nu_x = E_\text{c} \text{dz}\,(u)\,, \tag{4-5}$$

so that the anti-windup component is linear and static. With these definitions, let A_c, B_c, C_c, D_c and E_c be the controller state-space model and anti-windup gain matrices to be designed.

The closed-loop system resulting from the feedback interconnection of the input-saturated plant (4-1) and the controller (4-4) (depicted in Figure 4.1) can be compactly written as

$$\left|\begin{array}{l} \dot{x} = Ax + B\text{dz}\,(u) \\ u = Cx \end{array}\right. , \tag{4-6}$$

with $x := \begin{bmatrix} x_p^\mathsf{T} & x_c^\mathsf{T} \end{bmatrix}^\mathsf{T} \in \mathbb{R}^{2n}$ and

$$\left[\begin{array}{c|c} A & B \\ \hline C & - \end{array}\right] = \left[\begin{array}{cc|c} A_\text{p} + B_\text{p} D_\text{c} C_\text{p} & B_\text{p} C_\text{c} & -B_\text{p} \\ B_\text{c} C_\text{p} & A_\text{c} & E_\text{c} \\ \hline D_\text{c} C_\text{p} & C_\text{c} & - \end{array}\right] .$$

Remark 4.1: The null feedthrough matrix D_{p} in the definition (4-1) of the plant yields to a closed-loop system with no algebraic loop. □

Furthermore, define the extended vector

$$\eta := \left[x^{\mathsf{T}} \ \mathrm{dz}\,(Cx)^{\mathsf{T}}\right]^{\mathsf{T}} \tag{4-7}$$

and introduce

$$h(x) := H_1 x + H_2 \mathrm{dz}\,(Cx)\,, \tag{4-8}$$

where $H_1 \in \mathbb{R}^{m\times 2n}$, $H_2 \in \mathbb{R}^{m\times m}$ are both arbitrary design parameters. Then, note that exploiting the Lyapunov stability method, or more specifically, the second principle of Lyapunov applied to the Lyapunov function

$$W(x) := \begin{cases} V(x) & \text{if } x \in \mathcal{S}_h \\ 1 & \text{otherwise} \end{cases}, \tag{4-9}$$

where V is the sign-indefinite quadratic form

$$V(x) := \eta^{\mathsf{T}} P \eta = \eta^{\mathsf{T}} \begin{bmatrix} P_{11} & P_{12} \\ P_{12}^{\mathsf{T}} & P_{22} \end{bmatrix} \eta, \tag{4-10}$$

and $\mathcal{S}_h$ is the set

$$\mathcal{S}_h := \{x \in \mathbb{R}^{2n} : |h(x)|_\infty \leq 1\}, \tag{4-11}$$

it is possible to analyze the stability of the closed-loop (4-6), as it was shown in [56]. Define also the open sublevel set

$$\mathcal{S}(W) := \{x \in \mathbb{R}^{2n} : W(x) < 1\} \subset \mathcal{R}_A, \tag{4-12}$$

which will be shown to be to an estimate of the basin of attraction of (4-6), since W coincides with V in the set $\mathcal{S}_h$, and the set $\mathcal{S}_h$ in (4-11) and the definition (4-12) are designed in such a way that

$$\mathcal{S}(W) = \mathcal{S}(V) \cap \mathcal{S}_h. \tag{4-13}$$

For the particular case where only regional exponential stability is obtainable, i.e., when the input saturated plant is stabilizable but it has eigenvalues with positive real part (see Section 2.3.1), the Section 4.3.1 provides means to synthesize output-feedback controllers guaranteeing regional exponential stability and to determine an estimate of the basin of attraction of the origin of (4-6). Otherwise, Section 4.3.2 addresses the global exponential stabilization of exponentially stable plants.

The results presented in this chapter are derived in the form of LMIs and they provide sufficient conditions ensuring global or regional exponential stability of the controller-plant feedback (4-6). Leveraging Lemma 3.1, which allows to ignore the points where function W is not differentiable, and the fact that V coincides with W when $H_1 = 0$ and $H_2 = 0$ (see Remark 3.1), it is possible to state the following lemma, originally presented and proven in [56, Lemma 1].

Lemma 4.1

[56, Lemma 1] Considering the dynamics (4-6) and definitions (4-12), (4-11), if there exists a locally Lipschitz Lyapunov function $x \mapsto W(x)$ as defined in (4-9) and positive scalars β_1, β_2 and β_3 satisfying

$$\beta_1|x|^2 \leq W(x) \leq \beta_2|x|^2 \tag{4-14}$$

for all $x \in \mathcal{S}(W)$ and

$$\dot{W}(x) := \langle \nabla W(x), Ax + B\text{sat}(Cx) \rangle \leq -\beta_3|x|^2 \tag{4-15}$$

for almost all $x \in \mathcal{S}(W)$, then the origin of (4-6) is locally exponentially stable with a basin of attraction containing $\mathcal{S}(W)$. Moreover, if (4-14) and (4-15) are satisfied for all $x \in \mathbb{R}^n$, then the origin of (4-6) is globally exponentially stable.

Lemma 4.1 is a fundamental tool to show the stability results presented in the next section.

4.3 Lyapunov stability certificates

Generalizing the approach of [58], parameterize P introducing the full-rank matrices $\mathbf{X}$, $\mathbf{Y}$, $\tilde{X}$, $\tilde{Y} \in \mathbb{S}^n_{>0}$, and full-rank matrices $\mathbf{M}$, $N \in \mathbb{R}^{n\times n}$, such that

$$P_{11} = \begin{bmatrix} \mathbf{X} & \mathbf{M} \\ \mathbf{M}^\mathsf{T} & \tilde{X} \end{bmatrix}, \qquad P_{11}^{-1} = \begin{bmatrix} \mathbf{Y} & N \\ N^\mathsf{T} & \tilde{Y} \end{bmatrix}. \tag{4-16}$$

Using (4-16) and the fact that $P_{11}P_{11}^{-1} = P_{11}^{-1}P_{11} = I_n$, it can be seen that (4-16) holds for suitable selections of $\tilde{X}$ and $\tilde{Y}$ if and only if

$$\mathbf{X}\mathbf{Y} + \mathbf{M}N^\mathsf{T} = \mathbf{Y}\mathbf{X} + N\mathbf{M}^\mathsf{T} = I_n. \tag{4-17}$$

More specifically, under (4-16) and (4-17), the following symmetric selections for $\tilde{X}$ and $\tilde{Y}$ may be computed:

$$\begin{aligned} \tilde{X} &= -\mathbf{M}^\mathsf{T}\mathbf{Y}N^{-\mathsf{T}} & \tilde{Y} &= -\mathbf{M}^{-1}\mathbf{X}N \\ &= -N^{-1}(\mathbf{Y} - \mathbf{Y}\mathbf{X}\mathbf{Y})N^{-\mathsf{T}}, & &= -\mathbf{M}^{-1}(\mathbf{X} - \mathbf{X}\mathbf{Y}\mathbf{X})\mathbf{M}^{-\mathsf{T}}. \end{aligned} \tag{4-18}$$

Generalizing also the derivations in [58], it is possible to parameterize the controller matrices in (4-4) as

$$\begin{aligned} A_\text{c} &= \mathbf{M}^{-1}\big(\hat{\mathbf{A}}_\text{c} - \mathbf{X}\big(A_\text{p} + B_\text{p}D_\text{c}C_\text{p}\big)\mathbf{Y} - \mathbf{M}B_\text{c}C_\text{p}\mathbf{Y} - \mathbf{X}B_\text{p}C_\text{c}N^\mathsf{T}\big)N^{-\mathsf{T}}, \\ B_\text{c} &= \mathbf{M}^{-1}\big(\hat{\mathbf{B}}_\text{c} - \mathbf{X}B_\text{p}D_\text{c}\big), & C_\text{c} &= \big(\hat{\mathbf{C}}_\text{c} - D_\text{c}C_\text{p}\mathbf{Y}\big)N^{-\mathsf{T}}, \\ D_\text{c} &= \hat{\mathbf{D}}_\text{c}, & E_\text{c} &= \mathbf{M}^{-1}\hat{\mathbf{E}}_\text{c}\mathbf{S}^{-1} + \mathbf{M}^{-1}\mathbf{X}B_\text{p}, \end{aligned} \tag{4-19}$$

the remaining entries in (4-10) as

$$P_{12} = \begin{bmatrix} \mathbf{Y} & I_n \\ N^\mathsf{T} & 0 \end{bmatrix}^{-\mathsf{T}} \begin{bmatrix} \mathbf{Z}_\text{p} \\ \mathbf{Z}_\text{c} \end{bmatrix} \mathbf{S}^{-1}, \qquad P_{22} = \mathbf{S}^{-1}\hat{\mathbf{P}}_{22}\mathbf{S}^{-1} \tag{4-20}$$

and, finally, the parameters of (4-8) as

$$H_1 = \begin{bmatrix}\mathbf{G}_p & \mathbf{G}_c\end{bmatrix}\begin{bmatrix}\mathbf{Y} & I_n \\ N^{\mathsf{T}} & 0\end{bmatrix}^{-1}, \qquad H_2 = \hat{\mathbf{H}}_2\mathbf{S}^{-1}. \tag{4-21}$$

With this latter consideration and the parametrization above, the bold matrices $\hat{\mathbf{A}}_{\mathrm{c}} \in \mathbb{R}^{n\times n}$, $\hat{\mathbf{B}}_{\mathrm{c}} \in \mathbb{R}^{n\times m}$, $\hat{\mathbf{C}}_{\mathrm{c}} \in \mathbb{R}^{m\times n}$, $\hat{\mathbf{D}}_{\mathrm{c}} \in \mathbb{R}^{m\times m}$, $\hat{\mathbf{E}}_{\mathrm{c}} \in \mathbb{R}^{n\times m}$, $\mathbf{Z}_{\mathrm{p}} \in \mathbb{R}^{n\times m}$, $\mathbf{Z}_{\mathrm{c}} \in \mathbb{R}^{n\times m}$, $\hat{\mathbf{P}}_{22} \in \mathbb{S}^m$, $\mathbf{S} \in \mathbb{D}^m_{>0}$, $\mathbf{G}_{\mathrm{p}} \in \mathbb{R}^{m\times n}$, $\mathbf{G}_{\mathrm{c}} \in \mathbb{R}^{m\times n}$ and $\hat{\mathbf{H}}_2 \in \mathbb{R}^{m\times m}$ are the decision variables of the convex LMI-based synthesis formulated in the next sections, which allow designing linear dynamic output-feedback stabilizing controllers (4-4) for plant (4-1).

4.3.1 Regional stability results

Let the decentralized saturation function be symmetric, with $\underline{u} = \overline{u}$. Then, introduce the matrix $\overline{U} = \mathrm{diag}(\overline{u})$ and hence, using the Lyapunov function candidate W in (4-9), the following theorem presents a solution to Problem 3.1.

Theorem 4.1

If there exist matrices $\mathbf{X} \in \mathbb{S}^n_{>0}$, $\mathbf{Y} \in \mathbb{S}^n_{>0}$, $\mathbf{Z}_{\mathrm{p}} \in \mathbb{R}^{n\times m}$, $\mathbf{Z}_{\mathrm{c}} \in \mathbb{R}^{n\times m}$, $\hat{\mathbf{P}}_{22} \in \mathbb{S}^m$, $\mathbf{S} \in \mathbb{D}^m_{>0}$, $\mathbf{G}_{\mathrm{p}} \in \mathbb{R}^{m\times n}$, $\mathbf{G}_{\mathrm{c}} \in \mathbb{R}^{m\times n}$, $\hat{\mathbf{H}}_2 \in \mathbb{R}^{m\times m}$, $\hat{\mathbf{A}}_{\mathrm{c}} \in \mathbb{R}^{n\times n}$, $\hat{\mathbf{B}}_{\mathrm{c}} \in \mathbb{R}^{n\times m}$, $\hat{\mathbf{C}}_{\mathrm{c}} \in \mathbb{R}^{m\times n}$, $\hat{\mathbf{D}}_{\mathrm{c}} \in \mathbb{R}^{m\times m}$ and $\hat{\mathbf{E}}_{\mathrm{c}} \in \mathbb{R}^{n\times m}$ satisfying

$$\Psi_1 = \mathrm{He}\begin{bmatrix} \frac{1}{2}\mathbf{Y} & 0 & \mathbf{Z}_{\mathrm{p}} & 0 \\ I_n & \frac{1}{2}\mathbf{X} & \mathbf{Z}_{\mathrm{c}} & 0 \\ \overline{U}\mathbf{G}_{\mathrm{p}} - \hat{\mathbf{C}}_{\mathrm{c}} & \overline{U}\mathbf{G}_{\mathrm{c}} - \hat{\mathbf{D}}_{\mathrm{c}}C_{\mathrm{p}} & \frac{1}{2}\hat{\mathbf{P}}_{22} + \overline{U}\hat{\mathbf{H}}_2 + \mathbf{S} & 0 \\ \mathbf{G}_p & \mathbf{G}_c & \hat{\mathbf{H}}_2 & \frac{1}{2}I_m \end{bmatrix} > 0 \tag{4-22}$$

and

$$\Psi_2 = \mathrm{He}\begin{bmatrix} A_{\mathrm{p}}\mathbf{Y} + B_{\mathrm{p}}\hat{\mathbf{C}}_{\mathrm{c}} & A_{\mathrm{p}} + B_{\mathrm{p}}\hat{\mathbf{D}}_{\mathrm{c}}C_{\mathrm{p}} & -B_{\mathrm{p}}\mathbf{S} & 0 & 0 & \mathbf{Z}_{\mathrm{p}} \\ \hat{\mathbf{A}}_{\mathrm{c}} & \mathbf{X}A_{\mathrm{p}} + \hat{\mathbf{B}}_{\mathrm{c}}C_{\mathrm{p}} & \hat{\mathbf{E}}_{\mathrm{c}} & 0 & 0 & \mathbf{Z}_{\mathrm{c}} \\ \hat{\mathbf{C}}_{\mathrm{c}} - \overline{U}\mathbf{G}_{\mathrm{p}} & \hat{\mathbf{D}}_{\mathrm{c}}C_{\mathrm{p}} - \overline{U}\mathbf{G}_{\mathrm{c}} & -\mathbf{S} - \overline{U}\hat{\mathbf{H}}_2 & \mathbf{Z}_{\mathrm{p}}^{\mathsf{T}} - \hat{\mathbf{C}}_{\mathrm{c}} & \mathbf{Z}_{\mathrm{c}}^{\mathsf{T}} - \hat{\mathbf{D}}_{\mathrm{c}}C_{\mathrm{p}} & \hat{\mathbf{P}}_{22} \\ A_{\mathrm{p}}\mathbf{Y} + B_{\mathrm{p}}\hat{\mathbf{C}}_{\mathrm{c}} & A_{\mathrm{p}} + B_{\mathrm{p}}\hat{\mathbf{D}}_{\mathrm{c}}C_{\mathrm{p}} & -B_{\mathrm{p}}\mathbf{S} & -\mathbf{Y} & -I_n & 0 \\ \hat{\mathbf{A}}_{\mathrm{c}} & \mathbf{X}A_{\mathrm{p}} + \hat{\mathbf{B}}_{\mathrm{c}}C_{\mathrm{p}} & \hat{\mathbf{E}}_{\mathrm{c}} & -I_n & -\mathbf{X} & 0 \\ 0 & 0 & \mathbf{S} & \hat{\mathbf{C}}_{\mathrm{c}} & \hat{\mathbf{D}}_{\mathrm{c}}C_{\mathrm{p}} & -\mathbf{S} \end{bmatrix} < 0 \tag{4-23}$$

then function W in (4-9) is Lipschitz continuous, inclusion $\mathcal{S}(W) \subset \mathcal{S}_h$ holds and the origin of (4-6) with the controller state-space model matrices A_{c}, B_{c}, C_{c}, D_{c} and E_{c} as selected in (4-19) is locally exponentially stable from $\mathcal{S}(W)$.

Proof: First, notice that selections (4-19)-(4-21) can be uniquely inverted as

$$\begin{aligned}
\hat{\mathbf{A}}_{\mathrm{c}} &= \mathbf{X}\left(A_{\mathrm{p}} + B_{\mathrm{c}} D_{\mathrm{c}} C_{\mathrm{p}}\right)\mathbf{Y} + \mathbf{M} B_{\mathrm{c}} C_{\mathrm{p}} \mathbf{Y} + \mathbf{X} B_{\mathrm{p}} C_{\mathrm{c}} N^{\mathsf{T}} + \mathbf{M} A_{\mathrm{c}} N^{\mathsf{T}}, \\
\hat{\mathbf{B}}_{\mathrm{c}} &= \mathbf{X} B_{\mathrm{p}} D_{\mathrm{c}} + \mathbf{M} B_{\mathrm{c}}, & \hat{\mathbf{C}}_{\mathrm{c}} &= D_{\mathrm{c}} C_{\mathrm{p}} \mathbf{Y} + C_{\mathrm{c}} N^{\mathsf{T}}, \\
\hat{\mathbf{D}}_{\mathrm{c}} &= D_{\mathrm{c}}, & \hat{\mathbf{E}}_{\mathrm{c}} &= \mathbf{M} E_{\mathrm{c}} \mathbf{S} - \mathbf{X} B_{\mathrm{p}} \mathbf{S}, \\
\begin{bmatrix} \mathbf{Z}_{\mathrm{p}} \\ \mathbf{Z}_{\mathrm{c}} \end{bmatrix} &= \begin{bmatrix} \mathbf{Y} & I_n \\ N^{\mathsf{T}} & 0 \end{bmatrix}^{\mathsf{T}} P_{12} \mathbf{S}, & \hat{\mathbf{P}}_{22} &= \mathbf{S} P_{22} \mathbf{S}, \\
\begin{bmatrix} \mathbf{G}_{\mathrm{p}} & \mathbf{G}_{\mathrm{c}} \end{bmatrix} &= H_1 \begin{bmatrix} \mathbf{Y} & I_n \\ N^{\mathsf{T}} & 0 \end{bmatrix}, & \hat{\mathbf{H}}_2 &= H_2 \mathbf{S}.
\end{aligned} \tag{4-24}$$

Introduce the invertible matrix

$$\Pi := \begin{bmatrix} \mathbf{Y} & I_n \\ N^{\mathsf{T}} & 0 \end{bmatrix} \tag{4-25}$$

for which, using (4-17) and recalling the selection of P_{11} in (4-16), it may be easily verified that the properties

$$\Pi^{\mathsf{T}} P_{11} = \begin{bmatrix} I_n & 0 \\ \mathbf{X} & \mathbf{M} \end{bmatrix}, \qquad \Pi^{\mathsf{T}} P_{11} \Pi = \begin{bmatrix} \mathbf{Y} & I_n \\ I_n & \mathbf{X} \end{bmatrix}, \tag{4-26}$$

are satisfied. Observe that, according to definition (4-9), $W(x) > 0$ for all $x \notin \mathcal{S}_h$ and $W(x) = V(x)$ for all $x \in S_h$. Leveraging Facts 2.2 and 2.3 emerging from the sector models of the deadzone (see Section 2.4), note that, for any $T_1 \in \mathbb{D}^m_{>0}$, it holds that for all $x \in \mathcal{S}_h$,

$$\mathrm{dz}\left(Cx\right)^{\mathsf{T}} T_1 (Cx - \mathrm{dz}\left(Cx\right) - \overline{U} h(x)) \geq 0, \tag{4-27}$$

and that, for any $T_2 \in \mathbb{D}^m$, $T_3 \in \mathbb{D}^m$ and for all $x \in \mathbb{R}^{2n} : |u_i(x)| \neq \overline{u}_i$,

$$\mathrm{dz}\left(Cx\right)^{\mathsf{T}} T_2 (C\dot{x} - \dot{\mathrm{dz}}\left(Cx\right)) = 0, \tag{4-28}$$

$$\dot{\mathrm{dz}}\left(Cx\right)^{\mathsf{T}} T_3 (C\dot{x} - \dot{\mathrm{dz}}\left(Cx\right)) = 0, \tag{4-29}$$

where $\dot{x} = Ax + B\mathrm{dz}\left(u\right)$ as defined in (4-6) and where $\dot{\mathrm{dz}}\left(Cx\right)$ denotes the time-derivative of $x \mapsto \mathrm{dz}\left(Cx\right)$, which is well defined for almost all values of $x \in \mathbb{R}^{2n}$.

Now, exploiting the invertibility of Π and considering the selections in (4-24), pre- and post-multiply Ψ_1 in (4-22) by

$$\begin{bmatrix} \Pi & 0 & 0 \\ 0 & \mathbf{S} & 0 \\ 0 & 0 & I_m \end{bmatrix}^{-\mathsf{T}}$$

and its transpose to obtain the matrix

$$\mathrm{He} \begin{bmatrix} \frac{1}{2} P_{11} & P_{12} & 0 \\ \mathbf{S}^{-1} \overline{U} H_1 - \mathbf{S}^{-1} C & \frac{1}{2} P_{22} + \mathbf{S}^{-1} \overline{U} H_2 + \mathbf{S}^{-1} & 0 \\ H_1 & H_2 & \frac{1}{2} I_m \end{bmatrix},$$

which is positive-definite due to hypothesis (4-22). Applying a Schur complement

to the expression above, define

$$\bar{\Psi}_1 := P - \mathrm{He}\begin{bmatrix} 0 & 0 \\ \mathbf{S}^{-1}C - \mathbf{S}^{-1}\overline{U}H_1 & -\mathbf{S}^{-1} - \mathbf{S}^{-1}\overline{U}H_2) \end{bmatrix} - \begin{bmatrix} H_1^{\mathsf{T}} \\ H_2^{\mathsf{T}} \end{bmatrix} \begin{bmatrix} H_1 & H_2 \end{bmatrix} > 0, \quad (4\text{-}30)$$

which verifies that, for all $x \in \mathcal{S}_h$,

$$\begin{aligned} V(x) - h(x)^{\mathsf{T}}h(x) &\geq V(x) - h(x)^{\mathsf{T}}h(x) - 2\,\mathrm{dz}\,(Cx)^{\mathsf{T}}\,\mathbf{S}^{-1}(Cx - \mathrm{dz}\,(Cx) - \overline{U}h(x)) \\ &= \eta^{\mathsf{T}}\bar{\Psi}_1\eta \geq \lambda_{\min}(\bar{\Psi}_1)\,|\eta|^2 \geq \lambda_{\min}(\bar{\Psi}_1)\,|x|^2 = \beta_1\,|x|^2\,. \end{aligned} \quad (4\text{-}31)$$

Property (4-31) leads to $W(x) = V(x) \geq h^{\mathsf{T}}(x)h(x) > 0$, proving the inclusion $\mathcal{S}(W) \subset \mathcal{S}_h$, and ensures that $V(x) \geq 1$ at the boundary of $\mathcal{S}_h$, thus implying Lipschitz continuity of $W(x)$ for all $x \in \mathcal{S}_h$. Moreover, since $u = Cx$ is globally Lipschitz, using $|\mathrm{dz}\,(Cx)| \leq |Cx| \leq L\,|x|$, it can be stated that

$$W(x) = V(x) \leq \lambda_{\max}(P)\,|\eta|^2 \leq \lambda_{\max}(P)L\,|x|^2 = \beta_2\,|x|^2\,,$$

which, together with (4-31), implies the existence of positive scalars $\beta_1 = \lambda_{\min}(\bar{\Psi}_1)$ and $\beta_2 = \lambda_{\max}(P)L$ satisfying inequality (4-14) and, thus, positive-definiteness of W for all $x \in \mathcal{S}(W)$.

Furthermore, since $\dot{W}(x)$ coincides with $\dot{V}(x)$ for almost all $x \in \mathcal{S}(W)$, defining the extended state vector υ

$$\upsilon := \begin{bmatrix} x^{\mathsf{T}} & \mathrm{dz}\,(u)^{\mathsf{T}} & \dot{x}^{\mathsf{T}} & \dot{\mathrm{dz}}\,(u)^{\mathsf{T}} \end{bmatrix}^{\mathsf{T}}$$

and matrix K as

$$K := \begin{bmatrix} 0 & C^{\mathsf{T}}\mathbf{S}^{-1} - P_{12} & P_{11} & -C^{\mathsf{T}}\mathbf{S}^{-1} \end{bmatrix}^{\mathsf{T}},$$

due to continuity of (4-6), using Lemma 3.1 (see [14, Section 2.2]), the Lyapunov stability of the origin for the closed-loop system (4-6) from $\mathcal{S}(W)$ can be proven by showing that $\dot{W}(x) = \dot{V}(x) < -\beta_3|x|^2$ for some $\beta_3 > 0$ and for almost all $x \in \mathcal{S}(W) \subset \mathcal{S}_h$. To this end, with (4-24) and after some extensive derivations, pre and postmultiplying Ψ_2 in (4-23) by

$$\begin{bmatrix} \Pi & 0 & 0 & 0 \\ 0 & \mathbf{S} & 0 & 0 \\ 0 & 0 & \Pi & 0 \\ 0 & 0 & 0 & \mathbf{S} \end{bmatrix}^{\mathsf{T}}$$

and its transpose allows determining the symmetric matrix

$$\begin{aligned} \bar{\Psi}_2 :=& \mathrm{He}\begin{bmatrix} P_{11}A & (C - \overline{U}H_1)^{\mathsf{T}}\mathbf{S}^{-1} & 0 & P_{12} \\ B^{\mathsf{T}}P_{11} & -\mathbf{S}^{-1}(I_m + \overline{U}H_2) & P_{12}^{\mathsf{T}} - \mathbf{S}^{-1}C & P_{22} \\ P_{11}A & P_{11}B & -P_{11} & 0 \\ 0 & \mathbf{S}^{-1} & \mathbf{S}^{-1}C & -\mathbf{S}^{-1} \end{bmatrix} \\ =& \mathrm{He}\left(\begin{bmatrix} P_{11} & P_{12} \\ P_{12}^{\mathsf{T}} & P_{22} \\ 0 & 0 \\ 0 & 0 \end{bmatrix} \begin{bmatrix} A & B & 0 & 0 \\ 0 & 0 & 0 & I_m \end{bmatrix} \right) \end{aligned}$$

$$
\begin{aligned}
&+ \mathrm{He}\left(\begin{bmatrix} 0 \\ \mathbf{S}^{-1} \\ 0 \\ 0 \end{bmatrix} \begin{bmatrix} C - \overline{U}H_1 & -I_m - \overline{U}H_2 & 0 & 0 \end{bmatrix}\right) \\
&+ \mathrm{He}\left(\begin{bmatrix} 0 \\ -\mathbf{S}^{-1} \\ 0 \\ 0 \end{bmatrix} \begin{bmatrix} CA & CB & 0 & -I_m \end{bmatrix}\right) \\
&+ \mathrm{He}\left(\begin{bmatrix} 0 \\ 0 \\ 0 \\ \mathbf{S}^{-1} \end{bmatrix} \begin{bmatrix} CA & CB & 0 & -I_m \end{bmatrix}\right) \\
&+ \mathrm{He}\left(\begin{bmatrix} 0 \\ \mathbf{S}^{-1}C - P_{12}^{\mathsf{T}} \\ P_{11} \\ -\mathbf{S}^{-1}C \end{bmatrix} \begin{bmatrix} A & B & -I_{2n} & 0 \end{bmatrix}\right),
\end{aligned}
$$

which is negative-definite thanks to hypothesis (4-23). Exploiting the properties (4-27), (4-28) and (4-29) issued from Facts 2.2 and 2.3, the expression above implies

$$
\begin{aligned}
\dot{V}(x) \leq \dot{V}(x) &+ 2\,\mathrm{dz}\,(Cx)^{\mathsf{T}}\,\mathbf{S}^{-1}(Cx - \mathrm{dz}\,(Cx) - \bar{U}h(x)) \\
&- 2\,\mathrm{dz}\,(Cx)^{\mathsf{T}}\,\mathbf{S}^{-1}(C\dot{x} - \dot{\mathrm{dz}}\,(Cx)) \\
&+ 2\,\dot{\mathrm{dz}}\,(Cx)^{\mathsf{T}}\,\mathbf{S}^{-1}(C\dot{x} - \dot{\mathrm{dz}}\,(Cx)) \\
&+ 2\,\upsilon^{\mathsf{T}}K(Ax + B\mathrm{dz}\,(Cx) - \dot{x}) = \upsilon^{\mathsf{T}}\bar{\Psi}_2\upsilon
\end{aligned} \tag{4-32}
$$

for almost all $x \in \mathcal{S}_h$. Therefore, selecting $\beta_3 = \lambda_{\min}(-\bar{\Psi}_2) > 0$, it holds that

$$
-\upsilon^{\mathsf{T}}\bar{\Psi}_2\upsilon \geq \lambda_{\min}\left(-\bar{\Psi}_2\right)|\upsilon|^2 \geq \lambda_{\min}\left(-\bar{\Psi}_2\right)|x|^2 = \beta_3|x|^2
$$

for almost all $x \in \mathcal{S}(W)$, proving the existence of positive scalar $\beta_3 = \lambda_{\min}\left(-\bar{\Psi}_2\right)$ for the condition (4-15) in Lemma 4.1, and, therefore, ensuring regional exponential stability of the origin of (4-6) from $\mathcal{S}(W)$. □

Remark 4.2: The preliminary statement (4-27) requires T_1 to be positive-definite, while facts (4-28) and (4-29) admit diagonal sign-indefinite multipliers. Hence, to preserve the convexity and feasibility of conditions (4-22) and (4-23), Theorem 4.1 takes $T_1 = T_3 = \mathbf{S}^{-1} > 0$ but, specifically for the examples in Section 4.4, selecting $T_2 = -\mathbf{S}^{-1}$ was observed to produce more voluminous estimates of the basin of attraction for (4-6). Moreover, since the gains T_1, T_2 and T_3 rely on the same decision variable $\mathbf{S}$, some conservatism upcoming from these selections may be expected in the design stage, but the analysis tools of [56] may be used a posteriori to recompute a less conservative estimate of the basin of attraction. □

With Theorem 4.1 ensuring local exponential stability of (4-6), the resulting output feedback control system may have an arbitrarily slow convergence rate or arbitrarily fast dynamics. To address this fact, the next proposition allows ensuring a prescribed spectral abscissa of A smaller than or equal to $-\alpha < 0$, which leads

to a minimum given convergence rate α for dynamics (4-6) in the linear tail of the response, and a spectral radius of A smaller than a given scalar $\rho > \alpha$.

Proposition 4.1

Given a prescribed convergence rate $\alpha \geq 0$ and a prescribed spectral radius $\rho > \alpha$, if there exist matrices $\mathbf{X} \in \mathbb{S}^n_{>0}$, $\mathbf{Y} \in \mathbb{S}^n_{>0}$, $\mathbf{Z}_p \in \mathbb{R}^{n\times m}$, $\mathbf{Z}_c \in \mathbb{R}^{n\times m}$, $\mathbf{G}_p \in \mathbb{R}^{m\times n}$, $\mathbf{G}_c \in \mathbb{R}^{m\times n}$, $\hat{\mathbf{H}}_2 \in \mathbb{R}^{m\times m}$, $\hat{\mathbf{P}}_{22} \in \mathbb{S}^m$, $\mathbf{S} \in \mathbb{D}^m_{>0}$, $\hat{\mathbf{A}}_\mathrm{c} \in \mathbb{R}^{n\times n}$, $\hat{\mathbf{B}}_\mathrm{c} \in \mathbb{R}^{n\times m}$, $\hat{\mathbf{C}}_\mathrm{c} \in \mathbb{R}^{m\times n}$, $\hat{\mathbf{D}}_\mathrm{c} \in \mathbb{R}^{m\times m}$, $\hat{\mathbf{E}}_\mathrm{c} \in \mathbb{R}^{n\times m}$, $\hat{\mathbf{T}}_{pp} \in \mathbb{S}^n$, $\hat{\mathbf{T}}_{pc} \in \mathbb{R}^{n\times n}$ and $\hat{\mathbf{T}}_{cc} \in \mathbb{S}^n$ such that conditions (4-22), (4-23) are satisfied and, additionally

$$\hat{T} = \begin{bmatrix} \hat{\mathbf{T}}_{pp} & \hat{\mathbf{T}}_{pc} \\ \hat{\mathbf{T}}_{pc}^\mathsf{T} & \hat{\mathbf{T}}_{cc} \end{bmatrix} > 0, \tag{4-33}$$

$$\Psi_3 = \mathrm{He}\begin{bmatrix} A_\mathrm{p}\mathbf{Y} + B_\mathrm{p}\hat{\mathbf{C}}_\mathrm{c} + \alpha\mathbf{Y} & A_\mathrm{p} + B_\mathrm{p}\hat{\mathbf{D}}_\mathrm{c}C_\mathrm{p} + \alpha I_n & \hat{\mathbf{T}}_{pp} - \mathbf{Y} & \hat{\mathbf{T}}_{pc} - I_n \\ \hat{\mathbf{A}}_\mathrm{c} + \alpha I_n & \mathbf{X}A_\mathrm{p} + \hat{\mathbf{B}}_\mathrm{c}C_\mathrm{p} + \alpha\mathbf{X} & \hat{\mathbf{T}}_{pc}^\mathsf{T} - I_n & \hat{\mathbf{T}}_{cc} - \mathbf{X} \\ A_\mathrm{p}\mathbf{Y} + B_\mathrm{p}\hat{\mathbf{C}}_\mathrm{c} + \alpha\mathbf{Y} & A_\mathrm{p} + B_\mathrm{p}\hat{\mathbf{D}}_\mathrm{c}C_\mathrm{p} + \alpha I_n & -\mathbf{Y} & -I_n \\ \hat{\mathbf{A}}_\mathrm{c} + \alpha I_n & \mathbf{X}A_\mathrm{p} + \hat{\mathbf{B}}_\mathrm{c}C_\mathrm{p} + \alpha\mathbf{X} & -I_n & -\mathbf{X} \end{bmatrix} < 0, \tag{4-34}$$

$$\Psi_4 = \mathrm{He}\begin{bmatrix} -\frac{1}{2}\rho\mathbf{Y} & -\rho I_n & A_\mathrm{p}\mathbf{Y} + B_\mathrm{p}\hat{\mathbf{C}}_\mathrm{c} & A_\mathrm{p} + B_\mathrm{p}\hat{\mathbf{D}}_\mathrm{c}C_\mathrm{p} \\ 0 & -\frac{1}{2}\rho\mathbf{X} & \hat{\mathbf{A}}_\mathrm{c} & \mathbf{X}A_\mathrm{p} + \hat{\mathbf{B}}_\mathrm{c}C_\mathrm{p} \\ 0 & 0 & -\frac{1}{2}\rho\mathbf{Y} & -\rho I_n \\ 0 & 0 & 0 & -\frac{1}{2}\rho\mathbf{X} \end{bmatrix} < 0 \tag{4-35}$$

also hold, then the origin of (4-6) with the controller state-space model matrices A_c, B_c, C_c, D_c and E_c selected as in (4-19) is locally exponentially stable from $\mathcal{S}(W)$ and the eigenvalues of A in (4-6) have real part smaller than $-\alpha$ and a modulus smaller than ρ.

Proof: The proof of the local exponential stability of the origin of (4-6) from $\mathcal{S}(W)$ under (4-22), (4-23) has been given in the proof of Theorem 4.1. To show that $\lambda_{\max}(A) < -\alpha$, introduce the matrix

$$T := \Pi^{-\mathsf{T}}\hat{T}\Pi^{-1},$$

with $\hat{T}$ defined as in (4-33). Then, hypothesis (4-34) implies

$$\begin{bmatrix} \Pi & 0 \\ 0 & \Pi \end{bmatrix}^{-\mathsf{T}} \Psi_3 \begin{bmatrix} \Pi & 0 \\ 0 & \Pi \end{bmatrix}^{-1} = \mathrm{He}\begin{bmatrix} P_{11}(A + \alpha I_{2n}) & T - P_{11} \\ P_{11}(A + \alpha I_{2n}) & -P_{11} \end{bmatrix},$$

which is negative definite due to hypothesis (4-34) and, pre- and post-multiplied by

$$\begin{bmatrix} x^\mathsf{T} & x^\mathsf{T}(A + \alpha I_{2n})^\mathsf{T} \end{bmatrix}$$

and its transpose, reads

$$x^\mathsf{T}\mathrm{He}(T(A + \alpha I_{2n}))x < 0,$$

proving that matrix $A + \alpha I_{2n}$ is Hurwitz. Furthermore, exploiting the results of [8]

and the invertibility of Π in (4-25), to show that the spectral radius of A is smaller than ρ, pre- and post-multiply Ψ_4 in (4-35) by

$$\begin{bmatrix} \Pi^{-\mathsf{T}} & 0 \\ 0 & \Pi^{-\mathsf{T}} \end{bmatrix}$$

and its transpose. This product leads to

$$\mathrm{He}\begin{bmatrix} -\frac{1}{2}\rho P_{11} & P_{11}A \\ 0 & -\frac{1}{2}\rho P_{11} \end{bmatrix}, \tag{4-36}$$

which is negative-definite by assumption (4-35) and corresponds to the characteristic LMI region of a disk of radius ρ centered on the origin, ensuring that the eigenvalues of A in (4-6) have modulus smaller than ρ. □

Although Proposition 4.1 allows to determine an estimate of the basin of attraction of the origin of (4-6), it does not provide means to maximize the volume of $\mathcal{S}(W)$. Therefore, the following remark discuss about some supplementary elements that allow solving Problem 3.1 in its entirely.

Remark 4.3: Following a similar approach to [65, Section 3.4.3], minimizing

$$\mathrm{trace}(P_{11}) = \mathrm{trace}(\mathbf{X}) + \mathrm{trace}(\tilde{X}) \tag{4-37}$$

indirectly maximizes the volume of $\mathcal{S}(W)$. Moreover, from the definitions in (4-16), it can be found that $\tilde{X} = \mathbf{M}^{\mathsf{T}}\left(\mathbf{X} - \mathbf{Y}^{-1}\right)^{-1}\mathbf{M}$. Therefore, introducing a matrix $\mathbf{V} \in \mathbb{S}^n_{>0}$ and imposing

$$\mathbf{M} + \mathbf{M}^{\mathsf{T}} > 0 \tag{4-38}$$

inequality $\tilde{X} \leq \mathbf{V}$ can be enforced (by a Schur complement) via the LMI

$$\begin{bmatrix} \mathbf{V} & \mathbf{M}^{\mathsf{T}} & 0 \\ \mathbf{M} & \mathbf{X} & I_n \\ 0 & I_n & \mathbf{Y} \end{bmatrix} \geq 0. \tag{4-39}$$

As a consequence, the cost (4-37) can be replaced with

$$\mathrm{trace}(\mathbf{X}) + \mathrm{trace}\big(\tilde{X}\big) \;\leq\; \mathrm{trace}(\mathbf{X}) + \mathrm{trace}(\mathbf{V})$$

under constraint (4-39), which leads to the convex optimization problem

$$\begin{array}{ll} \min\limits_{\substack{\mathbf{V},\mathbf{X},\mathbf{Y},\mathbf{Z}_{\mathrm{p}},\mathbf{Z}_{\mathrm{c}},\hat{\mathbf{P}}_{22},\mathbf{S},\\ \hat{\mathbf{A}}_{\mathrm{c}},\hat{\mathbf{B}}_{\mathrm{c}},\hat{\mathbf{C}}_{\mathrm{c}},\hat{\mathbf{D}}_{\mathrm{c}},\hat{\mathbf{E}}_{\mathrm{c}},\\ \mathbf{G}_{\mathrm{p}},\mathbf{G}_{\mathrm{c}},\hat{\mathbf{H}}_2,\hat{\mathbf{T}}_{pp},\hat{\mathbf{T}}_{pc},\hat{\mathbf{T}}_{cc}}} & \mathrm{trace}(\mathbf{X}) + \mathrm{trace}(\mathbf{V}),\ \text{subject to} \\ & \text{(4-22), (4-23), (4-34), (4-35), (4-38), (4-39).} \end{array} \tag{4-40}$$

Due to Proposition 4.1, problem (4-40) allows determining optimal controller matrices $A_{\mathrm{c}} \in \mathbb{R}^{n\times n}$, $B_{\mathrm{c}} \in \mathbb{R}^{n\times m}$, $C_{\mathrm{c}} \in \mathbb{R}^{m\times n}$, $D_{\mathrm{c}} \in \mathbb{R}^{m\times m}$ and $E_{\mathrm{c}} \in \mathbb{R}^{n\times m}$ that maximize the volume of $\mathcal{S}(W)$ while ensuring a prescribed convergence rate α and a spectral radius smaller than ρ for matrix A in (4-6). Moreover, notice that whenever the optimization (4-40) produces any $P_{22} < 0$, the volume of $\mathcal{S}(W)$ increases since, in such a case, $\mathrm{trace}(P_{11}) > \mathrm{trace}(P)$. □

4.3.2 Global stability results

For the global stabilization, Problem 3.2, let $H_1 = 0$ and $H_2 = 0$ so that $\mathcal{S}_h = \mathbb{R}^n$ and let the saturation function be asymmetric, as originally defined in (4-2). Therefore, using the Lyapunov function candidate V in (4-10), the next theorem allows synthesize the dynamic output-feedback controller (4-4) globally exponentially stabilizing the input-saturated plant (4-1) under conditions formulated in form of LMIs.

Theorem 4.2

Given a desired convergence rate $\alpha \geq 0$, if there exist matrices $\mathbf{X} \in \mathbb{S}^n_{>0}$, $\mathbf{Y} \in \mathbb{S}^n_{>0}$, $\mathbf{Z}_\mathrm{p} \in \mathbb{R}^{n\times m}$, $\mathbf{Z}_\mathrm{c} \in \mathbb{R}^{n\times m}$, $\hat{\mathbf{P}}_{22} \in \mathbb{S}^m$, $\mathbf{S} \in \mathbb{D}^m_{>0}$, $\hat{\mathbf{A}}_\mathrm{c} \in \mathbb{R}^{n\times n}$, $\hat{\mathbf{B}}_\mathrm{c} \in \mathbb{R}^{n\times m}$, $\hat{\mathbf{C}}_\mathrm{c} \in \mathbb{R}^{m\times n}$, $\hat{\mathbf{D}}_\mathrm{c} \in \mathbb{R}^{m\times m}$, $\hat{\mathbf{E}}_\mathrm{c} \in \mathbb{R}^{n\times m}$, $\hat{\mathbf{T}}_{pp} \in \mathbb{S}^n$, $\hat{\mathbf{T}}_{pc} \in \mathbb{R}^{n\times n}$ and $\hat{\mathbf{T}}_{cc} \in \mathbb{S}^n$ satisfying

$$\hat{T} = \begin{bmatrix} \hat{\mathbf{T}}_{pp} & \hat{\mathbf{T}}_{pc} \\ \hat{\mathbf{T}}_{pc}^\mathsf{T} & \hat{\mathbf{T}}_{cc} \end{bmatrix} > 0, \tag{4-41}$$

$$\Psi_5 = \mathrm{He}\begin{bmatrix} \frac{1}{2}\mathbf{Y} & 0 & \mathbf{Z}_\mathrm{p} \\ I_{n_p} & \frac{1}{2}\mathbf{X} & \mathbf{Z}_\mathrm{c} \\ -\hat{\mathbf{C}}_\mathrm{c} & -\hat{\mathbf{D}}_\mathrm{c}C_\mathrm{p} & \frac{1}{2}\hat{\mathbf{P}}_{22} + \mathbf{S} \end{bmatrix} > 0, \tag{4-42}$$

$$\Psi_6 = \mathrm{He}\begin{bmatrix} A_\mathrm{p}\mathbf{Y} + B_\mathrm{p}\hat{\mathbf{C}}_\mathrm{c} & A_\mathrm{p} + B_\mathrm{p}\hat{\mathbf{D}}_\mathrm{c}C_\mathrm{p} & -B_\mathrm{p}\mathbf{S} & 0 & 0 & \mathbf{Z}_\mathrm{p} \\ \hat{\mathbf{A}}_\mathrm{c} & \mathbf{X}A_\mathrm{p} + \hat{\mathbf{B}}_\mathrm{c}C_\mathrm{p} & \hat{\mathbf{E}}_\mathrm{c} & 0 & 0 & \mathbf{Z}_\mathrm{c} \\ \hat{\mathbf{C}}_\mathrm{c} & \hat{\mathbf{D}}_\mathrm{c}C_\mathrm{p} & -\mathbf{S} & \mathbf{Z}_\mathrm{p}^\mathsf{T} + \hat{\mathbf{C}}_\mathrm{c} & \mathbf{Z}_\mathrm{c}^\mathsf{T} + \hat{\mathbf{D}}_\mathrm{c}C_\mathrm{p} & \hat{\mathbf{P}}_{22} \\ A_\mathrm{p}\mathbf{Y} + B_\mathrm{p}\hat{\mathbf{C}}_\mathrm{c} & A_\mathrm{p} + B_\mathrm{p}\hat{\mathbf{D}}_\mathrm{c}C_\mathrm{p} & -B_\mathrm{p}\mathbf{S} & -\mathbf{Y} & -I_n & 0 \\ \hat{\mathbf{A}}_\mathrm{c} & \hat{\mathbf{X}}A_\mathrm{p} + \hat{\mathbf{B}}_\mathrm{c}C_\mathrm{p} & \hat{\mathbf{E}}_\mathrm{c} & -I_n & -\mathbf{X} & 0 \\ 0 & 0 & -\mathbf{S} & \hat{\mathbf{C}}_\mathrm{c} & \hat{\mathbf{D}}_\mathrm{c}C_\mathrm{p} & -\mathbf{S} \end{bmatrix} < 0 \tag{4-43}$$

$$\Psi_7 = \mathrm{He}\begin{bmatrix} A_\mathrm{p}\mathbf{Y} + B_\mathrm{p}\hat{\mathbf{C}}_\mathrm{c} + \alpha\mathbf{Y} & A_\mathrm{p} + B_\mathrm{p}\hat{\mathbf{D}}_\mathrm{c}C_\mathrm{p} + \alpha I_n & \hat{\mathbf{T}}_{pp} - \mathbf{Y} & \hat{\mathbf{T}}_{pc} - I_n \\ \hat{\mathbf{A}}_\mathrm{c} + \alpha I_n & \mathbf{X}A_\mathrm{p} + \hat{\mathbf{B}}_\mathrm{c}C_\mathrm{p} + \alpha\mathbf{X} & \hat{\mathbf{T}}_{pc}^\mathsf{T} - I_n & \hat{\mathbf{T}}_{cc} - \mathbf{X} \\ A_\mathrm{p}\mathbf{Y} + B_\mathrm{p}\hat{\mathbf{C}}_\mathrm{c} + \alpha\mathbf{Y} & A_\mathrm{p} + B_\mathrm{p}\hat{\mathbf{D}}_\mathrm{c}C_\mathrm{p} + \alpha I_n & -\mathbf{Y} & -I_n \\ \hat{\mathbf{A}}_\mathrm{c} + \alpha I_n & \mathbf{X}A_\mathrm{p} + \hat{\mathbf{B}}_\mathrm{c}C_\mathrm{p} + \alpha\mathbf{X} & -I_n & -\mathbf{X} \end{bmatrix} < 0 \tag{4-44}$$

then the origin of (4-6) with the controller state-space model matrices A_c, B_c, C_c, D_c and E_c as selected in (4-19) is globally exponentially stable. Moreover, the eigenvalues of A in (4-6) have real part smaller than $-\alpha$.

Proof: Taking $H_1 = 0$ and $H_2 = 0$ in (4-8), W coincides with V in all the state-space $\mathbb{R}^{2n}$ and, therefore, the existence of the positive scalars β_1 and β_2 ensuring the positive-definiteness of V can be proven following a similar procedure to the one used in Theorem 4.1, in this case focusing on the positive-definiteness of the upper left three block rows and columns of matrix Ψ_1 in condition (4-22). Introducing the

invertible matrix

$$\Pi := \begin{bmatrix} \mathbf{Y} & I_n \\ N^\mathsf{T} & 0 \end{bmatrix}, \tag{4-45}$$

which certainly also satisfies the properties in (4-26), combined with the fact that

$$\mathrm{dz}\,(Cx)^\mathsf{T} T_4(Cx - \mathrm{dz}\,(Cx)) \geq 0, \tag{4-46}$$

derived from the global property (2-26) presented in Section 2.4, it is possible to obtain the matrix

$$\bar{\Psi}_5 := \mathrm{He}\begin{bmatrix} \frac{1}{2}P_{11} & P_{12} \\ -\mathbf{S}^{-1}C & \frac{1}{2}P_{22} + \mathbf{S}^{-1} \end{bmatrix} \tag{4-47}$$

by pre- and post-multiplying Ψ_5 in (4-42) by

$$\begin{bmatrix} \Pi & 0 \\ 0 & \mathbf{S} \end{bmatrix}^{-\mathsf{T}}$$

and its transpose. Since (4-47) is positive-definite due to hypothesis (4-42), it verifies, for all $x \in \mathbb{R}^{2n}$,

$$\begin{aligned} V(x) &\geq V(x) - 2\,\mathrm{dz}\,(Cx)^\mathsf{T}\mathbf{S}^{-1}(Cx - \mathrm{dz}\,(Cx)) \\ &= \eta^\mathsf{T}\bar{\Psi}_5\eta \geq \lambda_{\min}(\bar{\Psi}_5)\,|\eta|^2 \geq \lambda_{\min}(\bar{\Psi}_5)\,|x|^2 = \beta_1\,|x|^2\,. \end{aligned} \tag{4-48}$$

Moreover, using $|\mathrm{dz}\,(Cx)| \leq |Cx| \leq L\,|x|$, note that

$$V(x) \leq \lambda_{\max}(P)\,|\eta|^2 \leq \lambda_{\max}(P)L\,|x|^2 = \beta_2\,|x|^2\,,$$

which, together with (4-48), proves the existence of the scalars $\beta_1 = \lambda_{\min}(\bar{\Psi}_5)$ and $\beta_2 = \lambda_{\max}(P)$ with $W(x) = V(x)$ in (4-14) for all $x \in \mathbb{R}^{2n}$, ensuring the positive-definiteness and radial-unboundedness of V. On the other hand, selecting $H_1 = 0$ and $H_2 = 0$, as well as considering the global sector condition (4-46), it follows that $\Psi_6 = \Psi_2$ in (4-23) and $\Psi_7 = \Psi_3$ in (4-34), thus the proofs of the global exponential stability of the origin of (4-6) and the Hurwitz property of matrix $A + \alpha I_{2n}$ is shown as in the proofs of Theorem 4.1 and Proposition 4.1, respectively. □

4.4 Numerical examples

4.4.1 Balancing pointer

Consider the balancing pointer SISO example in [65, Example 3.4]. Thus let $\overline{u} = 5$, $\alpha = 0.5$, $\rho = 10$ and

$$A_\mathrm{p} = \begin{bmatrix} 0 & 1 \\ 1 & 0 \end{bmatrix}, \quad B_\mathrm{p} = \begin{bmatrix} 0 \\ -1 \end{bmatrix}, \quad C_\mathrm{p} = \begin{bmatrix} 1 & 0 \end{bmatrix}. \tag{4-49}$$

For this exponentially unstable plant, leveraging Theorem 4.1 and Remark 4.3, using the selections in (4-16), (4-18) and (4-19), the optimizer produces a controller

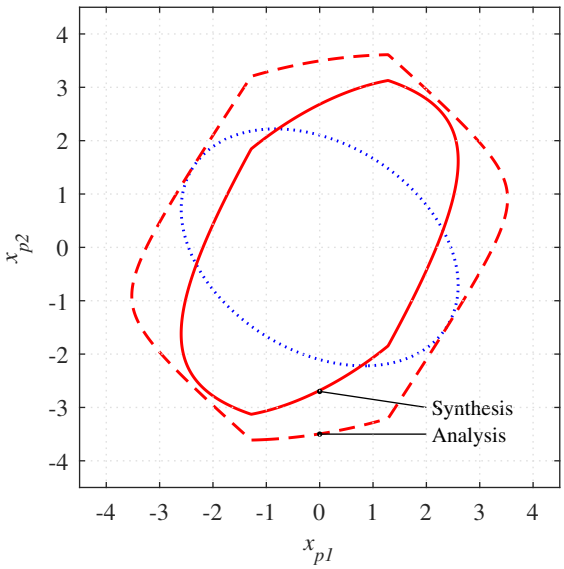

Figure 4.2: Estimate $\mathcal{S}(W)$ of the basin of attraction of the origin of the closed loop (4-49), (4-50) in the synthesis phase (solid red) and in the analysis phase (dashed red). Quadratic estimate obtained using the solution of [11] in dotted blue.

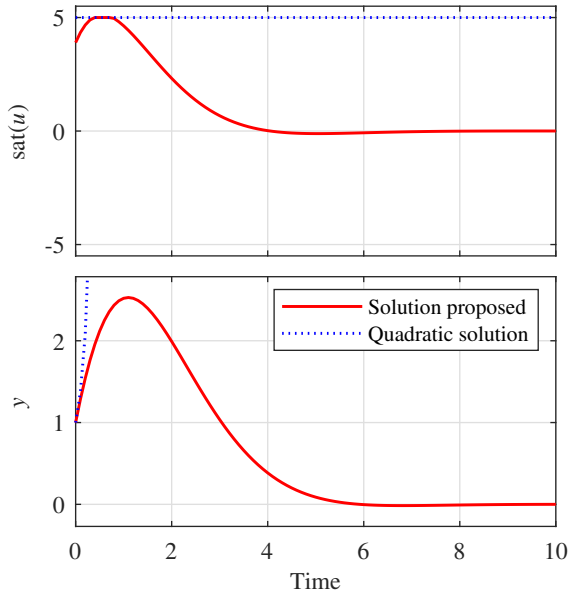

Figure 4.3: Controller (4-50) and plant (4-49) output responses from the initial state $x_0 = \begin{bmatrix}1 & 3 & 0 & 0\end{bmatrix}^\mathsf{T}$.

guaranteeing regional exponential stability with state-space matrices

$$A_c = \begin{bmatrix}-2.1075 & 0.5482\\ 0.5258 & -2.2020\end{bmatrix}, \qquad B_c = \begin{bmatrix}-2.0303\\ 2.1958\end{bmatrix}\cdot 10^3, \quad E_c = \begin{bmatrix}5.0368\\ -5.3993\end{bmatrix}\cdot 10^2$$
$$C_c = \begin{bmatrix}1.4809 & -1.6369\end{bmatrix}\cdot 10^{-3}, \quad D_c = 3.8971, \tag{4-50}$$

and a sign-indefinite matrix P with eigenvalues

$$\lambda(P) = \{2.0800\cdot 10^{-1}, 7.0724\cdot 10^{-2}, -5.7345\cdot 10^{-2}, 1.0860\cdot 10^{-12}, 1.8044\cdot 10^{-7}\}.$$

Figure 4.2 shows the solid red estimate $\mathcal{S}(W)$ of the basin of attraction of the controlled closed-loop system, obtained by running (4-40) to design the controller matrices. For the synthesis phase, $\mathcal{S}(W)$ is 27.5% larger than the quadratic estimate found with the solution of [11]. Furthermore, leveraging the results in [56], the

subsequent stability analysis of the closed-loop system produces a more voluminous non-ellipsoidal set $\mathcal{S}(W)$, which is coherent with Remarks 4.2 and 4.3. Figure 4.3 shows the saturated control signal sat (u) and the plant output response y from the initial state $x_0 = \begin{bmatrix}1 & 3 & 0 & 0\end{bmatrix}^\mathsf{T}$. The control signal is observed to converge to the origin with the procedure in Remark 4.3 (red solid), while it remains saturated with the solution of [11] (blue dotted).

4.4.2 MIMO academic Example 1

Consider the MIMO exponentially unstable plant in [23, Example 2] with

$$A_\mathrm{p} = \begin{bmatrix}0.1 & -0.1\\ 0.1 & -3\end{bmatrix}, \quad B_\mathrm{p} = \begin{bmatrix}5 & 0\\ 0 & 1\end{bmatrix}, \quad C_\mathrm{p} = I_2, \tag{4-51}$$

$\overline{u} = \begin{bmatrix}5 & 2\end{bmatrix}^\mathsf{T}$, $\alpha = 2.5$ and $\rho = 100$. In this case, exploiting the proposed stability certificates and parameterizations (4-16) to (4-19), the optimizer returns the controller state-space model matrices

$$\begin{aligned}
A_\mathrm{c} &= \begin{bmatrix}-2.8947 & -0.0064\\ 0.0046 & -2.8628\end{bmatrix}, & B_\mathrm{c} &= \begin{bmatrix}-0.8332 & -0.0624\\ -0.3043 & 1.4487\end{bmatrix},\\
C_\mathrm{c} &= \begin{bmatrix}-0.0247 & -0.0252\\ 0.6426 & 0.3646\end{bmatrix}\cdot 10^{-4}, & D_\mathrm{c} &= \begin{bmatrix}-5.7010 & 0.1093\\ 0.26670 & -1.7815\end{bmatrix}\cdot 10^{-1},\\
E_\mathrm{c} &= \begin{bmatrix}17.7281 & -0.4332\\ -0.3013 & 3.9641\end{bmatrix},
\end{aligned} \tag{4-52}$$

Furthermore, the obtained matrix P has eigenvalues

$$\lambda(P) = \{-2.6336\cdot 10^{-4}, 3.1426\cdot 10^{-5}, 1.4229\cdot 10^{-5},\\ -3.2326\cdot 10^{-6}, 1.9984\cdot 10^{-9}, 1.9913\cdot 10^{-9}\}.$$

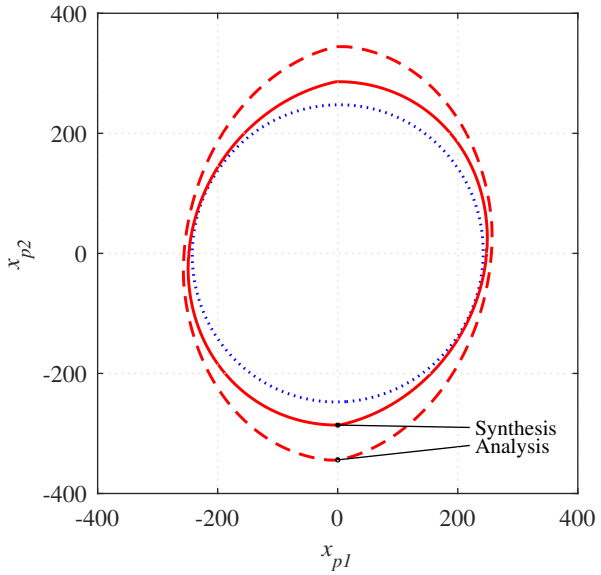

Figure 4.4: Estimate $\mathcal{S}(W)$ of the basin of attraction of the origin of the closed loop (4-51), (4-52) in the synthesis phase (solid red) and in the analysis phase (dashed red). Quadratic estimate obtained using the solution of [19] in dotted blue.

Figure 4.4 reports on the estimate of the basin of attraction of the controlled closed-loop system, which, in the synthesis phase, is 15.9% larger if estimated with the optimization criterion proposed in Section 4.3, as compared to the estimate obtained with the solution in [65, Section 3.4.3] using a classical quadratic Lyapunov function. On the other hand, Figures 4.5 and 4.6 show the faster response of the saturated control signal $\text{sat}(u)$ and plant output y from the initial state $x_0 = \begin{bmatrix} 250 & 0 & 0 & 0 \end{bmatrix}^\mathsf{T}$ obtained with the solution in Remark 4.3, as compared to the dynamics resulting from the quadratic construction of [65, Section 3.4.3].

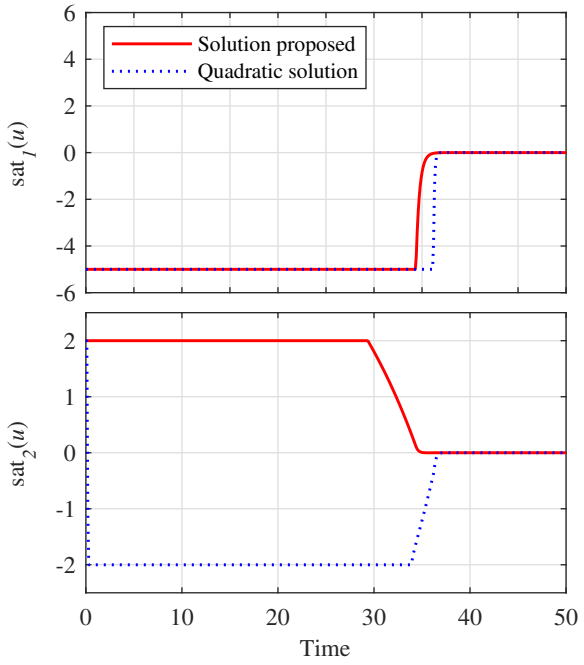

Figure 4.5: Controller (4-50) saturated output response from the initial state $x_0 = \begin{bmatrix} 250 & 0 & 0 & 0 \end{bmatrix}^\mathsf{T}$.

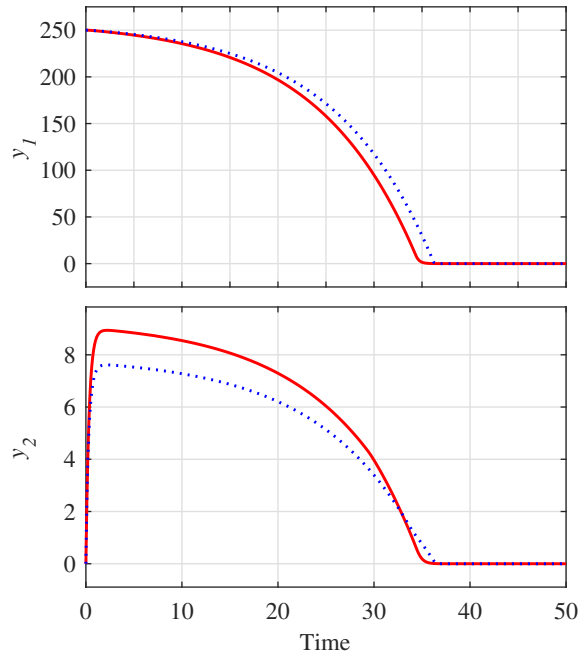

Figure 4.6: Plant (4-49) output response from the initial state $x_0 = \begin{bmatrix} 250 & 0 & 0 & 0 \end{bmatrix}^\mathsf{T}$.

4.4.3 SISO example 1

Consider the SISO exponentially stable plant with state-space model matrices

$$A_{\mathrm{p}} = \begin{bmatrix} -3 & 1 \\ 1 & -2 \end{bmatrix}, \qquad B_{\mathrm{p}} = \begin{bmatrix} 1 \\ 0.5 \end{bmatrix}, \qquad C_{\mathrm{p}} = \begin{bmatrix} 1 & 1 \end{bmatrix}, \tag{4-53}$$

and $\underline{u} = \overline{u} = 2$, $M = I_n$. In a first case, take $\alpha = 0.1$. The controller state-space model matrices obtained from Theorem 4.2 are then

$$\begin{aligned} A_{\mathrm{c}} &= \begin{bmatrix} -2.2293 & 0.7734 \\ 1.5373 & -2.2945 \end{bmatrix}, & B_{\mathrm{c}} &= \begin{bmatrix} -1.0674 \\ -2.4750 \end{bmatrix}, & E_{\mathrm{c}} &= \begin{bmatrix} 10.3178 \\ 9.4127 \end{bmatrix} \\ C_{\mathrm{c}} &= \begin{bmatrix} -0.0196 & 0.0567 \end{bmatrix}, & D_{\mathrm{c}} &= 0.6973, \end{aligned} \tag{4-54}$$

while the matrix P determined from (4-16), (4-18), (4-20) has eigenvalues

$$\lambda(P) = \{2.8377 \cdot 10^{3},\ 2.5999 \cdot 10^{2},\ -8.5063 \cdot 10^{-3}, 6.6814 \cdot 10^{-3},\ 7.1259 \cdot 10^{-4}\},$$

where there is a negative eigenvalue, showing that the optimizer exploits a sign-indefinite P for V in (4-10). Figure 4.7 shows, at top, the controller (4-54) saturated output, and, at bottom, the input-output response of (4-6) and with the plant and controller matrices in (4-53) and (4-54), respectively, from the initial state $x_0 = \begin{bmatrix} -2.5 & -2.5 & 0 & 0 \end{bmatrix}^{\mathsf{T}}$, carefully chosen to have an initial output $y(0) = -5$. It is possible to observe that the proposed controller synthesis (red solid) eliminates the overshoot and reduces the settling time, as compared to the response obtained with the solution proposed in [19] (blue dotted), which is based on positive-definite quadratic forms.

In a second case, let $\alpha = 1.5$. With this given prescribed convergence rate, the

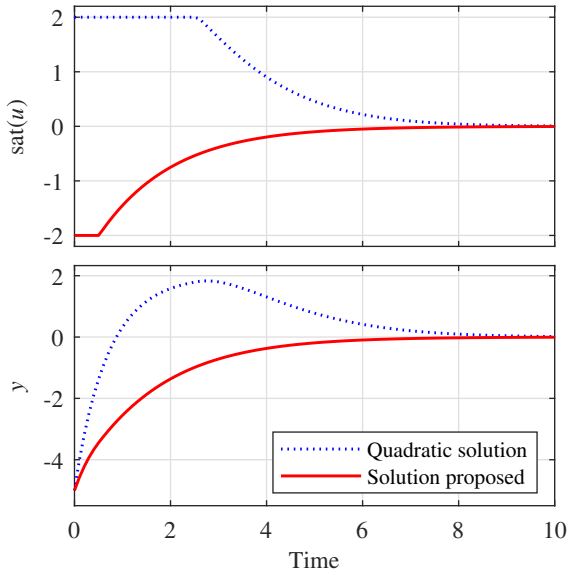

Figure 4.7: Controller (4-54) and plant (4-53) output responses from the initial state $x_0 = \begin{bmatrix} -2.5 & -2.5 & 0 & 0 \end{bmatrix}^{\mathsf{T}}$.

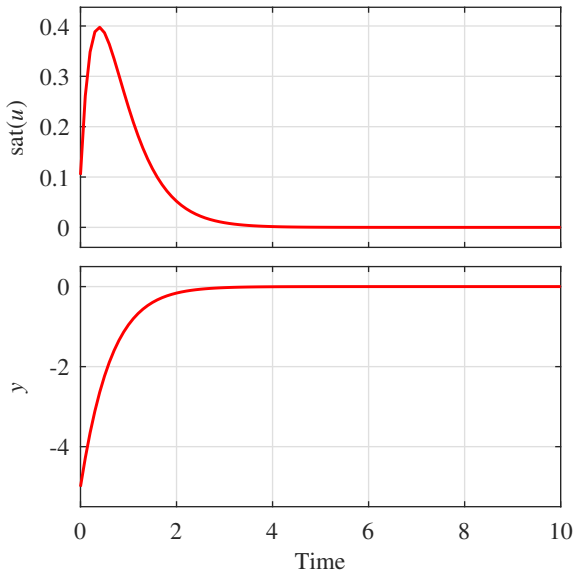

Figure 4.8: Controller (4-55) and plant (4-53) output responses from the initial state $x_0 = \begin{bmatrix}-2.5 & -2.5 & 0 & 0\end{bmatrix}^{\mathsf{T}}$.

controller obtained from Theorem 4.2 is

$$A_{\mathrm{c}} = \begin{bmatrix}-2.7776 & 0.5282\\ 0.6388 & -2.7664\end{bmatrix}, \qquad B_{\mathrm{c}} = \begin{bmatrix}0.4417\\ -4.9914\end{bmatrix}, \qquad E_{\mathrm{c}} = \begin{bmatrix}7.9591\\ 6.1248\end{bmatrix},$$
$$C_{\mathrm{c}} = \begin{bmatrix}-0.0285 & 0.0439\end{bmatrix}, \qquad D_{\mathrm{c}} = -0.0817. \tag{4-55}$$

Whereas the quadratic solution exposed in [19] is not able to find a feasible selection for the controller (4-4), the solution proposed in Theorem 4.2 returns a sign-indefinite matrix P with eigenvalues

$$\lambda(P) = \{1.0801\cdot 10^{3},\ 2.8081\cdot 10^{2},\ -9.2740\cdot 10^{-2}, 7.3939\cdot 10^{-3},\ 9.6861\cdot 10^{-4}\}.$$

Figure 4.8 shows the input-output response of the closed-loop (4-6) with the plant (4-53) and controller (4-55).

4.4.4 MIMO academic example 2

Apply now the proposed global controller design procedure in Theorem 4.2 to a MIMO example based on [69, Example 4.3.2]. Let $\bar{u} = \begin{bmatrix}1 & 1\end{bmatrix}^{\mathsf{T}}$, $M = I_n$, $\alpha = 5\cdot 10^{-3}$ and

$$A_{\mathrm{p}} = \begin{bmatrix}-0.01 & 0\\ 0 & -0.01\end{bmatrix}, \qquad B_{\mathrm{p}} = \begin{bmatrix}1 & 0\\ 0 & 1\end{bmatrix}, \qquad C_{\mathrm{p}} = \begin{bmatrix}-0.4 & 0.5\\ -0.1 & 0.1\end{bmatrix}. \tag{4-56}$$

For this exponentially stable plant, the optimizer produces a state-space model of the controller with

$$A_{\mathrm{c}} = \begin{bmatrix}-0.6882 & 0\\ 0 & -0.6882\end{bmatrix}, \quad B_{\mathrm{c}} = \begin{bmatrix}8.4412 & -10.5515\\ 2.1103 & -8.4412\end{bmatrix}, \quad E_{\mathrm{c}} = \begin{bmatrix}6.0818 & 0\\ 0 & 6.0818\end{bmatrix},$$

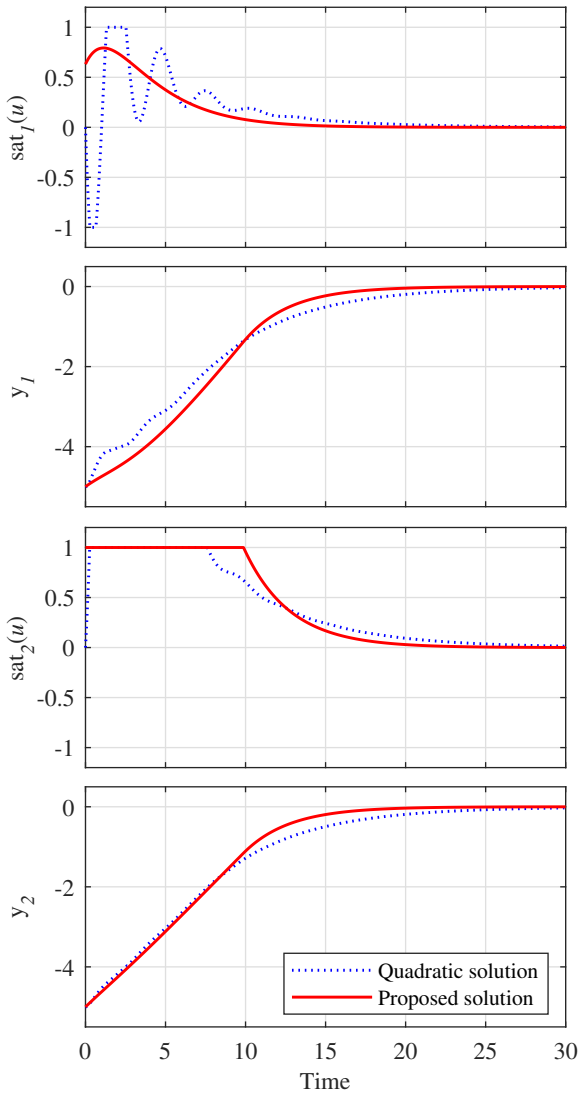

Figure 4.9: Saturated controller (4-57) and plant (4-56) output responses from the initial state $x_0 = \begin{bmatrix} -4.54 & -13.63 & 0 & 0 \end{bmatrix}^\mathsf{T}$.

$$C_\mathrm{c} = \begin{bmatrix} 0.0108 & 0 \\ 0 & 0.0108 \end{bmatrix}, \qquad D_\mathrm{c} = \begin{bmatrix} 0.7927 & -0.9909 \\ 0.1982 & -0.7927 \end{bmatrix}, \tag{4-57}$$

and a positive-definite matrix P with eigenvalues

$$\lambda(P) = \{2.6155 \cdot 10^{-3}, 2.4781 \cdot 10^{-1}, 2.2429 \cdot 10^{2}, \\ 2.2429 \cdot 10^{2}, 2.6155 \cdot 10^{-3}, 2.4781 \cdot 10^{-1}\}.$$

Figure 4.9 reports on the input-output response and the saturated control signal of (2-3) with the state-space matrices in (4-56) and (4-57) from the initial state $x_0 = \begin{bmatrix} -4.5455 & -13.6364 & 0 & 0 \end{bmatrix}^\mathsf{T}$. Analogous to Example 4.4.3, these initial conditions are chosen in such a way that $y(0) = \begin{bmatrix} -5 & -5 \end{bmatrix}^\mathsf{T}$. Notice that, despite the positive-definiteness condition of P, whic does not exploit the sign-indefiniteness of the quadratic form, a smoother and faster convergence of outputs y_1 and y_2 is obtained, as compared to the response found with the method suggested in [65, Proposition 3.18] using a classic quadratic Lyapunov function.

4.5 Conclusions

In this chapter, we addressed the design of a dynamic output-feedback controller including an anti-windup loop ensuring regional exponential stability of closed-loop systems with exponentially unstable plants subject to input saturation, as well as global exponential stability of closed-loop systems with ANCBC plants. Moreover, the designed controllers are of the same order as the plant order and respond to the synthesis Problems 3.1 and 3.2 stated in Section 3.2.2. The design conditions are formulated in terms of LMIs and derived by combining the use of sign-indefinite quadratic forms, appropriate changes of variables inspired from [58], and generalized sector conditions involving the dead-zone nonlinearity and its directional time derivative. Furthermore, the use of the deadzone nonlinearity in the Lyapunov function candidates used on the presented numerical examples allows for some conservativeness mitigation with respect to traditional quadratic approaches.

Chapter 5

Static linear anti-windup synthesis

5.1 Introduction

This chapter compiles static anti-windup gains design procedures for closed-loop linear systems with saturating inputs ensuring, for general linear plants, regional exponential stability of the origin [50] or, for exponentially stable plants, global exponential stability of the origin [55], thus responding to Problems 3.3 and 3.4 formulated in Section 3.2.2. The presented solutions also provide guarantees on the convergence rate for the global and regional results, and maximized non-ellipsoidal estimates of the basin of attraction when global exponential stability is not obtainable. The stability certificates are based on sign-indefinite quadratic forms leading to locally positive definite nonquadratic piecewise smooth Lyapunov functions and are formulated in terms of Bilinear Matrix Inequalities (BMIs).

Some preliminary concepts necessary for the approach used in this chapter are defined in Section 5.2. Section 5.3 presents the stability conditions certifying regional and global exponential stability. Additionally, to solve the BMI conditions inherent to this approach, four iterative algorithms based on a convex-concave decomposition are proposed in Section 5.4. Some numerical applications are presented in Section 5.5 to illustrate the effectiveness of the proposed methods.

5.2 Preliminaries

Consider the closed-loop system with plant

$$\left| \begin{array}{rcl} \dot{x}_p & = & A_{\mathrm{p}} x_p + B_{\mathrm{p}} \mathrm{sat}\,(u) \\ y & = & C_{\mathrm{p}} x_p + D_{\mathrm{p}} \mathrm{sat}\,(u) \end{array} \right. \tag{5-1}$$

and controller

$$\left| \begin{array}{rcl} \dot{x}_c &=& A_{\mathrm{c}} x_c + B_{\mathrm{c}} y + \nu_x \\ u &=& C_{\mathrm{c}} x_c + D_{\mathrm{c}} y + \nu_u \end{array} \right. , \tag{5-2}$$

where $x_p \in \mathbb{R}^{n_p}$, $y \in \mathbb{R}^p$ are the plant state and output, $x_c \in \mathbb{R}^{n_c}$, $u \in \mathbb{R}^m$ are the controller state and output, respectively. Moreover, the decentralized symmetric saturation function is denoted with components

$$\mathrm{sat}_i(u_i) := \max\{-\overline{u}_i, \min\{\overline{u}_i, u_i\}\}, \tag{5-3}$$

where $i = 1, ..., m$ and $\overline{u}_i > 0$ are the saturation limits and u_i and $\overline{u}_i$ are the ith entry of the vectors u and $\overline{u}$, respectively. According to the developments in section 2.3, the linear feedback (5-1)-(5-2) is locally well-posed if and only if there exist the inverses

$$\Delta_u := (I_m - D_{\mathrm{c}} D_{\mathrm{p}})^{-1}, \qquad \Delta_y := (I_p - D_{\mathrm{p}} D_{\mathrm{c}})^{-1}. \tag{5-4}$$

Assumption 5.1

The controller-plant feedback with (5-2), (5-1) is locally well-posed (the inverse matrices in (5-4) exist) and locally exponentially stable with $\nu_x = 0$, $\nu_u = 0$ and $\mathrm{sat}(u) = u$.

Define the deadzone as $\mathrm{dz}(u) := u - \mathrm{sat}(u)$ and select the Anti-windup inputs ν_x and ν_u as

$$\nu_x := \mathbf{E}_{\mathrm{c}} \mathrm{dz}(u), \qquad \nu_u := \mathbf{F}_{\mathrm{c}} \mathrm{dz}(u), \tag{5-5}$$

where $\mathbf{E}_{\mathrm{c}} \in \mathbb{R}^{n_c \times m}$ and $\mathbf{F}_{\mathrm{c}} \in \mathbb{R}^{m \times m}$ are the anti-windup gains to be designed. Notice that the algorithm design makes sense if and only if Assumption 5.1 is satisfied because the anti-windup inputs ν_x and ν_u are zero in a neighborhood of the origin. By applying definitions (5-4) and (5-5), the feedback interconnection (5-1)–(5-2) can be rewritten as

$$\left| \begin{array}{rcl} \dot{x} &=& Ax + \left(B_0 + B_{\mathrm{aw}} \begin{bmatrix} \mathbf{E}_{\mathrm{c}} \\ \mathbf{F}_{\mathrm{c}} \end{bmatrix} \right) \mathrm{dz}(u) \\ u &=& Cx + \left(D_0 + D_{\mathrm{aw}} \begin{bmatrix} \mathbf{E}_{\mathrm{c}} \\ \mathbf{F}_{\mathrm{c}} \end{bmatrix} \right) \mathrm{dz}(u) \end{array} \right. , \tag{5-6}$$

where $x := \begin{bmatrix} x_p^{\mathsf{T}} & x_c^{\mathsf{T}} \end{bmatrix}^{\mathsf{T}} \in \mathbb{R}^n$, with $n = n_p + n_c$, and

$$\left[\begin{array}{c|c|c} A & B_0 & B_{\mathrm{aw}} \\ \hline C & D_0 & D_{\mathrm{aw}} \end{array} \right] = \left[\begin{array}{cc|cc|c} A_{\mathrm{p}} + B_{\mathrm{p}} \Delta_u D_{\mathrm{c}} C_{\mathrm{p}} & B_{\mathrm{p}} \Delta_u C_{\mathrm{c}} & -B_{\mathrm{p}} \Delta_u & 0 & B_{\mathrm{p}} \Delta_u \\ B_{\mathrm{c}} \Delta_y C_{\mathrm{p}} & A_{\mathrm{c}} + B_{\mathrm{c}} \Delta_y D_{\mathrm{p}} C_{\mathrm{c}} & -B_{\mathrm{c}} \Delta_y D_{\mathrm{p}} & I_{n_c} & B_{\mathrm{c}} \Delta_y D_{\mathrm{p}} \\ \hline \Delta_u D_{\mathrm{c}} C_{\mathrm{p}} & \Delta_u C_{\mathrm{c}} & I_m - \Delta_u & 0 & \Delta_u \end{array} \right].$$

For compact notation, let

$$B := B_0 + B_{\mathrm{aw}} \begin{bmatrix} \mathbf{E}_{\mathrm{c}} \\ \mathbf{F}_{\mathrm{c}} \end{bmatrix}, \qquad D := D_0 + D_{\mathrm{aw}} \begin{bmatrix} \mathbf{E}_{\mathrm{c}} \\ \mathbf{F}_{\mathrm{c}} \end{bmatrix} = D_0 + \Delta_u \mathbf{F}_{\mathrm{c}}. \tag{5-7}$$

Additionally, define the extended vector

$$\eta := \begin{bmatrix} x^{\mathsf{T}} & \mathrm{dz}\left(v(x)\right)^{\mathsf{T}} \end{bmatrix}^{\mathsf{T}} \tag{5-8}$$

where $x \mapsto v(x)$ is the Lipschitz solution of the nonlinear algebraic loop specified by the second equation in (5-6) (see Section 2.3.4). Introduce

$$h(x) := \mathbf{H}_1 x + \mathbf{H}_2 \mathrm{dz}\left(v(x)\right), \tag{5-9}$$

where $\mathbf{H}_1 \in \mathbb{R}^{m\times n}$, $\mathbf{H}_2 \in \mathbb{R}^{m\times m}$ are both arbitrary design parameters. Then, introduce the Lyapunov function candidate

$$W(x) := \begin{cases} V(x) & \text{if } x \in \mathcal{S}_h \\ 1 & \text{otherwise} \end{cases}, \tag{5-10}$$

where V is the sign-indefinite quadratic form

$$V(x) := \eta^{\mathsf{T}} P \eta = \eta^{\mathsf{T}} \begin{bmatrix} \mathbf{P}_{11} & \mathbf{P}_{12} \\ \mathbf{P}_{12}^{\mathsf{T}} & \mathbf{P}_{22} \end{bmatrix} \eta, \tag{5-11}$$

with η in (5-8), and $\mathcal{S}_h$ is the set

$$\mathcal{S}_h := \{x \in \mathbb{R}^n : |h(x)|_\infty \leq 1\}. \tag{5-12}$$

Following the results of [56], it is possible to analyze the stability of the closed-loop (5-6) exploiting the second method of Lyapunov with (5-10). Define also the open sublevel set

$$\mathcal{S}(W) := \{x \in \mathbb{R}^n : W(x) < 1\}, \tag{5-13}$$

which will be shown to provide an estimate of the basin of attraction of the origin for (5-6), due to the fact that W coincides with V in the set $\mathcal{S}_h$ and that set $\mathcal{S}_h$ in (5-12) and definition (5-13) are designed in such a way that

$$\mathcal{S}(W) = \mathcal{S}(V) \cap \mathcal{S}_h. \tag{5-14}$$

For both regional and global procedures, two static linear anti-windup strategies guaranteeing exponential stability with a prescribed convergence rate are addressed in this chapter. On the one hand, the case where both anti-windup actions E_{c} and F_{c} on the dynamics and output of the controller are designed, and, on the other hand, the case where the anti-windup solution acts only on the dynamics of the controller, i.e. when $\mathbf{F}_{\mathrm{c}} = 0$ is imposed. Notice that, for the case where $D_{\mathrm{c}}D_{\mathrm{p}} \neq 0$, the linear well-posedness in (5-4) does not ensure the well-posedness of the nonlinear algebraic loop in (5-6), and, for the case where $D_{\mathrm{c}}D_{\mathrm{p}} = 0$ and $\mathbf{F}_{\mathrm{c}} = 0$, the well-posedness becomes structurally nonlinear because imposing $\mathbf{F}_{\mathrm{c}} = 0$ implies $u = Cx$ (see the discussion in [69, Section 2.3.7]). Moreover, for the cases where only regional exponential stability is attainable, sufficient conditions providing an estimate of the basin of attraction of the origin of (5-6) are given.

The results presented in this chapter are derived in the form of BMIs and they provide sufficient conditions ensuring global exponential stability for the closed-loop system (5-6) with exponentially stable plants and, when global exponential stability is not attainable, sufficient conditions ensuring regional exponential stability for the

closed-loop system are given. Leveraging the Lemma 3.1, which allows to ignore the points in which the function W is not differentiable, and the fact that V coincides with W when $\mathbf{H}_1 = 0$ and $\mathbf{H}_2 = 0$ (see Remark 3.1), it is possible to state the following lemma, originally presented and proven in [56, Lemma 1], which is the main basis for the results presented in the next section.

Lemma 5.1

[56, Lemma 1] Considering dynamics (5-6) and the definitions of $\mathcal{S}(W)$ in (4-12) and $\mathcal{S}_h$ in (4-11), if there exists a locally Lipschitz Lyapunov function $x \mapsto W(x)$ as defined in (4-9) and positive scalars β_1, β_2 and β_3 satisfying

$$\beta_1|x|^2 \leq W(x) \leq \beta_2|x|^2 \tag{5-15}$$

for all $x \in \mathcal{S}(W)$ and

$$\dot{W}(x) := \langle \nabla W(x), Ax + B\text{sat}(v(x)) \rangle \leq -\beta_3|x|^2 \tag{5-16}$$

for almost all $x \in \mathcal{S}(W)$, then the origin of (5-6) is local exponentially stable with a basin of attraction containing $\mathcal{S}(W)$. Moreover, if (5-15) and (5-16) are satisfied for all $x \in \mathbb{R}^n$, then the origin of (5-6) is globally exponentially stable.

5.3 Lyapunov stability certificates

5.3.1 Regional stability results

It is possible to show that W in (5-10) is shown to be Lipschitz continuous in $\mathcal{S}_h$ since V in (5-11) and h in (5-9) are designed in such a way that

$$\mathcal{S}(W) = \mathcal{S}(V) \cap \mathcal{S}_h. \tag{5-17}$$

Then, to enlarge as much as possible the volume of $\mathcal{S}(W)$, introduce the ellipsoidal set

$$\mathcal{E}\big(\hat{\mathbf{P}}\big) := \big\{x \in \mathbb{R}^n : x^\mathsf{T}\hat{\mathbf{P}}x < 1\big\}, \tag{5-18}$$

with $\hat{P} \in \mathbb{S}^n_{>0}$, and impose

$$\mathcal{E}\big(\hat{\mathbf{P}}\big) \subset \mathcal{S}(W) \tag{5-19}$$

while maximizing the volume of (5-18), or similarly (but not fully equivalently) by minimizing the trace of $\hat{\mathbf{P}}$. The above steps are necessary to state the next theorem, which is an adaptation of [56, Theorem 3], ensures regional exponential stability and provides an estimate of the basin of attraction of the origin for nonlinear system (5-6), responding to Problem 3.3.

Theorem 5.1

If there exist matrices $\hat{\mathbf{P}} \in \mathbb{S}^n_{>0}$, $\mathbf{P}_{11} \in \mathbb{S}^n_{>0}$, $\mathbf{P}_{12} \in \mathbb{R}^{n\times m}$, $\mathbf{P}_{22} \in \mathbb{S}^m$, $\hat{\mathbf{T}} \in \mathbb{D}^m_{>0}$, $\mathbf{T}_1 \in \mathbb{D}^m_{>0}$, $\mathbf{H}_1 \in \mathbb{R}^{m\times n}$, $\mathbf{H}_2 \in \mathbb{R}^{m\times m}$, $\mathbf{E}_{\mathrm{c}} \in \mathbb{R}^{n_c\times m}$ and $\mathbf{F}_{\mathrm{c}} \in \mathbb{R}^{m\times m}$ such that

$$\Psi_1 := \begin{bmatrix} \mathbf{P}_{11} & \mathbf{P}_{12} & 0 \\ \mathbf{P}_{12}^{\mathsf{T}} & \mathbf{P}_{22} & 0 \\ 0 & 0 & 1 \end{bmatrix} + \mathrm{He}\begin{bmatrix} 0 & \mathbf{H}_1^{\mathsf{T}}\mathbf{T}_1 - C^{\mathsf{T}}\mathbf{T}_1 & 0 \\ 0 & \mathbf{T}_1\mathbf{H}_2 + \mathbf{T}_1 - \mathbf{T}_1 D & 0 \\ \mathbf{H}_{1\,i} & \mathbf{H}_{2\,i} & 0 \end{bmatrix} > 0 \tag{5-20}$$

with $i = 1, ..., m$ being the i^{th} row of $\mathbf{H}_1$ and $\mathbf{H}_2$, and

$$\Psi_2 := \begin{bmatrix} \hat{\mathbf{P}} & 0 \\ 0 & 0 \end{bmatrix} - P + \mathrm{He}\begin{bmatrix} 0 & -C^{\mathsf{T}}\hat{\mathbf{T}} \\ 0 & \hat{\mathbf{T}}\,(I_m - D) \end{bmatrix} > 0 \tag{5-21}$$

with D as defined in (5-7) hold and, additionally, there exist a scalar $\boldsymbol{\alpha} \geq 0$ and matrices $\mathbf{T}_2 \in \mathbb{D}^m_{>0}$, $\mathbf{T}_3 \in \mathbb{D}^m_{>0}$ and $\mathbf{T}_4 \in \mathbb{D}^m$ satisfying

$$\begin{aligned} \Psi_3 := \mathrm{He}\left(\begin{bmatrix} \mathbf{P}_{11}\,(A + \boldsymbol{\alpha} I_n) & \mathbf{P}_{11}B & \mathbf{P}_{12} \\ \mathbf{P}_{12}^{\mathsf{T}}A & \mathbf{P}_{12}^{\mathsf{T}}B & \mathbf{P}_{22} \\ 0 & 0 & 0 \end{bmatrix}\right. \\ \left. + \begin{bmatrix} 0 & 0 & 0 \\ \mathbf{T}_2C - \mathbf{T}_2\mathbf{H}_1 + \mathbf{T}_4CA & \mathbf{T}_2D - \mathbf{T}_2 - \mathbf{T}_2\mathbf{H}_2 + \mathbf{T}_4CB & \mathbf{T}_4D - \mathbf{T}_4 \\ \mathbf{T}_3CA & \mathbf{T}_3CB & \mathbf{T}_3D - \mathbf{T}_3 \end{bmatrix}\right) < 0 \end{aligned} \tag{5-22}$$

with B defined as in (5-7), then the algebraic loop in (5-6) is well-posed and the origin of (5-6) is locally exponentially stable form $\mathcal{S}(W)$ in (5-13). Moreover, the eigenvalues of A in (5-6) have real part smaller than $-\boldsymbol{\alpha}$.

Proof: Exploiting the Facts 2.2 and 2.3 emerging from the sector models of the deadzone (see Section 2.4), note that the following facts are true:

1. For any $T \in \mathbb{D}^m_{>0}$ and any $u \in \mathbb{R}^m$,
$$\mathrm{dz}\,(u)^{\mathsf{T}}\, T(u - \mathrm{dz}\,(u)) \geq 0, \tag{5-23}$$
2. for any $T \in \mathbb{D}^m_{>0}$, for all $x \in \mathcal{S}_h$ and any $u \in \mathbb{R}^m$, it holds that
$$\mathrm{dz}\,(u)^{\mathsf{T}}\, T(u - \mathrm{dz}\,(u) - \overline{U}h(x)) \geq 0, \tag{5-24}$$
3. and for any $T \in \mathbb{D}^m$ and for all $x \in \mathbb{R}^n : |u_i(x)| \neq \overline{u}_i$,
$$\dot{\mathrm{dz}}\,(v(x))^{\mathsf{T}}\, T(\dot{v}(x) - \dot{\mathrm{dz}}\,(v(x))) = 0, \tag{5-25}$$
$$\mathrm{dz}\,(v(x))^{\mathsf{T}}\, T(\dot{v}(x) - \dot{\mathrm{dz}}\,(v(x))) = 0, \tag{5-26}$$
where $v(x)$ denotes the explicit solution of the nonlinear algebraic loop
$$u - D\mathrm{dz}\,(u) = Cx$$
stemming from the bottom equation in (5-6) and $\dot{\mathrm{dz}}\,(v(x))$ denotes the time-derivative of $x \mapsto \mathrm{dz}\,(v(x))$, which is defined for almost all values of $x \in \mathbb{R}^n$.

Then, thanks to Lemma 2.1 (see the results in [3, Proposition 1]) and the definition of T in (5-25), with $T = \mathbf{T}_3$, system (5-6) is well-posed due to the negative definiteness

of the (3,3) entry of Ψ_3 in condition (5-22). Under well-posedness, applying a Schur complement to (5-20) as

$$\bar{\Psi}_1 := P + \mathrm{He}\begin{bmatrix} 0 & \mathbf{H}_1^{\mathsf{T}}\mathbf{T}_1 - C^{\mathsf{T}}\mathbf{T}_1 \\ 0 & \mathbf{T}_1\mathbf{H}_2 + \mathbf{T}_1 - \mathbf{T}_1 D \end{bmatrix} - \begin{bmatrix} H_{1\,i}^{\mathsf{T}} \\ H_{2\,i}^{\mathsf{T}} \end{bmatrix} \begin{bmatrix} H_{1\,i} & H_{2\,i} \end{bmatrix} > 0 \tag{5-27}$$

and using (5-24), it can be shown that

$$V(x) - h(x)_i^2 \geq V(x) - h(x)_i^2 - 2\mathrm{dz}\left(v(x)\right)^{\mathsf{T}} \mathbf{T}_1 \left(v(x) - \mathrm{dz}\left(v(x)\right) - h(x)\right) \tag{5-28}$$

$$= \eta^{\mathsf{T}}\bar{\Psi}_1\eta \geq \lambda_{\min}(\bar{\Psi}_1)|\eta|^2 \geq \lambda_{\min}(\bar{\Psi}_1)|x|^2 = \beta_1|x|^2, \tag{5-29}$$

which yields $W(x) = V(x) > h(x)_i^2 > 0$, proving that $\mathcal{S}(W) \in \mathcal{S}_h$ and ensuring that $V(x) > 1$ in the boundary of $\mathcal{S}_h$, which implies Lipschitz continuity of $W(x)$ for all $x \in \mathcal{S}_h$. Moreover, using $|\mathrm{dz}\left(v(x)\right)| \leq |v(x)| \leq L\,|x|$ and the fact that u in (5-6) is globally Lipschitz, it can be stated that

$$W(x) = V(x) \leq \lambda_{\max}(P)|\eta|^2 \leq \lambda_{\max}(P)L|x|^2 = \beta_2|x|^2,$$

which, together with property (5-29), implies the existence of the positive scalars $\beta_1 = \lambda_{\min}(\bar{\Psi}_1)$ and $\beta_2 = \lambda_{\max}(P)L$ satisfying inequality (4-14) and, thus, positive-definiteness of W for all $x \in \mathcal{S}(W)$.

Furthermore, by hypothesis (5-21) and property (5-23),

$$x^{\mathsf{T}}\hat{\mathbf{P}}x - W(x) \geq x^{\mathsf{T}}\hat{\mathbf{P}}x - V(x) \geq x^{\mathsf{T}}\hat{\mathbf{P}}x - V(x) - 2\mathrm{dz}\left(v(x)\right)^{\mathsf{T}}\hat{\mathbf{T}}\left(v(x) - \mathrm{dz}\left(v(x)\right)\right)$$
$$= \eta^{\mathsf{T}}\Psi_2\eta > 0,$$

which leads to

$$x^{\mathsf{T}}\hat{\mathbf{P}}x > W(x), \qquad \forall x \in S_h. \tag{5-30}$$

Consequently, $x^{\mathsf{T}}\hat{\mathbf{P}}x > 1$ implies $W(x) > 1$ for all $x \in S_h$, which entails inclusion (5-19). Furthermore, with the proven existence of the scalars β_1 and β_2, local exponential stability from $\mathcal{S}(W)$ holds if there exists a positive scalar β_3 upper-bounding $\dot{W}$, according to Lemma 5.1. With this in mind, by exploiting the sector conditions (5-24) to (5-26), introduce the matrix

$$\begin{aligned}
\bar{\Psi}_3 := \mathrm{He}&\left(\begin{bmatrix} \mathbf{P}_{11} & \mathbf{P}_{12} \\ \mathbf{P}_{12}^{\mathsf{T}} & \mathbf{P}_{22} \\ 0 & 0 \end{bmatrix} \begin{bmatrix} A & B & 0 \\ 0 & 0 & I_m \end{bmatrix}\right) \\
&+ \mathrm{He}\left(\begin{bmatrix} 0 \\ \mathbf{T}_2 \\ 0 \end{bmatrix} \begin{bmatrix} C - \mathbf{H}_1 & D - I_m - \mathbf{H}_2 & 0 \end{bmatrix}\right) \\
&+ \mathrm{He}\left(\begin{bmatrix} 0 \\ 0 \\ \mathbf{T}_3 \end{bmatrix} \begin{bmatrix} CA & CB & D - I_m \end{bmatrix}\right) \\
&+ \mathrm{He}\left(\begin{bmatrix} 0 \\ \mathbf{T}_4 \\ 0 \end{bmatrix} \begin{bmatrix} CA & CB & D - I_m \end{bmatrix}\right),
\end{aligned} \tag{5-31}$$

and notice that

$$\bar{\Psi}_3 = \Psi_3 - \mathrm{He}\left(\begin{bmatrix}\mathbf{P}_{11}\\ 0\\ 0\end{bmatrix}\begin{bmatrix}\boldsymbol{\alpha} I_n & 0 & 0\end{bmatrix}\right), \tag{5-32}$$

thus $\bar{\Psi}_3 \leq \Psi_3 < 0$ due to the definitions of $\mathbf{P}_{11}$ and $\boldsymbol{\alpha}$ and hypothesis (5-22). Therefore, recalling that $W(x) = V(x)$, $\forall x \in \mathcal{S}(W)$, it may be found that, for almost all $x \in \mathcal{S}(W)$,

$$\begin{aligned}\dot{W}(x) \leq \dot{W}(x) &+ 2\mathrm{dz}\left(v(x)\right)^{\mathsf{T}}\mathbf{T}_2\left(v(x) - \mathrm{dz}\left(v(x)\right) - h(x)\right)\\ &+ 2\dot{\mathrm{dz}}\left(v(x)\right)^{\mathsf{T}}\mathbf{T}_3(\dot{v}(x) - \dot{\mathrm{dz}}\left(v(x)\right))\\ &+ 2\mathrm{dz}\left(v(x)\right)^{\mathsf{T}}\mathbf{T}_4(\dot{v}(x) - \dot{\mathrm{dz}}\left(v(x)\right))\\ &= \eta^{\mathsf{T}}\bar{\Psi}_3\eta\end{aligned} \tag{5-33}$$

and this, together with (5-32), leads to

$$-\eta^{\mathsf{T}}\Psi_3\eta \geq -\eta^{\mathsf{T}}\bar{\Psi}_3\eta \geq \lambda_{\min}\left(-\bar{\Psi}_3\right)|\eta|^2 \geq \lambda_{\min}\left(-\bar{\Psi}_3\right)|x|^2,$$

which shows that $A + \boldsymbol{\alpha} I_n$ is Hurwitz due to the fact that

$$x^{\mathsf{T}}\mathrm{He}(\mathbf{P}_{11}(A + \boldsymbol{\alpha} I_n))x < 0$$

with $\mathbf{P}_{11} > 0$ and, further, proves the existence of $\beta_3 = \lambda_{\min}\left(-\bar{\Psi}_3\right)$, ensuring regional exponential stability of the closed-loop system (5-6) with basin of attraction of the origin containing $\mathcal{S}(W)$. □

5.3.2 Global stability results

The results on synthesis of static linear anti-windup gains using Lyapunov stability certificates based on the sign-indefinite quadratic form in (5-11) is presented in [55], which responds to Problem 3.4 and may be derived from the regional results in the previous section. Taking $\mathbf{H}_1 = 0$ and $\mathbf{H}_2 = 0$, notice that $\mathcal{S}_h = \mathbb{R}^n$ (see Remark 3.1). Hence, using the Lyapunov function candidate V in (5-11), the following theorem allows computing the static linear anti-windup gains $\mathbf{E}_{\mathrm{c}}$ and $\mathbf{F}_{\mathrm{c}}$ in (5-5) while guaranteeing global exponential stability of the closed-loop system (5-6) with anti-windup loop.

Theorem 5.2

If there exist matrices $\mathbf{P}_{11} \in \mathbb{S}^n_{>0}$, $\mathbf{P}_{12} \in \mathbb{R}^{n\times m}$, $\mathbf{P}_{22} \in \mathbb{S}^m$, $\mathbf{T}_1 \in \mathbb{D}^m_{>0}$, $\mathbf{E}_{\mathrm{c}} \in \mathbb{R}^{n_c\times m}$ and $\mathbf{F}_{\mathrm{c}} \in \mathbb{R}^{m\times m}$ such that

$$\Psi_4 := \begin{bmatrix}\mathbf{P}_{11} & \mathbf{P}_{12}\\ \mathbf{P}_{12}^{\mathsf{T}} & \mathbf{P}_{22}\end{bmatrix} + \mathrm{He}\begin{bmatrix}0 & 0\\ -\mathbf{T}_1 C & \mathbf{T}_1 - \mathbf{T}_1 D\end{bmatrix} > 0 \tag{5-34}$$

with D as defined in (5-7) holds and, additionally, there exist a scalar $\boldsymbol{\alpha} \geq 0$ and matrices $\mathbf{T}_2 \in \mathbb{D}^m_{>0}$, $\mathbf{T}_3 \in \mathbb{D}^m_{>0}$ and $\mathbf{T}_4 \in \mathbb{D}^m$ satisfying

$$\Psi_5 := \mathrm{He}\left(\begin{bmatrix} \mathbf{P}_{11}\left(A+\boldsymbol{\alpha} I_n\right) & \mathbf{P}_{11}B & \mathbf{P}_{12} \\ \mathbf{P}_{12}^{\mathsf{T}}A & \mathbf{P}_{12}^{\mathsf{T}}B & \mathbf{P}_{22} \\ 0 & 0 & 0 \end{bmatrix} + \begin{bmatrix} 0 & 0 & 0 \\ \mathbf{T}_2C+\mathbf{T}_4CA & \mathbf{T}_2D-\mathbf{T}_2+\mathbf{T}_4CB & \mathbf{T}_4D-\mathbf{T}_4 \\ \mathbf{T}_3CA & \mathbf{T}_3CB & \mathbf{T}_3D-\mathbf{T}_3 \end{bmatrix}\right) < 0 \quad (5\text{-}35)$$

with B as defined in (5-7), then the algebraic loop in (5-6) is well-posed and the origin of (5-6) is globally exponentially stable. Moreover, the eigenvalues of A in (5-6) have real part smaller than $-\boldsymbol{\alpha}$.

Proof: Following the same procedure used in the proof of Theorem 5.1 and taking $\mathbf{H}_1 = 0$ and $\mathbf{H}_2 = 0$, notice that $\Psi_5 = \Psi_3$ in (5-22) and, therefore, the well-posedness of the algebraic loop in the bottom equation of (5-6), the existence of the positive scalar $\beta_3 = \lambda_{\min}\left(-\bar{\Psi}_5\right)$ satisfying (5-16) with

$$\bar{\Psi}_5 := \mathrm{He}\left(\begin{bmatrix} \mathbf{P}_{11}A & \mathbf{P}_{11}B & \mathbf{P}_{12} \\ \mathbf{P}_{12}^{\mathsf{T}}A & \mathbf{P}_{12}^{\mathsf{T}}B & \mathbf{P}_{22} \\ 0 & 0 & 0 \end{bmatrix} + \begin{bmatrix} 0 & 0 & 0 \\ \mathbf{T}_2C+\mathbf{T}_4CA & \mathbf{T}_2D-\mathbf{T}_2+\mathbf{T}_4CB & \mathbf{T}_4D-\mathbf{T}_4 \\ \mathbf{T}_3CA & \mathbf{T}_3CB & \mathbf{T}_3D-\mathbf{T}_3 \end{bmatrix}\right),$$

and the Hurwitz property of $A+\boldsymbol{\alpha} I_n$ may be shown. Moreover, under well-posedness, observe that, using the sector condition (5-23),

$$\begin{aligned} V(x) &\geq V(x) - 2\mathrm{dz}\left(v(x)\right)^{\mathsf{T}}\mathbf{T}_1\left(v(x)-\mathrm{dz}\left(v(x)\right)\right) \\ &= \eta^{\mathsf{T}}\Psi_4\eta \geq \lambda_{\min}(\Psi_4)|\eta|^2 \geq \lambda_{\min}(\Psi_4)|x|^2 = \beta_1|x|^2 \end{aligned} \quad (5\text{-}36)$$

with η defined as in (5-8), leading to $V(x) > 0$ for all $x \in \mathbb{R}^n$ and proving the radial unboundedness of V. Besides, since the control signal u is globally Lipschitz, using $|\mathrm{dz}\left(v(x)\right)| \leq |v(x)| \leq L\,|x|$, it can be stated that

$$V(x) \leq \lambda_{\max}(P)|\eta|^2 \leq \lambda_{\max}(P)L|x|^2 = \beta_2|x|^2,$$

which, together with (5-36), proves the existence of the scalars $\beta_1 = \lambda_{\min}(\Psi_4)$ and $\beta_2 = \lambda_{\max}(P)L$, ensuring global exponential stability of the origin for the closed-loop system (5-6). □

5.4 Iterative algorithms for the anti-windup design

For both the regional and global exponential stability results of Theorems 5.1, 5.2, an iterative approach is proposed to design the anti-windup gains $\mathbf{E}_{\mathrm{c}}$ and $\mathbf{F}_{\mathrm{c}}$,

applying a convex-conxave decomposition to convexify the synthesis problem since the sufficient conditions in Theorems 5.1 and 5.2 are formulated in terms of BMIs in the decision variables. Additionally, for the regional case, the algorithm iteratively increases the volume of the estimate of the basin of attraction $\mathcal{S}(W)$ in (5-13) by minimizing the trace of $\hat{\mathbf{P}}$ within the inclusion (5-19).

5.4.1 Feasible initial conditions

In order to be able to initialize the iterative algorithm, the following initial conditions for the decision variables are used to find a first feasible solution for the sufficient conditions presented in Theorems 5.1 and 5.2.

$$\mathbf{E}_{\mathrm{c}} = 0, \tag{5-37}$$

$$\mathbf{F}_{\mathrm{c}} = D_c D_p, \tag{5-38}$$

$$\begin{gathered}
\mathbf{P}_{11} = I_n, \qquad \mathbf{P}_{12} = 0, \qquad \mathbf{P}_{22} = 0, \\
\boldsymbol{\alpha} = -\frac{1}{2}\lambda_{\max}\left(A + A^{\mathsf{T}} + I_n + \left(B + C^{\mathsf{T}}\right)\left(B^{\mathsf{T}} + C\right)\right), \\
\mathbf{T}_1 = \lambda_{\max}\left(CC^{\mathsf{T}}\right)^{-1} I_m, \qquad \mathbf{T}_2 = I_m, \\
\mathbf{T}_3 = \lambda_{\max}\left(C\begin{bmatrix}A & B\end{bmatrix}\begin{bmatrix}A^{\mathsf{T}} \\ B^{\mathsf{T}}\end{bmatrix}C^{\mathsf{T}}\right)^{-1} I_m, \qquad \mathbf{T}_4 = 0, \\
\hat{\mathbf{T}} = \lambda_{\max}\left(CC^{\mathsf{T}}\right)^{-1} I_m, \qquad \hat{\mathbf{P}} = 2I_n.
\end{gathered} \tag{5-39}$$

and, specifically for conditions (5-20) and (5-22), take

$$\mathbf{H}_1 = 0, \qquad \mathbf{H}_2 = 0. \tag{5-40}$$

Observe that the selections in (5-39) are often not stabilizing because $\alpha < 0$ in most cases. However, the selections above are suitable for the initialization of the iterative algoithm. The next proposition ensures the initial feasibility of the conditions in Theorems 5.1 and 5.2 for the closed loop (5-6) with anti-windup action on both the dynamics and the output of the system.

Proposition 5.1

Conditions (5-20), (5-21) and (5-22) of Theorem 5.1 hold with selections (5-37), (5-38), (5-39) and (5-40) and conditions (5-34) and (5-35) of Theorem 5.2 hold with selections (5-37), (5-38) and (5-39).

Proof: Take $\mathbf{P}_{11} = I_n$, $\mathbf{P}_{12} = 0$, $\mathbf{P}_{22} = 0$, $\mathbf{H}_1 = 0$ and $\mathbf{H}_2 = 0$. Then,

$$\Psi_1 = \mathrm{He}\begin{bmatrix}\frac{1}{2}I_n & -C^{\mathsf{T}}\mathbf{T}_1 & 0 \\ 0 & \mathbf{T}_1 - \mathbf{T}_1 D & 0 \\ 0 & 0 & \frac{1}{2}\end{bmatrix}$$

Then, notice that with $\mathbf{E}_{\mathrm{c}} = 0$, $\mathbf{F}_{\mathrm{c}} = D_c D_p$, it can be shown that $D = 0$ from

(5-7). Therefore,

$$\Psi_1 = \mathrm{He}\begin{bmatrix} \frac{1}{2}I_n & -C^\mathsf{T}\mathbf{T}_1 & 0 \\ 0 & \mathbf{T}_1 & 0 \\ 0 & 0 & \frac{1}{2}I_m \end{bmatrix} = \begin{bmatrix} I_n & -C^\mathsf{T}\mathbf{T}_1 & 0 \\ -\mathbf{T}_1 C & 2\mathbf{T}_1 & 0 \\ 0 & 0 & 1 \end{bmatrix},$$

which is positive definite if and only if the upper left block matrix of rows and columns 1 and 2 satisfies

$$\begin{bmatrix} I_n & -C^\mathsf{T}\mathbf{T}_1 \\ -\mathbf{T}_1 C & 2\mathbf{T}_1 \end{bmatrix} > 0, \tag{5-41}$$

which also corresponds to Ψ_4 with $\mathbf{P}_{11} = I_n$, $\mathbf{P}_{12} = 0$, $\mathbf{P}_{22} = 0$, $\mathbf{H}_1 = 0$, $\mathbf{H}_2 = 0$, $\mathbf{E}_\mathrm{c} = 0$ and $\mathbf{F}_\mathrm{c} = D_c D_p$. Therefore, to show (5-20) and (5-34), apply Schur complement and observe that

$$\begin{aligned} &2\mathbf{T}_1 - \mathbf{T}_1 C C^\mathsf{T}\mathbf{T}_1 > 0 \\ \equiv\ &2\mathbf{T}_1^{-1} - CC^\mathsf{T} > 0, \end{aligned}$$

which holds with $\mathbf{T}_1 = \lambda_{\max}\left(CC^\mathsf{T}\right)^{-1} I_m$ and guarantees initial $\Psi_1 > 0$ and initial $\Psi_4 > 0$. Recalling selections in (5-39), notice that, with $\hat{\mathbf{P}} = 2I_n$,

$$\Psi_2 = \begin{bmatrix} I_n & -C^\mathsf{T}\hat{\mathbf{T}} \\ -\hat{\mathbf{T}}C & 2\hat{\mathbf{T}} \end{bmatrix} > 0,$$

which is equivalent to (5-41) and holds with $\hat{\mathbf{T}} = \lambda_{\max}\left(CC^\mathsf{T}\right)^{-1} I_m$. Finally, the selections (5-37), (5-38), (5-39) and (5-40) and let $\mathbf{T}_4 = 0$ so that

$$\Psi_3 = \Psi_5 = \mathrm{He}\begin{bmatrix} A - \boldsymbol{\alpha} I_n & B & 0 \\ \mathbf{T}_2 C & -\mathbf{T}_2 & 0 \\ \mathbf{T}_3 CA & \mathbf{T}_3 CB & -\mathbf{T}_3 \end{bmatrix} < 0,$$

of which the first two rows and columns read

$$\mathrm{He}\begin{bmatrix} A - \boldsymbol{\alpha} I_n & B \\ \mathbf{T}_2 C & -\mathbf{T}_2 \end{bmatrix} = \begin{bmatrix} A + A^\mathsf{T} - 2\boldsymbol{\alpha} I_n & B + C^\mathsf{T}\mathbf{T}_2 \\ B^\mathsf{T} + \mathbf{T}_2 C & -2\mathbf{T}_2 \end{bmatrix} < 0. \tag{5-42}$$

Changing the sign of the matrix inequality (5-42) above, force

$$\begin{bmatrix} -A - A^\mathsf{T} + 2\boldsymbol{\alpha} I_n & -B - C^\mathsf{T}\mathbf{T}_2 \\ -B^\mathsf{T} - \mathbf{T}_2 C & 2\mathbf{T}_2 \end{bmatrix} > I_{m+n},$$

or

$$\begin{bmatrix} -A - A^\mathsf{T} + 2\boldsymbol{\alpha} I_n - I_n & -B - C^\mathsf{T}\mathbf{T}_2 \\ -B^\mathsf{T} - \mathbf{T}_2 C & 2\mathbf{T}_2 - I_m \end{bmatrix} > 0.$$

As established in selection (5-39), let $\mathbf{T}_2 = I_m$ so that $2\mathbf{T}_2 - I_m = I_m > 0$. Hence, applying Schur complement,

$$-A - A^\mathsf{T} + 2\boldsymbol{\alpha} I_n - I_n - \left(-B - C^\mathsf{T}\right)\left(-B^\mathsf{T} - C\right) > 0$$

which holds with

$$\boldsymbol{\alpha} = \frac{1}{2}\lambda_{\max}\left(A + A^\mathsf{T} + I_n + \left(B + C^\mathsf{T}\right)\left(B^\mathsf{T} + C\right)\right)$$

and guarantees

$$-\Psi_3 = -\Psi_5 > \begin{bmatrix} & I_{m+n} & & -A^\mathsf{T}C^\mathsf{T}\mathbf{T}_3 \\ & & & -B^\mathsf{T}C^\mathsf{T}\mathbf{T}_3 \\ -\mathbf{T}_3 CA & -\mathbf{T}_3 CB & & 2\mathbf{T}_3 \end{bmatrix} > 0$$

Finally, applying Schur complement and defining $\tilde{C} := C\begin{bmatrix} A & B \end{bmatrix}$,

$$\begin{aligned} & 2\mathbf{T}_3 - \mathbf{T}_3\tilde{C}\tilde{C}^{\mathsf{T}}\mathbf{T}_3 > 0 \\ \equiv\ & 2\mathbf{T}_3^{-1} - \tilde{C}\tilde{C}^{\mathsf{T}} > 0, \end{aligned}$$

which holds with

$$\mathbf{T}_3 = \lambda_{\max}\left(\tilde{C}\tilde{C}^{\mathsf{T}}\right)^{-1} I_m,$$

ensures initial $\Psi_3 < 0$ and $\Psi_5 < 0$, completing the proof. □

The following proposition ensures the initial feasibility of the conditions in Theorems 5.1 and 5.2 for the controller-plant feedback (5-6) with anti-windup loop acting only on the dynamics of the closed-loop system.

Proposition 5.2

When the product $D_cD_p = 0$, conditions (5-20), (5-21) and (5-22) of Theorem 5.1 hold with selections (5-37), (5-39), (5-40) and $\mathbf{F}_{\mathrm{c}} = 0$, and conditions (5-34) and (5-35) of Theorem 5.2 holds with selections (5-37), (5-39) and $\mathbf{F}_{\mathrm{c}} = 0$.

Proof: Notice that $D_cD_p = 0$ implies $\Delta_u = I_m$ and, therefore, imposing $\mathbf{F}_{\mathrm{c}} = 0$, together with selection (5-37), results in $D = 0$. Additionally, selections in (5-39) and (5-40) lead to the same reasoning as in Proposition 5.1. □

5.4.2 Convex-concave decomposition

Conditions (5-20), (5-21) and (5-22) in Theorem 5.1, as well as conditions (5-34) and (5-35) in Theorem 5.2, are BMIs in the decision variables that need to be linearized in order to be suitable for LMI solvers. First, observe that (5-20) can be reformulated as

$$\begin{aligned} \Psi_1 = & \begin{bmatrix} \mathbf{P}_{11} & \mathbf{P}_{12} & 0 \\ \mathbf{P}_{12}^{\mathsf{T}} & \mathbf{P}_{22} & 0 \\ 0 & 0 & I_m \end{bmatrix} + \mathrm{He}\left(\begin{bmatrix} 0 \\ \mathbf{T}_1 \\ 0 \end{bmatrix}\begin{bmatrix} \mathbf{H}_1 - C & \mathbf{H}_2 + I_m - D & 0 \end{bmatrix}\right) \\ & + \mathrm{He}\left(\begin{bmatrix} 0 \\ 0 \\ I_m \end{bmatrix}\begin{bmatrix} \mathbf{H}_1 & \mathbf{H}_2 & 0 \end{bmatrix}\right) \end{aligned}$$

and, making use of the convex-concave linearization presented in [15], introduce

$$\left[\begin{array}{c|c|c} X_1 & -Y_{1\,i} & \bar{Y}_1 \end{array}\right] := \left[\begin{array}{ccc|ccc|ccc} 0 & \mathbf{T}_1 & 0 & \mathbf{H}_1 & \mathbf{H}_2 - D_{\mathrm{aw}}\begin{bmatrix}\mathbf{E}_{\mathrm{c}} \\ \mathbf{F}_{\mathrm{c}}\end{bmatrix} & 0 & -C & I_m - D_0 & 0 \\ 0 & 0 & I_m & \mathbf{H}_{1\,i} & \mathbf{H}_{2\,i} & 0 & 0 & 0 & 0 \end{array}\right]. \tag{5-43}$$

Moreover, Ψ_2 in (5-21) can be rewritten as

$$\Psi_2 = \begin{bmatrix} \hat{\mathbf{P}} & 0 \\ 0 & 0 \end{bmatrix} - P + \mathrm{He}\begin{bmatrix} 0 \\ \hat{\mathbf{T}} \end{bmatrix}\begin{bmatrix} -C & I_m - D \end{bmatrix}$$

which facilitates the introduction of

$$\left[\begin{array}{c|c|c} X_2 & -Y_2 & \bar{Y}_2 \end{array}\right] := \left[\begin{array}{cc|c|cc} 0 & \hat{\mathbf{T}} & 0 & -D_{\text{aw}}\begin{bmatrix}\mathbf{E}_{\text{c}}\\ \mathbf{F}_{\text{c}}\end{bmatrix} & -C & I_m - D_0 \end{array}\right], \tag{5-44}$$

and, combining (5-31) and (5-32), define

$$\left[\begin{array}{c|c|c} X_3 & Y_3 & \bar{Y}_3 \end{array}\right] :=$$

$$\left[\begin{array}{ccc|ccc|ccc} \mathbf{P}_{11} & 0 & 0 & -\boldsymbol{\alpha} I_n & 0 & 0 & 0 & 0 & 0 \\ \mathbf{P}_{11} & \mathbf{P}_{12} & 0 & 0 & B_{\text{aw}}\begin{bmatrix}\mathbf{E}_{\text{c}}\\ \mathbf{F}_{\text{c}}\end{bmatrix} & 0 & A & B_0 & 0 \\ \mathbf{P}_{12}^{\mathsf{T}} & \mathbf{P}_{22} & 0 & 0 & 0 & 0 & 0 & 0 & I_m \\ 0 & \mathbf{T}_2 & 0 & -\mathbf{H}_1 & D_{\text{aw}}\begin{bmatrix}\mathbf{E}_{\text{c}}\\ \mathbf{F}_{\text{c}}\end{bmatrix} - \mathbf{H}_2 & 0 & C & D_0 - I_m & 0 \\ 0 & \mathbf{T}_4 & \mathbf{T}_3 & 0 & CB_{\text{aw}}\begin{bmatrix}\mathbf{E}_{\text{c}}\\ \mathbf{F}_{\text{c}}\end{bmatrix} & D_{\text{aw}}\begin{bmatrix}\mathbf{E}_{\text{c}}\\ \mathbf{F}_{\text{c}}\end{bmatrix} & CA & CB_0 & D_0 - I_m \end{array}\right]. \tag{5-45}$$

Furthermore, rewrite (5-35) as

$$\Psi_4 = \begin{bmatrix}\mathbf{P}_{11} & \mathbf{P}_{12}\\ \mathbf{P}_{12}^{\mathsf{T}} & \mathbf{P}_{22}\end{bmatrix} + \text{He}\left(\begin{bmatrix}0\\ \mathbf{T}_1\end{bmatrix}\begin{bmatrix}-C & I_m - D\end{bmatrix}\right)$$

to introduce

$$\left[\begin{array}{c|c|c} X_4 & -Y_4 & \bar{Y}_4 \end{array}\right] := \left[\begin{array}{cc|c|cc} 0 & \mathbf{T}_1 & 0 & -D_{\text{aw}}\begin{bmatrix}\mathbf{E}_{\text{c}}\\ \mathbf{F}_{\text{c}}\end{bmatrix} & -C & I_m - D_0 \end{array}\right], \tag{5-46}$$

and notice that, considering Ψ_5 in (5-35), following the same reasoning used to determine (5-45) and taking $\mathbf{H}_1 = 0$ and $\mathbf{H}_2 = 0$, it may be directly defined

$$\left[\begin{array}{c|c|c} X_5 & Y_5 & \bar{Y}_5 \end{array}\right] :=$$

$$\left[\begin{array}{ccc|ccc|ccc} \mathbf{P}_{11} & 0 & 0 & -\boldsymbol{\alpha} I_n & 0 & 0 & 0 & 0 & 0 \\ \mathbf{P}_{11} & \mathbf{P}_{12} & 0 & 0 & B_{\text{aw}}\begin{bmatrix}\mathbf{E}_{\text{c}}\\ \mathbf{F}_{\text{c}}\end{bmatrix} & 0 & A & B_0 & 0 \\ \mathbf{P}_{12}^{\mathsf{T}} & \mathbf{P}_{22} & 0 & 0 & 0 & 0 & 0 & 0 & I_m \\ 0 & \mathbf{T}_2 & 0 & 0 & D_{\text{aw}}\begin{bmatrix}\mathbf{E}_{\text{c}}\\ \mathbf{F}_{\text{c}}\end{bmatrix} & 0 & C & D_0 - I_m & 0 \\ 0 & \mathbf{T}_4 & \mathbf{T}_3 & 0 & CB_{\text{aw}}\begin{bmatrix}\mathbf{E}_{\text{c}}\\ \mathbf{F}_{\text{c}}\end{bmatrix} & D_{\text{aw}}\begin{bmatrix}\mathbf{E}_{\text{c}}\\ \mathbf{F}_{\text{c}}\end{bmatrix} & CA & CB_0 & D_0 - I_m \end{array}\right]. \tag{5-47}$$

Then, for the regional case, using definitions (5-43), (5-44) and (5-45), the convex-concave decompositions of Ψ_1, Ψ_2 and Ψ_3 in BMIs (5-20) to (5-22) are

$$\begin{aligned} -\Psi_1 &= \Phi_1 + X_1^{\mathsf{T}} Y_{1\,i} - Y_{1\,i}^{\mathsf{T}} X_1 = \Phi_1 + M_{1\,i} - N_{1\,i} < 0, \\ -\Psi_2 &= \Phi_2 + X_2^{\mathsf{T}} Y_2 - Y_2^{\mathsf{T}} X_2 = \Phi_2 + M_2 - N_2 < 0, \\ \Psi_3 &= \Phi_3 + X_3^{\mathsf{T}} Y_3 - Y_3^{\mathsf{T}} X_3 = \Phi_3 + M_3 - N_3 < 0, \end{aligned} \tag{5-48}$$

where

$$\begin{aligned} \Phi_1 &:= -\begin{bmatrix}P & 0\\ 0 & 1\end{bmatrix} - X_1^{\mathsf{T}}\bar{Y}_1 - \bar{Y}_1^{\mathsf{T}} X_1, \\ \Phi_2 &:= -\begin{bmatrix}\hat{\mathbf{P}} & 0\\ 0 & 0\end{bmatrix} + P - X_2^{\mathsf{T}}\bar{Y}_2 - \bar{Y}_2^{\mathsf{T}} X_2, \end{aligned}$$

$$\begin{aligned}
\Phi_3 &:= X_3^{\mathsf{T}}\bar{Y}_3 + \bar{Y}_3^{\mathsf{T}}X_3,\\
M_j &:= \frac{1}{2}\left(X_j + Y_j\right)^{\mathsf{T}}\left(X_j + Y_j\right),\\
N_j &:= \frac{1}{2}\left(X_j - Y_j\right)^{\mathsf{T}}\left(X_j - Y_j\right), \qquad \forall j \in \{1\, i, 2, 3\},
\end{aligned} \tag{5-49}$$

for all $i = 1, \cdots, m$, and for the global case, considering the definitions in (5-46) and (5-47), the convex-concave decompositions of Ψ_4 and Ψ_5 in BMis (5-34) and (5-35) are

$$\begin{aligned}
-\Psi_4 &= \Phi_4 + X_4^{\mathsf{T}}Y_{4\,i} - Y_{4\,i}^{\mathsf{T}}X_4 = \Phi_4 + M_4 - N_4 < 0,\\
\Psi_5 &= \Phi_5 + X_5^{\mathsf{T}}Y_5 - Y_5^{\mathsf{T}}X_5 = \Phi_5 + M_5 - N_5 < 0,
\end{aligned} \tag{5-50}$$

where

$$\begin{aligned}
\Phi_4 &:= -P - X_4^{\mathsf{T}}\bar{Y}_4 - \bar{Y}_4^{\mathsf{T}}X_4,\\
\Phi_5 &:= X_5^{\mathsf{T}}\bar{Y}_5 + \bar{Y}_5^{\mathsf{T}}X_5,\\
M_j &:= \frac{1}{2}\left(X_j + Y_j\right)^{\mathsf{T}}\left(X_j + Y_j\right),\\
N_j &:= \frac{1}{2}\left(X_j - Y_j\right)^{\mathsf{T}}\left(X_j - Y_j\right), \qquad \forall j \in \{4, 5\},
\end{aligned} \tag{5-51}$$

Now, for all $j = 1, \cdots, 5$, observe that Φ_j are linear in the decision variables and that M_j, $-N_j$ are convex and concave, respectively. Therefore, resorting to $-\Psi_1 < 0$, $-\Psi_2 < 0$ and $-\Psi_4 < 0$ instead of $\Psi_1 > 0$, $\Psi_2 > 0$ and $\Psi_4 > 0$ in (5-48) and (5-50) allows to apply the convex semidefinite program presented in [15, Section IV], where the main LMI requires negative-semidefiniteness.

5.4.3 Iterative solver algorithms

Regional synthesis

Algorithm 5.1 designs the anti-windup gains $(\mathbf{E}_{\mathrm{c}}, \mathbf{F}_{\mathrm{c}})$ both for $\mathbf{F}_{\mathrm{c}} = 0$ (when $D_c D_p = 0$) and generic $\mathbf{F}_{\mathrm{c}}$. In the first design (where $\mathbf{F}_{\mathrm{c}} = 0$), the variable $\mathbf{F}_{\mathrm{c}}$ (indicated in square brackets) must not be considered in problems (5-57), (5-59) and $\mathbf{F}_{\mathrm{c}}$ should be set to zero in (5-43), (5-44) and (5-45). The algorithm involves two optimization loops. In the first loop, starting from the (non-necessarily stabilizing) selection of Section 5.4.1, $\boldsymbol{\alpha}$ is maximized to seek for a stabilizing solution. In the second loop, starting from the stabilizing solution, the ellipsoid $\mathcal{E}\big(\hat{\mathbf{P}}, 1\big)$ in (5-18) included in the basin of attraction (through (5-19)) is enlarged.

First, exploit (5-48) and (5-49) to define

$$\begin{aligned}
N_j(k) &:= \tfrac{1}{2}\big(X_j(k) - Y_j(k)\big)^{\mathsf{T}}\big(X_j(k) - Y_j(k)\big),\\
\tilde{N}_j(k) &:= \tfrac{1}{2}\mathrm{He}\Big(\big(X_j(k) - Y_j(k)\big)^{\mathsf{T}}\big(X_j - X_j(k) - Y_j + Y_j(k)\big)\Big),
\end{aligned}$$

where k is the iteration index of the algorithm. As explained in [15], any solution

Algorithm 5.1: Anti-windup design without [or with] $\mathbf{F}_c$ action

Input: α_0, $E_{c\,0}$, $[F_{c\,0}]$, P_0, $\hat{P}_0$, $\hat{T}_0$, $T_{1\,0}$, $T_{2\,0}$, $T_{3\,0}$, $T_{4\,0}$, $H_{1\,0}$, $H_{2\,0}$
Parameters: A_p, B_p, C_p, D_p, A_c, B_c, C_c, D_c
Construct $X_1(0)$, $Y_{1\,i}(0)$, $X_2(0)$, $Y_2(0)$, $X_3(0)$, $Y_3(0)$ from (5-37), (5-38), (5-39), (5-40)
Set $k = 0$
Optimization Loop 1
do
  Solve (5-57) for X_1, $Y_{1\,i}$, X_2, Y_2, X_3, Y_3
  $k \leftarrow k + 1$
  Set $X_1(k){=}X_1$, $Y_{1\,i}(k){=}Y_{1\,i}$, $X_2(k){=}X_2$, $Y_2(k){=}Y_2$, $X_3(k){=}X_3$, $Y_3(k){=}Y_3$, $\boldsymbol{\alpha}(k){=}\boldsymbol{\alpha}$
while $|\boldsymbol{\alpha}(k) - \boldsymbol{\alpha}(k-1)| > \epsilon$
if $\boldsymbol{\alpha}(k) \geq 0$ **then**
  Optimization Loop 2
  do
    Solve (5-59) for X_1, $Y_{1\,i}$, X_2, Y_2, X_3, Y_3
    $k \leftarrow k + 1$
    Set $X_1(k){=}X_1$, $Y_{1\,i}(k){=}Y_{1\,i}$, $X_2(k){=}X_2$, $Y_2(k){=}Y_2$, $X_3(k){=}X_3$, $Y_3(k){=}Y_3$, ... $\mathrm{trace}\{\hat{\mathbf{P}}\}(k){=}\mathrm{trace}\{\hat{\mathbf{P}}\}$
  while $\left|\mathrm{trace}\{\hat{\mathbf{P}}\}(k) - \mathrm{trace}\{\hat{\mathbf{P}}\}(k-1)\right| > \epsilon$
  return $\mathbf{E}_c$, $[\mathbf{F}_c]$, P, $\mathbf{H}_1$, $\mathbf{H}_2$
else
  return No stabilizing solution found
end

of the convexified problem $\Phi_j + M_j - \left(N_j(k) + \tilde{N}_j(k)\right) < 0$ is also feasible for the original nonconvex constraints $\Psi_1 > 0$, $\Psi_2 > 0$ and $\Psi_3 < 0$, because concavity of $-N_j$ implies, for all $j \in \{1\,i, 2, 3\}$, with $i = 1, ..., m$,

$$\Phi_j + M_j - N_j \leq \Phi_j + M_j - \left(N_j(k) + \tilde{N}_j(k)\right) < 0. \tag{5-52}$$

Applying a Schur complement, define

$$\hat{\Psi}_{1\,i} := \begin{bmatrix} N_{1\,i}(k) + \tilde{N}_{1\,i}(k) - \Phi_1 & (X_1 + Y_{1\,i})^{\mathsf{T}} \\ (X_1 + Y_{1\,i}) & 2I_{m+1} \end{bmatrix} > 0, \tag{5-53}$$

$$\hat{\Psi}_2 := \begin{bmatrix} N_2(k) + \tilde{N}_2(k) - \Phi_2 & (X_2 + Y_2)^{\mathsf{T}} \\ (X_2 + Y_2) & 2I_m \end{bmatrix} > 0, \tag{5-54}$$

$$\hat{\Psi}_3 := \begin{bmatrix} N_3(k) + \tilde{N}_3(k) - \Phi_3 & (X_3 + Y_3)^{\mathsf{T}} \\ (X_3 + Y_3) & 2I_{2n+3m} \end{bmatrix} > 0. \tag{5-55}$$

Recall then

$$\hat{\mathbf{P}} > 0,\ \mathbf{P}_{11} > 0,\ \hat{\mathbf{T}} > 0,\ \mathbf{T}_1 > 0,\ \mathbf{T}_2 > 0,\ \mathbf{T}_3 > 0, \tag{5-56}$$

and the optimization to be solved in the first loop for the stabilization of (5-6) is

$$\max_{\substack{\mathbf{P}_{11},\mathbf{P}_{12},\mathbf{P}_{22},\hat{\mathbf{P}},\\ \hat{\mathbf{T}},\mathbf{T}_1,\mathbf{T}_2,\mathbf{T}_3,\mathbf{T}_4,\\ \mathbf{H}_1,\mathbf{H}_2,\mathbf{E}_c,[\mathbf{F}_c],\boldsymbol{\alpha}}} \boldsymbol{\alpha}, \text{ subject to (5-53), (5-54), (5-55), (5-56).} \tag{5-57}$$

Convex optimization (5-57) ensures the stability of (2-3) with the estimate $\mathcal{S}(W)$ whenever an

$$\boldsymbol{\alpha} \geq 0 \tag{5-58}$$

is returned and, in order to enlarge this estimate, recalling inclusion (5-19), it is useful to solve, in the second loop,

$$\min_{\substack{\mathbf{P}_{11},\mathbf{P}_{12},\mathbf{P}_{22},\hat{\mathbf{P}},\\ \hat{\mathbf{T}},\mathbf{T}_1,\mathbf{T}_2,\mathbf{T}_3,\mathbf{T}_4,\\ \mathbf{H}_1,\mathbf{H}_2,\mathbf{E}_c,[\mathbf{F}_c]}} \text{trace}\{\hat{\mathbf{P}}\}, \text{ subject to (5-53), (5-54), (5-55), (5-56), (5-58),} \tag{5-59}$$

which motivates including two do-while loops in Algorithm 5.1, namely Optimization Loops 1 and 2. Furthermore, the values of P, $\mathbf{H}_1$ and $\mathbf{H}_2$ returned by Algorithm 1 allow computing the sublevel set $\mathcal{S}(W)$, which corresponds to an inner approximation or estimate of the basin of attraction of the origin of the closed loop. Therefore, for each $x \in \mathcal{S}(W)$ uniform convergence to zero is guaranteed.

The following proposition ensures the termination of Algorithm 5.1 in a finite time and ensures the feasibility of problems (5-57) and (5-59) at each iteration of the Optimization Loops 1 and 2, respectively.

Proposition 5.3

Algorithm 5.1 terminates in a finite number of iterations and feasibility of the ensuing optimizations is guaranteed at each iteration.

Proof: Problem (5-57) is feasible at the initial step of Optimization Loop 1 since its constraints hold with selections (5-37), (5-38), (5-39) and (5-40). Under the hypotheses of Theorem 5.1, feasibility of (5-59) in the first step of Optimization Loop 2 is only guaranteed if a stabilizing solution is found at the last iteration of Optimization Loop 1. Furthermore, feasibility of (5-57) and (5-59) at each iteration is ensured by (5-52), as it implies monotonicity of $\boldsymbol{\alpha}$, with $\boldsymbol{\alpha} \geq \boldsymbol{\alpha}(k)$, and $\hat{\mathbf{P}}$, with $\text{trace}(\hat{\mathbf{P}}) \geq \text{trace}(\hat{\mathbf{P}})(k)$, at their corresponding optimization loops. Finally, since $\hat{\mathbf{P}}$ and $\boldsymbol{\alpha}$ are respectively bounded by expressions (5-54) and (5-55), Algorithm 5.1 stops in a finite number of iterations, thus completing the proof. □

Global synthesis

Following the same reasoning used for the regional synthesis, exploiting (5-50) and (5-51), as well as the results of [15], define

$$\hat{\Psi}_4 := \begin{bmatrix} N_4(k) + \tilde{N}_4(k) - \Phi_4 & (X_4 + Y_4)^{\mathsf{T}} \\ (X_4 + Y_4) & 2I_m \end{bmatrix} > 0, \tag{5-60}$$

$$\hat{\Psi}_5 := \begin{bmatrix} N_5(k) + \tilde{N}_5(k) - \Phi_5 & (X_5 + Y_5)^{\mathsf{T}} \\ (X_5 + Y_5) & 2I_{2n+3m} \end{bmatrix} > 0. \tag{5-61}$$

Algorithm 5.2: Anti-windup design without [or with] $\mathbf{F}_\mathrm{c}$ action

Input: α_0, $E_{c\,0}$, $[F_{c\,0}]$, P_0, $T_{1\,0}$, $T_{2\,0}$, $T_{3\,0}$, $T_{4\,0}$
Parameters: A_p, B_p, C_p, D_p, A_c, B_c, C_c, D_c
Construct $X_4(0)$, $Y_4(0)$, $X_5(0)$, $Y_5(0)$ from (5-37), (5-38), (5-39),
Set $k = 0$
do
    Solve (5-63) for X_4, Y_4, X_5, Y_5
    $k \leftarrow k + 1$
    Set $X_4(k) = X_4$, $Y_4(k) = Y_4$, $X_5(k) = X_5$, $Y_5(k) = Y_5$, $\boldsymbol{\alpha}(k) = \boldsymbol{\alpha}$
while $|\boldsymbol{\alpha}(k) - \boldsymbol{\alpha}(k-1)| > \epsilon$
if $\boldsymbol{\alpha}(k) \geq 0$ **then**
    return $\boldsymbol{\alpha}$, $\mathbf{E}_\mathrm{c}$, $[\mathbf{F}_\mathrm{c}]$, P
else
    return No stabilizing solution found
end

and, considering the definitions of

$$\mathbf{P}_{11} > 0,\ \mathbf{T}_1 > 0,\ \mathbf{T}_2 > 0,\ \mathbf{T}_3 > 0, \tag{5-62}$$

in Theorem 5.2, the optimization to be solved for the stability of (2-3) is

$$\max_{\substack{\mathbf{P}_{11},\mathbf{P}_{12},\mathbf{P}_{22},\mathbf{T}_1,\mathbf{T}_2,\\ \mathbf{T}_3,\mathbf{T}_4,\mathbf{E}_\mathrm{c},[\mathbf{F}_\mathrm{c}],\boldsymbol{\alpha}}} \boldsymbol{\alpha}, \text{ subject to (5-60), (5-61), (5-62).} \tag{5-63}$$

The following proposition ensures the termination of Algorithm 5.2 in a finite time and ensures the feasibility of problem (5-63) at each iteration.

Proposition 5.4

Algorithm 5.2 terminates in a finite number of iterations and feasibility of the ensuing optimizations is guaranteed at each iteration.

Proof: The proof of feasibility, convergence and finite-time termination of Algorithm 5.2 follows the same reasoning as in Proposition 5.3 and may be originally found in [55]. □

5.5 Numerical examples

5.5.1 SISO academic example 2

Algorithm 5.1 is applied to a numerical example inspired from [23, Example 1]. The matrices of the state-space dynamics model of the controller and the plant are

$$A_p = \begin{bmatrix} -1 & 0 \\ 0 & 0.1 \end{bmatrix}, \qquad B_p = \begin{bmatrix} 1 \\ 1 \end{bmatrix}, \qquad C_p = \begin{bmatrix} 1 & 1 \end{bmatrix}, \qquad D_p = 0,$$

$$A_c = \begin{bmatrix} -100 & 0 \\ 1 & 0 \end{bmatrix}, \quad B_c = \begin{bmatrix} 8 \\ 0 \end{bmatrix}, \quad C_c = \begin{bmatrix} 11 & -1 \end{bmatrix}, \quad D_c = -2, \tag{5-64}$$

with $\overline{u} = 1$. Fix $\epsilon = 10^{-6}$. With non-restricted $\mathbf{F}_c$ for the anti-windup design, Algorithm 5.1 performs 77 iterations to find $\boldsymbol{\alpha} = 2.9689 \cdot 10^{-9}$,

$$\mathbf{E}_c = 10^{-1} \cdot \begin{bmatrix} -1.1776 \\ 1.3831 \end{bmatrix}, \qquad \mathbf{F}_c = -4.6185 \cdot 10^{-1}, \tag{5-65}$$

and guarantees regional stability of the origin from $\mathcal{S}(W)$. We also have

$$\lambda(P) = \{-1.3371,\ 1.1205,\ 1.7455,\ 8.8673,\ 16.7379\} \cdot 10^{-3},$$

$H_1 = 10^{-3} \cdot \begin{bmatrix} 2.8978 & -98.3088 & -10.1507 & 1.7932 \end{bmatrix}$ and $H_2 = 1.3467 \cdot 10^{-3}$. For the case without F_c, we obtain $\boldsymbol{\alpha} = 5.5616 \cdot 10^{-9}$ and

$$\mathbf{E}_c = 10^{-2} \cdot \begin{bmatrix} 1.2690 \\ 9.2057 \end{bmatrix} \tag{5-66}$$

after 76 iterations, ensuring regional stability as well. Moreover, we find

$$\lambda(P) = \{-1.2337,\ 1.0944,\ 1.7446,\ 8.8641,\ 16.7666\} \cdot 10^{-3},$$

$H_1 = 10^{-3} \cdot \begin{bmatrix} 2.9752 & -98.2399 & -10.5768 & 1.8457 \end{bmatrix}$ and $H_2 = 9.6084 \cdot 10^{-4}$. Notice that in both cases P is sign-indefinite, which is an allowable selection exploited by the optimizer.

Figure 5.2 shows the input-output response with initial states $x = \begin{bmatrix} 4 & 4 & 0 & 0 \end{bmatrix}^\mathsf{T}$. Both anti-windup solutions allow eliminating the overshoot. In addition to this, Figure 5.3 reports on the monotonic evolution of the maximization of α and the minimization of the trace of $\hat{P}$ in their respective Optimization Loop, as established in Proposition 3. For both cases with and without $\mathbf{F}_c$ action, the Optimization

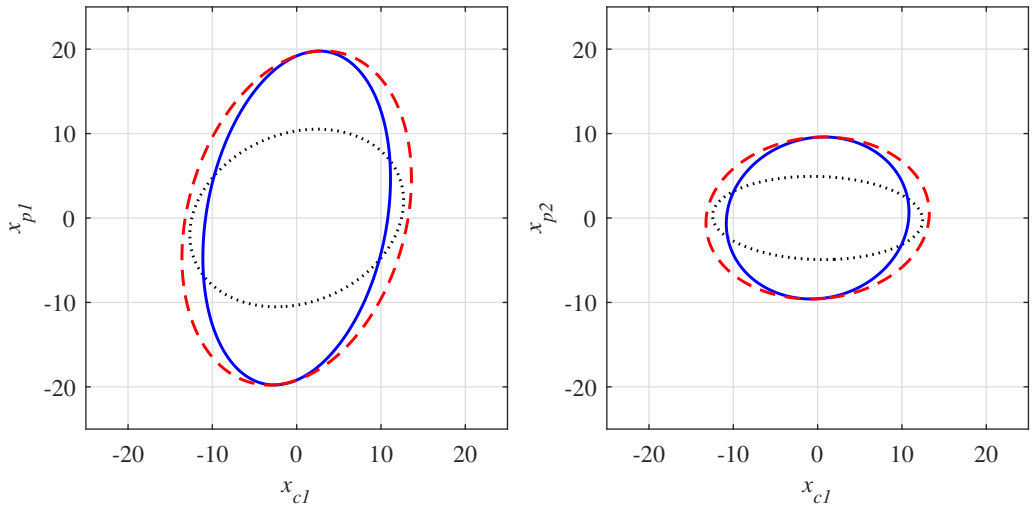

Figure 5.1: Estimate $\mathcal{S}(W)$ of the basin of attraction of the origin of the closed-loop with (5-64), in solid blue without $\mathbf{F}_c$, and in dashed red with $\mathbf{F}_c$. Quadratic estimate obtained using the solution of [23] in dotted black.

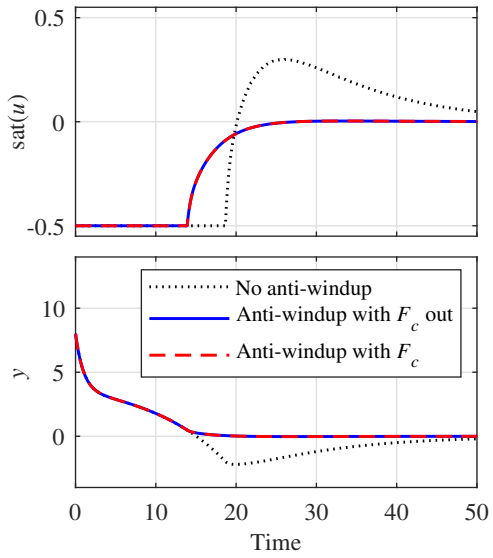

Figure 5.2: Simulation of the response of system (5-64) from the initial state $x_0 = \begin{bmatrix} 4 & 4 & 0 & 0 \end{bmatrix}^\mathsf{T}$ on top and its control input below.

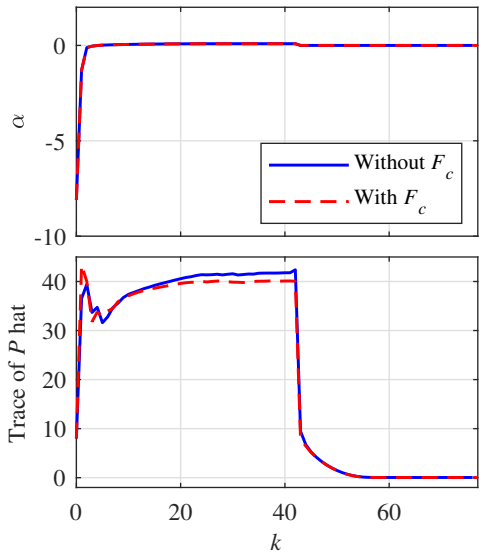

Figure 5.3: Evolution of α (top) and of the trace of $\hat{P}$ (bottom) as a function of the index k in the execution of Algorithm 5.1.

Loop 1 starts with a negative $\boldsymbol{\alpha}(1)$ but is able to maximize $\boldsymbol{\alpha}$ and find a stabilizing solution, allowing running the Optimization Loop 2, which maximizes the volume of the estimate $\mathcal{S}(W)$ by minimizing the trace of $\hat{\mathbf{P}}$. Furthermore, Figure 5.1 presents two sections of the estimates of the region of attraction $\mathcal{S}(W)$ with and without $\mathbf{F}_\mathrm{c}$ action, evincing an important enlargement of these estimates as compared to the results obtained with the quadratic method presented in [23].

5.5.2 SISO academic example 3

Consider now the closed-loop system with the exponentially stable plant of [55, Section V], for which the controller-plant dynamics are represented by the state-space model with matrices

$$A_p = \begin{bmatrix} -0.2 & -0.2 \\ 1 & 0 \end{bmatrix}, \quad B_p = \begin{bmatrix} 1 \\ 0 \end{bmatrix}, \quad C_p = \begin{bmatrix} -0.4 \\ -0.9 \end{bmatrix}^\mathsf{T}, \quad D_p = -0.5,$$
$$A_c = 0, \quad B_c = 1, \quad C_c = 2, \quad D_c = 2, \tag{5-67}$$

and $\overline{u} = 0.5$. Algorithm 5.2 is executed with a fixed $\epsilon = 10^{-6}$. With generic $\mathbf{F}_\mathrm{c}$, Algorithm 5.2 terminates successfully after 169 iterations and produces minimum convergence rate $\boldsymbol{\alpha} = 5.3207 \cdot 10^{-2}$ and

$$\mathbf{E}_\mathrm{c} = -1.5473, \qquad \mathbf{F}_\mathrm{c} = -8.3670 \cdot 10^{-2}, \tag{5-68}$$

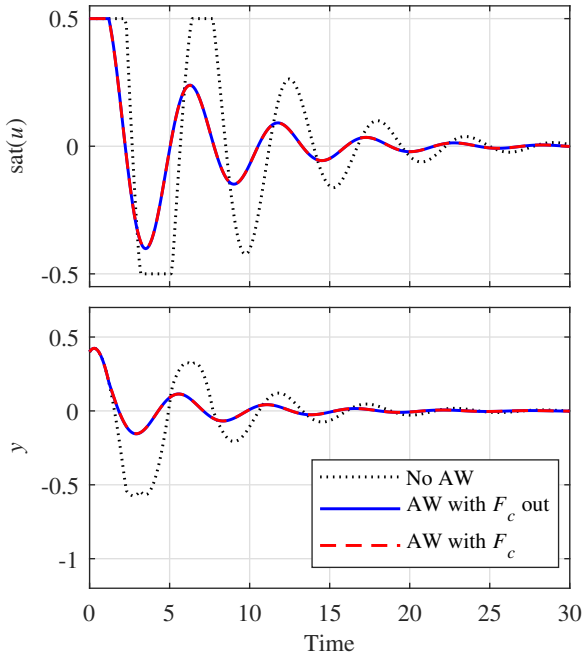

Figure 5.4: Response of the controller-plant feedback (5-67) from the initial state $x_0 = \begin{bmatrix}-0.5 & -0.5 & -0.5\end{bmatrix}^\mathsf{T}$ on top and its control input below.

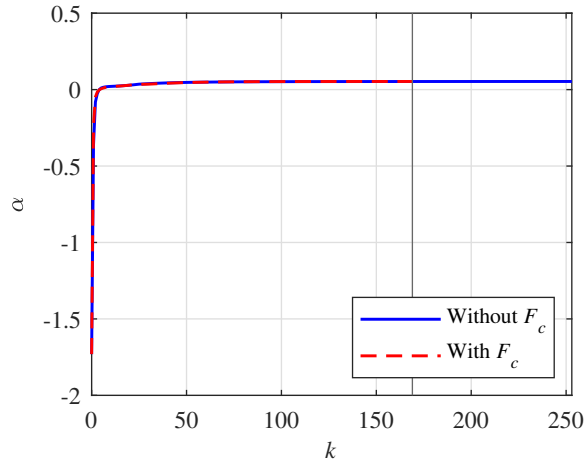

Figure 5.5: Evolution of $\boldsymbol{\alpha}$ as a function of the index k in the execution of Algorithm 5.1.

and a matrix P with eigenvalues

$$\lambda(P) = \{-7.3046,\ 2.9697,\ 11.4224,\ 21.4812\} \cdot 10^{-1},$$

ensuring global exponential stability. For the case with null $\mathbf{F}_\mathrm{c}$, Algorithm 5.2 performs 253 iterations to find $\boldsymbol{\alpha} = 5.3166 \cdot 10^{-2}$, a linear anti-windup gain

$$\mathbf{E}_\mathrm{c} = -1.6179 \tag{5-69}$$

and a matrix P with eigenvalues

$$\lambda(P) = \{-7.1475,\ 2.5823,\ 9.8896,\ 18.7561\} \cdot 10^{-1}.$$

Notice that in both cases, with and without $\mathbf{F}_\mathrm{c}$ in the anti-windup scheme, the matrix P is sign-indefinite, which is an allowable selection exploited by the optimizer.

Figure 5.4 reports on the input-output response and saturated control signal of

(2-3) with the state-space matrices in (5-67) from $x_0 = \begin{bmatrix}-0.5 & -0.5 & -0.5\end{bmatrix}^{\mathsf{T}}$. Notice that, with the computed anti-windup gains, a smoother and faster convergence of the output is obtained, as compared to the response found without any anti-windup compensation. Moreover, Figure 5.5 shows the monotonic evolution of $\boldsymbol{\alpha}$ along the iterations of Algorithm 5.2. Furthermore, it is worth to remark that, since $D_{\mathrm{p}} \neq 0$ for the controller-plant feedback, then the solution proposed in [23] is not able to provide any solution to this anti-windup design example.

5.5.3 Potter's wheel

Consider once again Example 2.3, in which the controller and plant state-space matrices are

$$\begin{aligned} &A_{\mathrm{p}} = -0.6960, && B_{\mathrm{p}} = 0.7030, && C_{\mathrm{p}} = 1, && D_{\mathrm{p}} = 0, \\ &A_{\mathrm{c}} = \begin{bmatrix}0 & 0\\ 0 & -100\end{bmatrix}, && B_{\mathrm{c}} = \begin{bmatrix}1\\ -100\end{bmatrix}, && C_{\mathrm{c}} = \begin{bmatrix}-20 & -30\end{bmatrix}, && D_{\mathrm{c}} = 20. \end{aligned} \tag{5-70}$$

and the saturation limit of the voltage supplier is $\overline{u} = 5V$. Moreover, Algorithm 5.2 is executed with a fixed $\epsilon = 10^{-6}$. For this example, Algorithm 5.2 terminates successfully after 214 iterations for the case with generic $\mathbf{F}_{\mathrm{c}}$ and finds $\boldsymbol{\alpha} = 2.4081$ and

$$\mathbf{E}_{\mathrm{c}} = \begin{bmatrix}14.1628\\ 78.9263\end{bmatrix}, \qquad \mathbf{F}_{\mathrm{c}} = -1.4743 \cdot 10^{2}, \tag{5-71}$$

and a matrix P with eigenvalues

$$\lambda(P) = \left\{-3.2926 \cdot 10^{2},\ 4.0717,\ 4.9107 \cdot 10^{2},\ 8.4001 \cdot 10^{2}\right\},$$

ensuring global exponential stability. For the case where $\mathbf{F}_{\mathrm{c}} = 0$ is imposed, Algorithm 5.2 produces $\boldsymbol{\alpha} = 2.4081$, a linear anti-windup gain

$$\mathbf{E}_{\mathrm{c}} = \begin{bmatrix}9.4175\\ 33.8953\end{bmatrix} \cdot 10^{-2} \tag{5-72}$$

and a matrix P with eigenvalues

$$\lambda(P) = \left\{-1.8557,\ 1.5282,\ 6.5636 \cdot 10^{2},\ 1.9177 \cdot 10^{3}\right\}$$

after 807 iterations. Notice that in both cases, with and without $\mathbf{F}_{\mathrm{c}}$ in the anti-windup scheme, the matrix P is sign-indefinite, which is an allowable selection exploited by the optimizer.

Figure 5.4 shows the plant output and saturated control output response of (2-3) with the state-space matrices in (5-70) from $x_0 = \begin{bmatrix}-10 & 0 & 0\end{bmatrix}^{\mathsf{T}}$. Notice that, with the computed anti-windup gains, a smoother and faster convergence of the output is obtained, in comparison to the response found without any anti-windup compensation, and, for this example, the solution with generic $\mathbf{F}_{\mathrm{c}}$ is able to produce a slightly smoother response with less iterations, as compared to the results obtained when imposing $\mathbf{F}_{\mathrm{c}} = 0$. On the other hand, Figure 5.5 shows the monotonic evolution

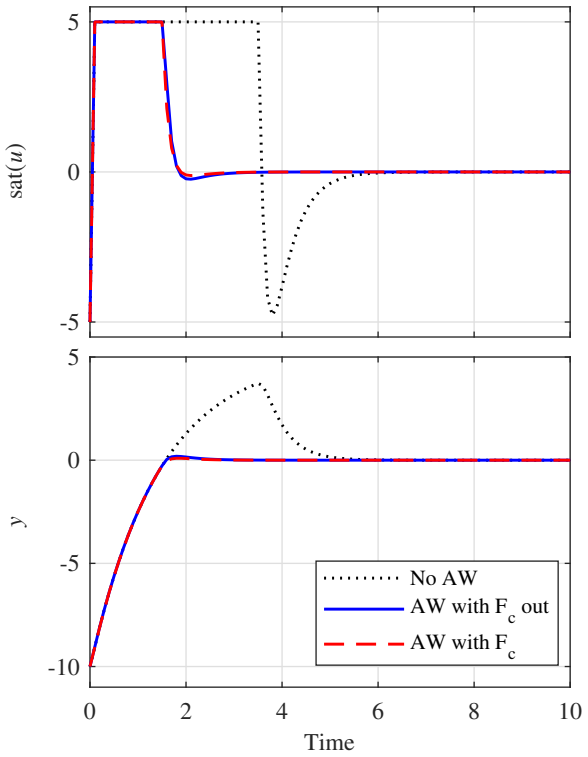

Figure 5.6: Response of the controller-plant feedback (5-67) from the initial state $x_0 = \begin{bmatrix} -10 & 0 & 0 \end{bmatrix}^\mathsf{T}$ on top and its control input below.

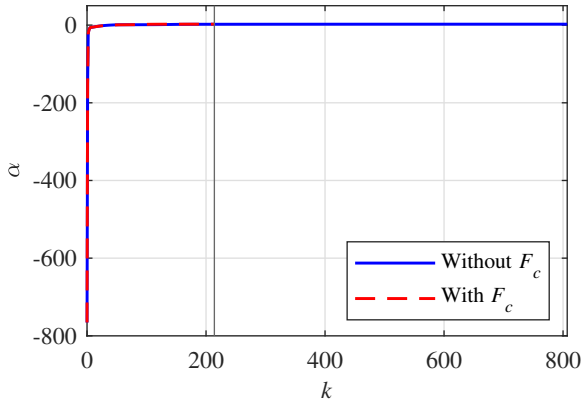

Figure 5.7: Evolution of $\boldsymbol{\alpha}$ as a function of the index k in the execution of Algorithm 5.1.

of $\boldsymbol{\alpha}$ along the iterations of Algorithm 5.2.

5.6 Conclusions

In this chapter, we addressed the design of static linear anti-windup gains guaranteeing regional exponential stability of closed-loop systems with plants subject to input saturation or global exponential stability of closed-loop systems with exponentially stable plants subject to input saturation by using nonquadratic smooth Lyapunov functions comprising sign-indefinite quadratic forms. The stability cer-

tificates are formulated in temrs of bilinear matrix inequalities, which are solved with iterative LMI-based algorithms based on a convex-concave decomposition that admit closed-loop systems with and without algebraic loops. The convergence of the presented algorithms is ensured by constructing a feasible initial solution to the BMI conditions, making these algorithms a complete solution to the static linear anti-windup design.

Chapter 6

General conclusion

The presence of amplitude constraints for the control signal in real-life control systems forbids the application of unlimited control effort. Disregarding these limitations on the control design phase may produce the degradation of performance or even the loss of stability for the closed loop. For this reason, this thesis proposed novel methods to

- synthesize a dynamic output-feedback controller for plants subject to input saturation, and
- synthesize a static linear anti-windup loop for systems subject to input saturation with a prescribed linear stabilizing controller.

The synthesized control laws guarantee exponential stability of the controller-plant feedback.

In the beginning of the manuscript, we discussed the notions of Lyapunov stability, for both nonlinear and linear autonomous systems. The concept of basin of attraction was also revised, recalling that its analytical determination may be a difficult or even impossible task, but its estimation is also a primary problem in the study of the stability of control systems.

Then, we have introduced the concept of input saturated systems, together with their mathematical modeling for the open-loop system and the closed-loop system with state-feedback and dynamic output-feedback control laws. Furthermore, we mentioned some important properties of systems subject to input saturation. Here, we discussed that global exponential stability of the closed-loop system is only attainable when the plant is already exponentially stable. Moreover, the concepts of region of linearity, region of saturation and windup phenomenon were also revised. Additionally, we studied the properties of the algebraic loop induced by the implementation of an anti-windup scheme.

With these latter concepts defined and discussed, we presented the motivations

and problems addressed in this work, as well as the main tool used to build the constructive results presented in this work: the sign-indefinite quadratic form of [56]. Indeed, we discussed the advantages of selecting piecewise smooth Lyapunov functions based on such sign-indefinite quadratic form, which result in the mitigation of conservativeness as compared to the classical quadratic methods thanks to the consideration of the gradient of the deadzone nonlinearity and the relaxation of some positivity conditions for the piecewise smooth Lyapunov functions.

Exploiting the versatility of the sign-indefinite quadratic forms of [56], we constructed then two certificates allowing computing a dynamic output-feedback controller for plants subject to input saturation guaranteeing regional exponential stability with maximized estimate of the basin of attraction. Moreover, we also stated conditions to compute a dynamic output-feedback control law ensuring global exponential stability of the closed loop and a prescribed local convergence rate when the plant is exponentially stable. The presented conditions are formulated in the form of linear matrix inequalities (LMIs), for which suitable commercial solvers can be used.

In the last chapter of this manuscript we presented four iterative algorithms based on the convex-concave decomposition of [15] allowing designing static linear anti-windup gains through the solution of the stability conditions of the closed-loop system derived from sign-indefinite piecewise smooth and sign-indefinite piecewise quadratic Lyapunov functions. Such conditions are formulated in terms of bilinear matrix inequalities (BMIs) and certify, for the general case, regional exponential stability, or global exponential stability for the cases where the closed-loop system has an exponentially stable plant. Moreover, for both the regional and global cases, an algorithm returning only the anti-windup gain acting on the state of the controller is given.

Considering the results proposed in this thesis, we can refer to some problems that remain open and that may deserve to be studied in the future:

- The $\mathcal{L}_2$ performance and external stabilization of closed-loop systems subject to input saturation with sign-indefinite quadratic forms.
- The internal and external stability analysis and stabilization of discrete time closed-loop systems subject to input saturation with sign-indefinite quadratic forms.
- The synthesis of dynamic output-feedback control laws for input-saturated plants with anti-windup term directly acting on the control signal using the sign-indefinite quadratic forms.

Indeed, we consider that the results presented in this manuscript can serve as the basis to address the above mentioned problems.

Bibliography

[1] K J Astrom and A B Ostberg. A teaching laboratory for process control. In *1985 American Control Conference*, pages 1380–1385, 1985.

[2] K.J. Aström and L. Rundqwist. Integrator windup and how to avoid it. In *1989 American Control Conference*, pages 1693–1698, 1989.

[3] Franco Blanchini, Giulia Giordano, Francesco Riz, and Luca Zaccarian. Solving nonlinear algebraic loops arising in input-saturated feedbacks. *IEEE Transactions on Automatic Control*, pages 1–1, 2022.

[4] Stephen Boyd, Laurent El Ghaoui, Eric Feron, and Venkataramanan Balakrishnan. *Linear Matrix Inequalities in System and Control Theory*. Society for Industrial and Applied Mathematics, 1994.

[5] C. Burgat, S. Tarbouriech, and M. Klai. Continuous-time saturated state feedback regulators: theory and design. *International Journal of Systems Science*, 25(2):315–336, 1994.

[6] Y. Cao, Z. Lin, and D.G. Ward. An antiwindup approach to enlarging domain of attraction for linear systems subject to actuator saturation. *IEEE Transactions on Automatic Control*, 47(1):140–145, 2002.

[7] Y. Cao, Z. Lin, and D.G. Ward. $\mathcal{H}_\infty$ antiwindup design for linear systems subject to input saturation. *Journal of Guidance, Control, and Dynamics*, 25(3):455–463, 2002.

[8] M. Chilali and P. Gahinet. H_∞ design with pole placement constraints: an LMI approach. *IEEE Transactions on Automatic Control*, 41(3):358–367, 1996.

[9] S. Crawshaw and G. Vinnicombe. Anti-windup synthesis for guaranteed $\mathcal{L}_2$ performance. In *Proceedings of the 39th IEEE Conference on Decision and Control (Cat. No.00CH37187)*, volume 2, pages 1063–1068 vol.2, 2000.

[10] A. Cristofaro, S. Galeani, S. Onori, and L. Zaccarian. A switched and scheduled design for model recovery anti-windup of linear plants. *European Journal of Control*, 46:23–35, 2019.

[11] D. Dai, T. Hu, A.R. Teel, and L. Zaccarian. Output feedback design for saturated linear plants using deadzone loops. *Automatica*, 45(12):2917–2924, 2009.

[12] D. Dai, T. Hu, A.R. Teel, and L. Zaccarian. Piecewise-quadratic Lyapunov functions for systems with deadzones or saturations. *Systems & Control Letters*, 58(5):365–371, 2009.

[13] Dan Dai, Tingshu Hu, Andrew R. Teel, and Luca Zaccarian. Analysis of systems with saturation/deadzone via piecewise-quadratic Lyapunov functions. In *2007 American Control Conference*, pages 5822–5827, 2007.

[14] M. Della Rossa, R. Goebel, A. Tanwani, and L. Zaccarian. Piecewise structure of Lyapunov functions and densely checked decrease conditions for hybrid systems. *Mathematics of Control, Signals, and Systems*, 33:123–149, 2021.

[15] Q. Tran Dinh, S. Gumussoy, W. Michiels, and M. Diehl. Combining convex–concave decompositions and linearization approaches for solving bmis, with application to static output feedback. *IEEE Transactions on Automatic Control*, 57(6):1377–1390, 2012.

[16] H. A. Fertik and C.W. Ross. Direct digital control algorithm with anti-windup feature. *ISA Transactions*, 6(4):317–328, 1967.

[17] S. Galeani, A.R. Teel, and L. Zaccarian. Constructive nonlinear anti-windup design for exponentially unstable linear plants. *Systems & Control Letters*, 56(5):357–365, 2007.

[18] Sergio Galeani, Sophie Tarbouriech, Matthew Turner, and Luca Zaccarian. A tutorial on modern anti-windup design. *European Journal of Control*, 15(3):418–440, 2009.

[19] G. Garcia, S. Tarbouriech, J.M. Gomes da Silva, and D. Eckhard. Finite $\mathcal{L}_2$ gain and internal stabilisation of linear systems subject to actuator and sensor saturations. *IET Control Theory & Applications*, 3:799–812(13), July 2009.

[20] J.M. Gomes da Silva Jr, A. Fischman, S. Tarbouriech, J.M. Dion, and L. Dugard. Synthesis of state feedback for linear systems subject to control saturation by an lmi-based approach. *IFAC Proceedings Volumes*, 30(16):207–212, 1997. IFAC Symposium on Robust Control Design (ROCOND'97), Budapest, Hungary, 25-27 June 1997.

[21] J.M. Gomes da Silva Jr and S. Tarbouriech. Local stabilization of discrete-time linear systems with saturating controls: an lmi-based approach. In *American Control Conference*, pages 92–96, 1998.

[22] J.M. Gomes da Silva Jr and S. Tarbouriech. Local stabilization of discrete-time linear systems with saturating controls: an LMI-based approach. *IEEE Transactions on Automatic Control*, 46(1):119–125, 2001.

[23] J.M. Gomes da Silva Jr and S. Tarbouriech. Anti-windup design with guaranteed regions of stability: an LMI-based approach. *IEEE Transactions on Automatic Control*, 50(1):106–111, 2005.

[24] J.M Gomes da Silva Jr, S. Tarbouriech, and R. Reginatto. Analysis of regions of stability for linear systems with saturating inputs through an anti-windup scheme. In *Proceedings of the International Conference on Control Applications*, volume 2, pages 1106–1111 vol.2, 2002.

[25] G.C. Goodwin, S.F. Graebe, and M.E. Salgado. *Control System Design*. Prentice Hall, 2001.

[26] G. Grimm, J. Hatfield, I. Postlethwaite, A.R. Teel, M.C. Turner, and L. Zaccarian. Anti-windup for stable linear systems with input saturation: an LMI-based synthesis. *IEEE Transactions on Automatic Control*, 48(9):1509–1525, 2003.

[27] Gene Grimm, Andrew R. Teel, and Luca Zaccarian. Linear LMI-based external anti-windup augmentation for stable linear systems. *Automatica*, 40(11):1987–1996, 2004.

[28] P. Hippe. Windup prevention for unstable systems. *Automatica*, 39(11):1967–1973, 2003.

[29] P. Hippe. *Windup in Control: Its Effects and Their Prevention*. Advances in Industrial Control. Springer London, 2006.

[30] T. Hu and Z. Lin. *Control Systems with Actuator Saturation: Analysis and Design*. Birkhauser Boston, Inc., USA, 2001.

[31] T. Hu, A.R. Teel, and L. Zaccarian. Stability and performance for saturated systems via quadratic and nonquadratic lyapunov functions. *IEEE Transactions on Automatic Control*, 51(11):1770–1786, 2006.

[32] Tingshu Hu, Zongli Lin, and Ben M. Chen. An analysis and design method for linear systems subject to actuator saturation and disturbance. *Automatica*, 38(2):351–359, 2002.

[33] The MathWorks Inc. Matlab simulink version 10.5 (r2022a), 2022.

[34] R.E. Kalman and J. E. Bertram. Control system analysis and design via the "second method" of lyapunov: Ii—discrete-time systems. *Journal of Basic Engineering*, 82:394–400, 1960.

[35] V. Kapila, A. Sparks, and H. Pan. Control of systems with actuator nonlinearities: An lmi approach. *Proceedings of the American Control Conference*, 5:3201 – 3205 vol.5, 02 1999.

[36] T.A. Kendi, M.L. Brockman, M. Corless, and F.J. Doyle. Controller synthesis for input-constrained nonlinear systems subject to unmeasured disturbances. In *Proceedings of the 1997 American Control Conference (Cat. No.97CH36041)*, volume 5, pages 3088–3092 vol.5, 1997.

[37] H.K. Khalil. *Nonlinear systems; 3rd ed.* Prentice-Hall, Upper Saddle River, NJ, 2002.

[38] Mayuresh V. Kothare, Peter J. Campo, Manfred Morari, and Carl N. Nett. A unified framework for the study of anti-windup designs. *Automatica*, 30(12):1869–1883, 1994.

[39] V.A. Kubovich, G.A. Leonov, and A.K. Gelig. *Stability of Stationary Sets in Control Systems with Discontinuous Nonlinearities*. Series on stability. World Scientific, 2004.

[40] J.B. Lasserre. Reachable, controllable sets and stabilizing control of constrained linear systems. *Automatica*, 29(2):531–536, 1993.

[41] Y. Li. *Stability and Performance of Control Systems with Actuator Saturation*. Control Engineering. Springer Nature, Cham, 1st ed. 2018 edition. edition, 2017.

[42] Y. Li and Z. Lin. A generalized piecewise quadratic Lyapunov function approach to estimating the domain of attraction of a saturated system. In *IFAC-PapersOnLine*, volume 48, pages 120–125, 2015.

[43] Yuanlong Li, Zongli Lin, and Ning Li. Stability and performance analysis of saturated systems using an enhanced max quadratic lyapunov function. *IFAC-PapersOnLine*, 50(1):11847–11852, 2017. 20th IFAC World Congress.

[44] K. Liu and D. Akasaka. A partial parameterization of nonlinear output feedback controllers for saturated linear systems. *Automatica*, 50(1):233–239, 2014.

[45] J. Lozier. A steady state approach to the theory of saturable servo systems. *IRE Transactions on Automatic Control*, 1(1):19–39, 1956.

[46] Duane T. McRuer. Pilot-induced oscillations and human dynamic behavior. Technical report, NASA, 1995.

[47] E.F. Mulder and M.V. Kothare. Synthesis of stabilizing anti-windup controllers using piecewise quadratic lyapunov functions. In *Proceedings of the 2000 American Control Conference. ACC (IEEE Cat. No.00CH36334)*, volume 5, pages 3239–3243 vol.5, 2000.

[48] Eric F. Mulder, Pradeep Y. Tiwari, and Mayuresh V. Kothare. Simultaneous linear and anti-windup controller synthesis using multiobjective convex optimization. *Automatica*, 45(3):805–811, 2009.

[49] T. Nguyen and F. Jabbari. Output feedback controllers for disturbance attenuation with actuator amplitude and rate saturation. In *Proceedings of the 1999 American Control Conference (Cat. No. 99CH36251)*, volume 3, pages 1997–2001 vol.3, 1999.

[50] S. Pantano Calderón, S. Tarbouriech, and L. Zaccarian. Local static anti-windup design with sign-indefinite quadratic forms. *IEEE Control Systems Letters*, 7:3090–3095, 2023.

[51] S. Pantano Calderón, S. Tarbouriech, and L. Zaccarian. Global exponential saturated output feedback design with sign-indefinite quadratic forms. In *European Control Conference (ECC)*, 2024.

[52] S. Pantano Calderón, S. Tarbouriech, and L. Zaccarian. Plant-order saturated output-feedback regional controller synthesis with sign-indefinite quadratic forms. *IEEE Control Systems Letters*, 8:562–567, 2024.

[53] C. Pittet, S. Tarbouriech, and C. Burgat. Stability regions for linear systems with saturating controls via circle and popov criteria. In *Proceedings of the 36th IEEE Conference on Decision and Control*, volume 5, pages 4518–4523 vol.5, 1997.

[54] Ian Postlethwaite, Matthew C. Turner, and Guido Herrmann. Robust control applications. *Annual Reviews in Control*, 31(1):27–39, 2007.

[55] A. Priuli, S. Tarbouriech, and L. Zaccarian. Static linear anti-windup design with sign-indefinite quadratic forms. *IEEE Control Systems Letters*, 6:3158–3163, 2022.

[56] I. Queinnec, S. Tarbouriech, G. Valmorbida, and L. Zaccarian. Design of saturating state feedback with sign-indefinite quadratic forms. *IEEE Transactions on Automatic Control*, 67(7):3507–3520, 2022.

[57] Hanus Raymond and Kinnaert Michel. Control of constrained multivariable systems using the conditioning technique. In *1989 American Control Conference*, pages 1712–1718, 1989.

[58] C. Scherer, P. Gahinet, and M. Chilali. Multiobjective output-feedback control via LMI optimization. *IEEE Transactions on Automatic Control*, 42(7):896–911, 1997.

[59] W. E. Schmitendorf and B. R. Barmish. Null controllability of linear systems with constrained controls. *SIAM Journal on Control and Optimization*, 18(4):327–345, 1980.

[60] Jorge Sofrony, Matthew C. Turner, and Ian Postlethwaite. Anti-windup synthesis using riccati equations. *IFAC Proceedings Volumes*, 38(1):171–176, 2005. 16th IFAC World Congress.

[61] E.D. Sontag. An algebraic approach to bounded controllability of linear systems. *International Journal of Control*, 39(1):181–188, 1984.

[62] G. Stein. Respect the unstable. *IEEE Control Systems Magazine*, 23(4):12–25, 2003.

[63] H.J. Sussmann, E.D. Sontag, and Y. Yang. A general result on the stabilization of linear systems using bounded controls. *IEEE Transactions on Automatic Control*, 39(12):2411–2425, 1994.

[64] A. Syaichu-Rohman and R.H. Middleton. On the robustness of multivariable algebraic loops with sector nonlinearities. In *Proceedings of the 41st IEEE Conference on Decision and Control, 2002.*, volume 1, pages 1054–1059, 2002.

[65] S. Tarbouriech, G. Garcia, J.M. Gomes da Silva Jr., and I. Queinnec. *Stability and stabilization of linear systems with saturating actuators*. Springer-Verlag London Ltd., 2011.

[66] S. Tarbouriech, C. Prieur, and J.M. Gomes da Silva Jr. Stability analysis and stabilization of systems presenting nested saturations. *IEEE Transactions on Automatic Control*, 51(8):1364–1371, 2006.

[67] G. Valmorbida, A. Garulli, and L. Zaccarian. Regional $\mathcal{L}_{2m}$ gain analysis for linear saturating systems. *Automatica*, 76:164–168, 2017.

[68] G. Valmorbida, L. Zaccarian, S. Tarbouriech, I. Queinnec, and A. Papachristodoulou. Nonlinear static state feedback for saturated linear plants via a polynomial approach. *IEEE Transactions on Automatic Control*, 62(1):469–474, 2017.

[69] L. Zaccarian and A.R. Teel. *Modern Anti-windup Synthesis: Control Augmentation for Actuator Saturation*. Princeton Series in Applied Mathematics. Princeton University Press, 2011.

[70] Luca Zaccarian and Andrew R. Teel. A common framework for anti-windup, bumpless transfer and reliable designs. *Automatica*, 38(10):1735–1744, 2002.